Synergistic inflammatory signaling in airway epithelial cells: control of expression levels of protease-activated receptors and interleukin-8 release

Dissertation

Zur Erlangung des akademischen Grades

doctor rerum naturalium

(Dr. rer. nat.)

genehmigt durch die Fakultät für Naturwissenschaften

der Otto-von-Guericke Universität Magdeburg

von Dipl. -Pharm. Ewa Ostrowska

geb. am 09. November 1978 in Brzeg Dolny, Polen

Gutachter: **Prof. Dr. Georg Reiser**

Privatdozent Dr. Frank Bühling

Eingereicht am: **25. September 2007**

Verteidigt am: **31. März 2008**

Danksagung

An dieser Stelle möchte ich all den Menschen von Herzen danken, die mir bei der Erstellung dieser Arbeit geholfen haben und meine Arbeitszeit einer wertvollen Erinnerung machen werden.

Herrn Prof. Georg Reiser möchte ich ganz, ganz herzlich für Betreuung, Unterstützung, Förderung und besonders für den Glauben an mich danken.

Frau Dr. Sokolova möchte ich vor allem dafür danken, dass durch die zahlreichen Diskussionen mit ihr, meine Arbeit die jetzige Form annehmen konnte.

Allen Kolleginnen und Kollegen, Mitarbeitern des Instituts für Neurobiochemie, die ich durch meine Arbeit kennenlernen durfte, danke ich ganz herzlich für alles was ich von Ihnen gelernt habe und was ich mit ihnen erlebt habe. Vielen Dank für jede Hilfe, Unterstützung und für jedes Lächeln.

Table of content

1. Introduction

1.1 The family of protease-activated receptors (PARs).

The “history” of protease-activated receptors (PARs; more correctly, but less commonly referred to as proteinase-activated receptors) is relatively young. Only in the early nineties PARs were cloned and their unique activation mechanism was described . There are 4 subtypes of PARs, PAR-1, PAR-2, PAR-3 and PAR-4, named in chronological order of their discovery. PAR-1, formerly known as the thrombin receptor, was identified using RNA derived from thrombin-responsive cells and is still the one of the four family members which is the best characterised. Three years later the second proteolytically activated receptor, PAR-2, was cloned from a mouse genomic library, and subsequently found to be activated by trypsin . The third family member, PAR-3, was identified as a second thrombin receptor in PAR-1 knockout mouse cells , cloned and characterized . PAR-4 was cloned following database search using conserved domains of other PARs. PAR-4 was identified in PAR-3 deficient mouse platelets with persisting response to thrombin .

All the PAR genes, in human and mouse, share a similar two exon structure with a very long intron of 4-22 kb in case of PAR-1-3 and only 0.25 kb for PAR-4. PAR-1, PAR-2 and PAR-3 genes are located closely together on a single chromosome in humans (5q13) and mice (13D2), whereas the gene for PAR-4 is located separately in both species (chromosome 19p2 and 8B3.3, respectively) .

1.1.1 Mechanism of activation and signal transduction.

PARs consist of the typical 7-transmembrane helices connected by 3 extracellular and 3 intracellular loops together with an extracellular N-terminal and intracellular C-terminal domain (Fig. 1.1). Despite the fact that these receptors belong to a large superfamily of G protein-coupled receptors, the activation mechanism is very distinct from that of other receptors from this family. The mechanism of receptor activation involves cleavage of the receptor at a specific site within the extracellular amino terminus, called “activation site”, thus unmasking a new N-terminal “tethered” ligand. The “tethered” ligand binds intramolecularly to the receptor resulting in the initiation of signal transduction (Fig. 1.1). Six or more specific amino acid residues within the newly exposed tethered ligand

interact with extracellular loop 2 (Lerner et al., 1996). Thus, PARs are peptide receptors carrying their own ligands, which remains cryptic until unmasked by receptor cleavage .

Ultimately, the activated receptor interacts with heterotrimeric G proteins, which catalyze the exchange of GDP for GTP on the α-subunit of the G-protein. It results in transducing numerous intracellular signals, e.g. stimulation of phospholipase C (PLC)-catalyzed hydrolysis of polyphosphoinositides. PLC activation causes the formation of diacylglycerol and of inositol 1,4,5-trisphosphate ($InsP_3$) with further mobilization of intracellular Ca^{2+} and activation of protein kinase C. This triggers activation of mitogen-activated protein kinases (MAPKs) and other Ca^{2+}-modulated kinases.

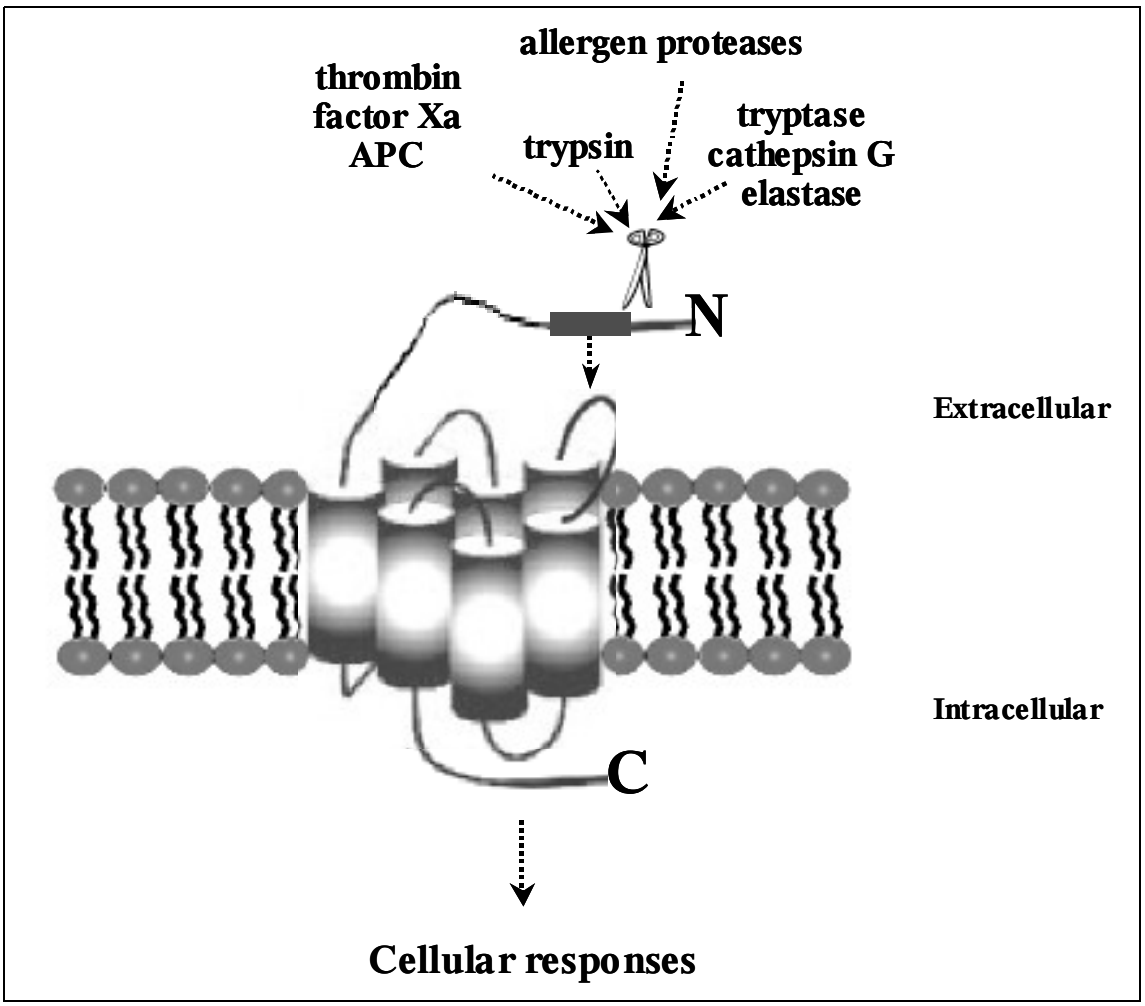

Figure 1.1: Activation of PARs. The protease cleaves irreversibly the PAR at the "activation site", unmasking a new N-terminus acting as a tethered ligand. This ligand interacts with the second extracellular loop of the receptor initiating G protein coupling. A synthetic activating peptide (AP) derived from the N-terminal sequence of PAR is able to activate the receptor in the absence of protease-mediated cleavage of the N terminus.

PARs are activated by an irreversible mechanism, and once cleaved, are destined for lysosomal degradation. Once activated, the receptors rapidly uncouple from the transmembrane signaling and internalize by a phosphorylation-dependent mechanism . The internalized receptor is mostly targeted to lysosomes for degradation and only few molecules recycle back to the cell surface but remain inactive. Resensitization of the receptor involves mobilization of the intracellular receptor pools, the Golgi apparatus and vesicles, where PARs are stored. Alternatively, PARs are synthesized *de novo* . The level of expression of receptors at the cell surface is a balance between removal by endocytosis and replenishment by mobilization of intracellular pools .

1.1.2 Agonists of PARs.

Three of the PAR receptors can be activated by thrombin, the main effector protease of the coagulation cascade . Thrombin is a serine protease generated at sites of vascular injury, produced from its precursor molecule prothrombin by the coagulation factor Xa in association with factor Va. Further, thrombin converts fibrinogen to fibrin which forms clots . Apart from the function in coagulation, thrombin has multiple biological effects, including platelet aggregation and endothelial cells proliferation, mostly via PARs . Thrombin exhibits high potency to activate PAR-1 and PAR-3, whereas PAR-4 activation requires 10-100 fold higher concentration. This apparently results from different primary structures of the receptors. The extracellular amino terminus of PAR-1 and PAR-3 contains a sequence of negatively charged residues, the so called “hirudin-like domain” that is distal to the thrombin cleavage site. This domain binds to an exosite I of thrombin to cause allosteric activation of thrombin and thus promotes efficient receptor activation. That explains thrombin’s potency at its receptor. The name of this region of the receptor comes from the fact that it resembles a domain of the leech anticoagulant hirudin, which inhibits thrombin by binding to its anionic site .

Differences in potency of thrombin to activate different PARs have interesting functional consequences. For example, human platelets express both PAR-1 and PAR-4, what allows them to respond to a broad range of concentrations of thrombin in a regulated manner. PAR-1 mediates responses to low concentrations of thrombin, whereas in the absence of PAR-1 function, PAR-4 can mediate platelet activation but only at high thrombin concentrations. However, the functional expression of PAR-3, in contrast to PAR-1 and PAR-4, was not detected in human platelets, what suggests that in humans PAR-3 does not play a major role for platelet activation, in contrast to the mouse system.

Other members of the coagulation cascade, factors Xa and VIIa, can also activate PAR-1 or PAR-2 .

Interestingly, activated protein C (APC), the major protease of anticoagulation pathway, can also trigger cellular responses via PAR-1 . However, very high concentrations of APC are required for the PAR-1 cleavage .

Another main PAR agonist, trypsin, activates PAR-2 , PAR-4 and PAR-1 . Trypsin is secreted from pancreas into the small intestine as inactive trypsinogen, where it is activated by enteropeptidase. The major two trypsinogen isoforms are cationic and anionic trypsinogens and the third less abundant form mesotrypsinogen, which possesses resistance to common trypsin inhibitors . Trypsin was thought to be restricted to the pancreas. However, now several studies have demonstrated the presence of trypsin in a variety of tissues such lung, brain, kidney, pancreas, spleen and cells such as leukocytes, neurons, epithelial and endothelial cells .

Mast cells tryptase, an important inflammatory mediator, detected in fluids from inflamed tissues is also a PAR-2 activator .

Cathepsin G from neutrophils is a potential activator of PAR-4 . Neutrophil proteinase 3 can activate PAR-2 . Granzyme A, released by activated T lymphocytes appears to activate the thrombin receptor PAR-1 .

Only recent reports show that matrix metalloprotease-1 (MMP-1) in the stromal tumor can alter the behaviour of cancer cells through PAR-1 to promote cell migration and invasion . Furthermore, tumor-derived MMP-1 cleaves endothelial PAR-1, thus generating a prothrombotic and proinflammatory cell adhesion . However, the ability of MMPs to activate PARs needs to be further evaluated systematically.

An interesting aspect is that a number of non-mammalian proteases from mites, bacteria, and fungi have been found to activate PARs in mammalian cells. For instance, dust mite *Dermatophagoides pteronyssinus* (Der p) produce serine proteases, cysteine proteases, and metalloproteases that are allergens in airway epithelium. It has been shown that these proteases can act via PAR. The effects of the proteases Der p3 and Der p9, Der p1 is mediated by PAR-2 .

Similarly, proteases from bacteria *Porphyromonas gingivalis* can activate PAR-1, PAR-2 and PAR-4 . Proteases from fungal extract might activate cells through PAR-2 .

Because of the unique activating mechanism of PARs, it is possible to directly use the synthetic peptides (activating peptides: AP) mimicking the tethered ligand sequence to activate the receptor without the proteolytic cleavage. The advantage of applying these

small peptides is manifested in 1) specificity, what gives the opportunity to avoid the use of proteases, which have many additional biological effects, and 2) possibility of development of antagonists, for which APs serve as a template. On the other hand the APs have some disadvantages limiting particular implications: 1) there is a low potency of APs. They require concentrations in excess of minimally several micromolar concentrations; 2) peptides are not always specific, e.g. SFLLR-NH2, PAR-1 AP derived from the human PAR-1 sequence can activate both PAR-1 and PAR-2 ; 3) there is no reliably effective AP for PAR-3 known.

An overview of the cleavage sites and the unmasked new terminus that function as tethered ligand on human and murine PARs is presented in Table 1.1. The synthetic peptide mimics the tethered ligand sequence and functions as an agonist independent of receptor cleavage.

	PAR-1	**PAR-2**	**PAR-3**	**PAR-4**
Activator	Thrombin>Trypsin	Trypsin	Thrombin	Thrombin=Trypsin
Cleavage site, human	R^{41}↓SFLLRN	R^{34}↓SLIGVK	K^{38}↓TFRGAP [a]	R^{47}↓GYPGQV
Cleavage site, murine	R^{41}↓SFFLRN	R^{38}↓SLIGRL	K^{37}↓SFNGGP [a]	R^{59}↓GYPGKF
Improved agonist	TFLLR	tc-LIGRLO		AYPGKF

Table 1.1: Summary of general properties of "tethered" ligand of human and murine PARs. Symbol abbreviation for amino acids are numbered accordingly, beginning from the amino terminus of the translated protein sequence. Appropriate cleavage site (↓) by activating proteases and predicted TLS after cleavage, what sequence serves for synthetic peptides analogues. Sensitivity to thrombin or trypsin is a basic defining feature of the PAR subtypes. [a]Inactive as peptide agonist. TLS, tethered ligand sequence.

1.1.3 PAR distribution in human tissue and cell types.

As it is shown in Table 1.2, PARs are receptors with widespread distribution and are abundant in almost every tissue in the human body. Cells can express more than one PAR family member and more than one may be thrombin-responsive.

Table 1.2: Localization of PARs in human tissues.

Organ (tissue and cell type)	References
PAR-1	
Brain (astrocytes, neurons)	
Eye (corneal cells)	
Lung (fibroblasts, alveolar macrophages, epithelium, smooth muscle)	
Pancreas	
Liver	
Epidermis (keratinocytes, fibroblasts)	
Vascular system (endothelial umbilical cells, smooth muscle)	
Platelets	
Cell of immune system (monocytes, macrophages)	
PAR-2	
Brain (neurons, astrocytes)	
Eye (corneal cells)	
Lung (epithelium, smooth muscle, fibroblasts)	
Heart	
Pancreas	
Liver	
Intestine (epithelium, nonvascular smooth muscle)	
Kidney	
Prostate (epithelium, myofibroblats)	
Uterus (smooth muscle)	
Vascular system (smooth muscle cells, endothelium)	
Epidermis (keratinocytes, endothelial cells)	
Cell of immune system (macrophages, neutrophils, eosinophils)	

Organ (tissue and cell type)	References
PAR-3	
Bone marrow	
Lung (fibroblasts, epithelium, smooth muscle)	
Heart	
Pancreas	
Liver	
Small intestine	
Vascular system (endothelial umbilical cells, smooth muscle)	
Cells of immune system (monocytes, macrophages, neutrophils)	
PAR-4	
Lung (epithelium, smooth muscle)	
Pancreas	
Liver	
Small intestine	
Thyroid	
Prostate	
Vascular system (endothelial cells, smooth muscle)	
Platelets	

1.1.4 PAR-3 signaling

The knowledge about PAR-3 signaling and its functional role, in contrast to the other members of the PAR family, is still unclear and confined to relatively few findings that have been published until now. A specific feature of this receptor is its different species-specific susceptibility and consequently physiological function in mouse and human. The responsiveness of human PAR-3 to thrombin was confirmed in heterologous expression systems, in COS7 cells and *Xenopus* oocytes . However, the experiments on murine PAR-3, overexpressed in COS7 cells as well as platelets from PAR-4 deficient mouse, demonstrated that murine PAR-3 itself does not mediate intracellular signaling but serves as a cofactor for PAR-4 cleavage . It might indicate that during evolution, murine PAR-3 has lost its ability to function autonomously. Additionally, the independent differential expression patterns of PAR-3 and PAR-4 in these two species, human and mouse, further indicate differences in the functional role of PAR-3. Particularly platelets, where thrombin is a potent activator, represent a good model of PAR-3 signaling. Consistently, human and mouse platelets display distinct PAR-3 expression as well as signaling. Murine PAR-3 is necessary for complete thrombin-mediated platelet activation, however its role seems to be restricted to act as cofactor for PAR-4 . In human platelets,

thrombin is signaling through the activation of PAR-1 and PAR-4, whereas PAR-3 is not involved in this process .

The presence of a considerably shorter C-terminal tail in PAR-3 (15 amino acids for hPAR-3) than in other PARs (about 40 amino acids) suggests that PAR-3 signaling and desensitization differs from that of other PARs. However, there are no investigations of this aspect available until now. Furthermore, the great obstacle in the extension of studies on PAR-3 signaling is the lack of PAR-3 selective agonist or antagonist. Synthetic peptides that mimic the putative tethered ligand of PAR-3 were found to be inactive in terms of PAR-3 activation . However, there are studies reporting these peptides that mimic the putative tethered ligand of human and murine PAR-3 may activate PAR-1 and PAR-2 . Nevertheless, our and other groups previously showed that the PAR-3-activating peptide is able to induce cellular responses in rat astrocytes , human smooth muscle cells and Jurkat T cells . Therefore, the issue of selective agonists for PAR-3 remains controversial.

A most recent report discloses interesting findings about the function of endothelial PAR-3 . The authors show that PAR-3 can form heterodimers with PAR-1. These PAR-1/3 dimers are formed constitutively and, upon activation, induce signaling distinct from PAR-1/1 homodimers, involving coupling to $G\alpha_{13}$. PAR-3 functions as an allosteric regulator of thrombin to enhance PAR-1 cleavage what leads to increased endothelial permeability.

However, PAR-3, particularly of human origin has remained largely unexplored and leaves plenty of questions open. The abundant distribution of this receptor in human tissues indicates the high biological relevance of PAR-3 activation. Therefore the unequivocal establishment of a signaling cascade connected to PAR-3 without crosstalk to other PARs underlines the eminent importance of PAR-3.

1.2 Inflammatory mediators and processes in lung.

Inflammation can be broadly defined as nonspecific protective reaction of vascular tissue to injury, extremely important for the clearance of exogenous toxins and pathogens. This process is accompanied by vasodilation, increased blood flow, enhanced permeability that augments the recruitment of inflammatory cells and delivery of plasma proteins to the site of injury. In general, this process is self-limiting and leads to a return to the normal state .

The early-phase of the inflammatory reaction is characterized by the rapid activation of airway mast cells and macrophages which release proinflammatory mediators such as early cytokines, TNF-α and IL-β1, histamine and eicosanoids, as well as reactive oxygen species, which induce contraction of airway smooth muscle, mucous secretion, vasodilation and enhanced permeability. These changes maximize the recruitment of peripheral blood cells: eosinophils, basophils, neutrophils, lymphocytes, and monocytes into inflamed airways. The involvement of these cells initiates the late-phase reaction and results further in adhesive interactions between circulating inflammatory and microvascular endothelial cells via the production of proinflammatory mediators, cytokines, chemokines and the expression of cell surface adhesion molecules . These late-phase reactions represent the model for studying the mechanisms of chronic inflammation in asthma. In asthma, the airway wall is infiltrated with mononuclear cells and eosinophils. Eosinophilic inflammation is the characteristics for asthma and once eosinophils have been recruited to the respiratory tract, their activation leads to secretion of toxic products like eosinophilic cationic protein, neurotoxin and free radicals, but also growth factors, elastase, metalloproteases and cytokines. The release of these eosinophilic mediators results in vascular leakage, hypersecretion of mucus, smooth muscle contraction, epithelial shedding, and eventual irreversible airway hyperresponsiveness and also initiates the process of remodeling. Therefore, eosinophils are able to play an important part in both, boost of airway inflammation and remodeling . Other cells like T-cells, macrophages, neutrophils and mast cells are also variably increased in the inflamed airways. Mast cells localize within the bronchial smooth muscle in asthma. They secrete tryptase, histamine, prostaglandin (PG) D_2, leukotriene (LT) C_4, as well as numerous pro-inflammatory cytokines like IL-4, IL-5, IL-13, IL-6, TGF-β1 and TNF-α, which contribute to all features of asthma like bronchoconstriction, mucus secretion, mucosal oedemas and airway remodeling . The evidence of up-regulation of TNF-α in asthma suggests that mast cells, as a source of this cytokine, play an important role in initiating and maintaining the inflammatory response in asthma . Another study shows that mast cells both release and respond to TNF-α what indicates, that there is a positive autocrine loop which leads to augmentation of mast cell activation and further production of TNF-α and other cytokines . Therefore, TNF-α, as a potential mediator of severe asthma, serves nowadays as target for development of novel therapies applied in asthma .

As it is shown in Figure 1.2, not only migratory cells of the airways, such as lymphocytes, macrophages, but also resident cells like fibroblasts, epithelial cells and

even bronchial smooth muscle cells, are involved in pathological states such as asthma and become activated during acute inflammation.

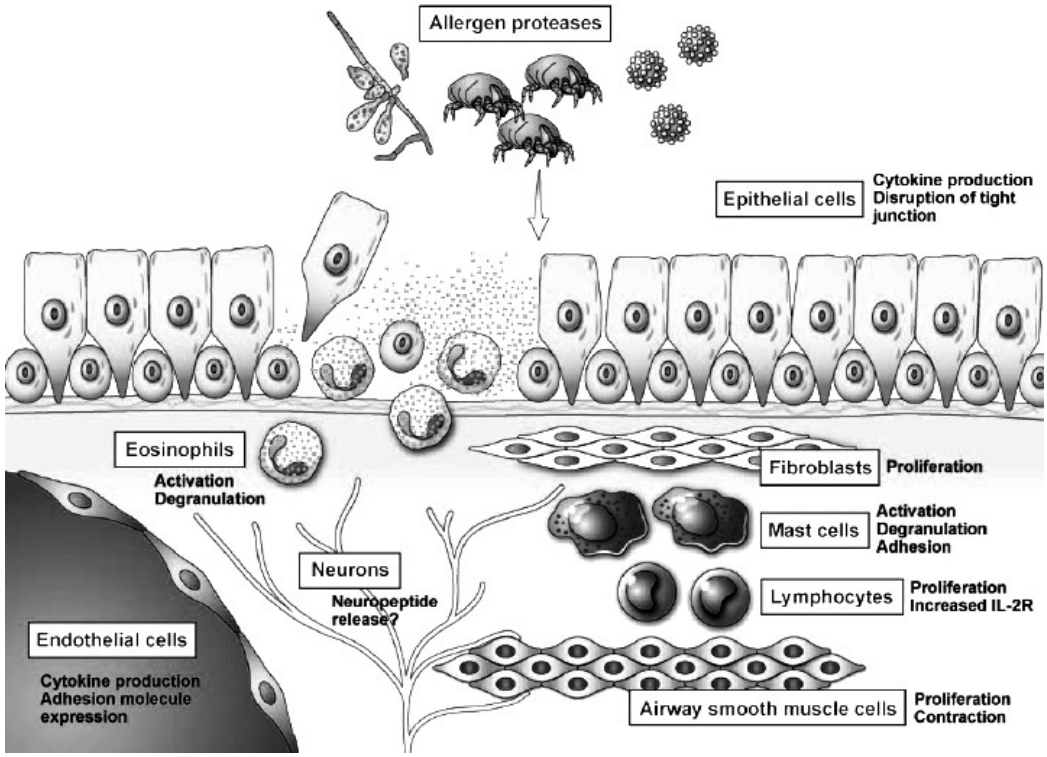

Figure 1.2: Network of inflammatory stimuli and responses in airways .

1.2.1 The involvement of epithelium in inflammatory processes in lung.

Epithelium was considered to act mainly as a natural physical barrier to external agents like bacteria, viruses and toxic substances participating in reactions protecting against injuries such as mucociliary clearance and removal of noxious agents. However, recently it has been shown that epithelial cells, in addition to the cells of the immune system, actively participate in inflammatory reactions . The epithelial surface regulates a variety of biologic reactions including protection against injuries and remodeling processes through the secretion of extracellular matrix proteins and the interaction with the other cells. Exposure of epithelial cells to deleterious factors like allergens, bacteria, pollutants, and to endogenous proinflammatory factors, such as the early cytokines interleukin-1β (IL-1β) and (TNF-α), triggers defence mechanisms and secretion of pro- and anti-inflammatory mediators including cytokines, growth factors and metalloproteases . Epithelial cells represent also a target for cytokines and growth factors acting in a paracrine manner.

1.2.2 The role of cytokines IL-8 and TGF-β1 in airway inflammation.

In general, cytokines are released by a variety of cells and play a highly important role in the immune system. They are produced mostly along with other cytokines in the patterns characteristic for particular organ dysfunctions. They are characterized by a wide pleiotropy (a single type of cytokine molecule can produce many diverse effects) and redundancy (overlapping functions, different cytokines can perform the same actions). Moreover, the effect of one particular cytokine may be influenced by other cytokines released simultaneously, inducing synergistic or antagonistic effects. Cytokines can induce the expression of receptors that may in turn change the properties of participating cells, stimulate their own synthesis or production of different cytokines, that can cause positive or negative feedback . One of the important members of the cytokine family is the chemokine interleukin-8. IL-8 is a secretory product of numerous cell types including monocytes, neutrophils, basophils, eosinophils, fibroblasts, alveolar macrophages, bronchial epithelial cells, airway smooth muscle cells (ASM). IL-8 is a potent chemo-attractant for neutrophils and comprises part of the inflammatory response induced by microbial infection. This chemokine mediates its effect through CXCR2 to picomolar IL-8 concentration and to higher concentrations of IL-8 through CXCR1 . The IL-8 production was highly up-regulated in patients with asthma, COPD and cystic fibrosis . Therefore elevated IL-8 was identified as a marker implicated in the development of airway inflammation. Moreover, elevated expression of IL-8 together with another cytokine, transforming growth factor-β1 (TGF-β1), has been observed in respiratory disorders. The release of both cytokines was enhanced in bronchiolar epithelium from smokers with COPD compared with those levels without COPD and in patients with asthma or microbiologically positive pneumonia . Furthermore, an increased activity of TGF-β1 was found in the lung of patients with chronic bronchitis when compared with healthy control subjects .

However, the action of TGF-β is very complex and not clear until now. TGF-β1 is a potent fibrotic cytokine and induces pulmonary fibrosis . In addition, TGF-β1 is an immunomodulatory cytokine. This factor seems to play a central role in regulating the balance between burst and resolution of inflammatory responses. The state of activation and differentiation of the target cells, the presence of other stimuli and the functional consequences of inappropriately large or small amounts of TGF-β1 are different at each site . For example, low concentrations of active TGF-β1 are required to maintain alveolar homeostasis and prevent the development of emphysema, whereas high concentrations

can induce emphysema, apparently through a pathway that involves apoptosis of alveolar epithelial cells . In response to lung injury, activation of TGF-β1 on the apical surface of the alveolar epithelium inhibits the increase in macrophage protease (MMP12) expression. At the same time, on the basolateral surface TGF-β1 induces production of collagen and other extracellular matrix proteins from alveolar fibroblast and contributes to influx of clotting factors and other proteins from the serum . Therefore it appears that TGF-β1 contributes to limiting the damage and initiating the process of alveolar repair. Furthermore, TGF-β1 is a chemoattractant for mast cells and is released by ASM after exposure to tryptase from mast cells and activation of PAR-2, providing a mechanism of an autoactivation loop involving smooth muscle, TGF-β1 and mast cells . Moreover, animal studies show that deficiency of the TGF-β1 gene in mouse causes a multifocal, inflammatory cell response and tissue necrosis, leading to organ failure and death . Delayed wound healing was observed in TGF-β1 immunodeficient mouse . Similarly, data from in vitro studies showed that TGF-β1 increases the speed of epithelial repair and even suppresses apoptosis . Thus, TGF-β1, a fibrogenic and immunomodulatory factor, plays multifunctional roles contributing to airway repair and remodeling and is involved in complex processes associated with the development of respiratory disorders like asthma .

1.3 PARs in respiratory disorders.

1.3.1 PAR agonists and inactivators in lung.

There are many potential PAR activators of endogenous as well as exogenous origin that can interact with PARs in airway tissue. Especially in the diseased lung, increased activity of potential biological activators of PARs has been detected. In acute and chronic inflammation, vascular leakage results in the accumulation of plasma proteins in the airways and activation of coagulation . The consequence is an increased activity of the coagulation protease thrombin, the main PAR-1 activator. Thrombin was found in bronchoalveolar lavage fluid (BALF) and in the sputum of asthmatic patients that was significantly higher than in non-asthmatic subjects . Increased thrombin activity was also

detected in BALF of patients with acute lung injury and chronic lung diseases with characteristics of pulmonary fibrosis .

Fibrinolysis-related proteases (plasmin, tissue plasminogen activator, urokinase) exhibit small effects on the uninflamed airways, but can be recruited into the lung during pulmonary oedema and inflammation . It has been shown that plasmin can display mitogenic effects via PAR-1 activation on lung fibroblasts .

The airways of patients with chronic airway diseases contain another PAR-2 activator, human trypsin-like protease (HAT) . The enzyme is localized to epithelial cells and is released into the airway wall during airway disease where it mediates regeneration and remodeling by stimulation of fibroblast proliferation through a PAR-2-mediated pathway .

Another well established activator of PAR-2, trypsin, co-localizes immunohistochemically in epithelial cells with PAR-2 . The ability of trypsin to activate PAR-2 as well as PAR-1 in the respiratory tract has been confirmed by *in vitro* studies. However, the knowledge about the action and importance of trypsin outside the pancreas, *in vivo* is still incomplete .

In the inflamed airways, there is also elevated activity of proteases secreted into the cellular space by migratory inflammatory cells, which have an effect on PARs. The asthmatic epithelium is characterized by mast cell infiltration and release of the potent PAR-2 activator tryptase upon cell degranulation . Similarly in nasal lavage fluid and in BALF tryptase levels were higher in asthmatics and patients with allergic rhinitis . Released into diseased airways, tryptase regulates homeostatic functions in lung by activating PAR-2, for example in fibroproliferative responses .

Various airway cells express other catalytically active proteases, like tryptase Clara, miniplasmin, but their ability to cleave PARs has not yet been determined . Relatively new findings show that MMPs can act via PARs . MMPs are actively secreted by the airway epithelium, alveolar macrophages, and neutrophils during airway inflammation and remodeling and can cleave biologically active peptides, such as endothelins and calcitonin gene-related peptide

There is increasing evidence that inhaled airborne allergens also play an eminent role in activation of respiratory PARs by contributing to elevated levels of proteases in airways. Recent reports show that the effect of airborne allergens from house dust mite faecal pellets or fungi stimulate the release of pro-inflammatory cytokines through the activation of PARs. As presented in Table 1.3, house dust mite allergen Der p 1, Der p 3

and Der p 9-induced release of proinflammatory cytokines from respiratory epithelial cells is, in part, mediated by activation of PAR-2 . Mold protease, Pen c 13, exhibits its proteolytic activity by cleavage of PAR-1 and PAR-2 in airway epithelial cells what mediates IL-8 release . The bacterial protease serralysin elicits inflammatory responses via PAR-2 in lung squamous cell carcinoma . On the contrary, bacterial proteases like thermolysin and *P. aeruginosa* elastase function as a disabling protease for PAR-1 and PAR-2, respectively . This may alter the host's innate defense mechanisms and respiratory functions.

Although proteolysis is the physiological mechanism for PAR activation, proteases can also inactivate receptors. Neutrophil proteases such as elastase, cathepsin G, proteinase-3, that contribute to chronic obstructive pulmonary disease, can inactivate PAR-1 and PAR-2 preventing activation of PARs by other proteases . Similarly, human PAR-3 is disabled by elastase and cathepsin G . On the other hand, neutrophil proteinase 3 can activate PAR-2 and cathepsin G activates PAR-4 .

The effect of all these proteases becomes notably important in diseases involving airway inflammation. When the level of these pro-inflammatory proteases of the immune system and coagulation-related proteases is elevated in the extracellular space, PARs can be activated. The consequences of PAR-mediated effects might have supplementary impact on the development of airway inflammation.

Concluding, several PAR agonists that are able to activate epithelial PARs occur in the airways, as summarized in Table 1.3. Thrombin, factor VIIa and Xa, originated from the blood circulation or proteases released by cells of the immune system e.g. tryptase have easy access to the airway epithelium during inflammatory reaction or disruption of the blood barrier. Even epithelial cells themselves are an important source of a PAR agonist, trypsin.

Table 1.3: Sources of proteases in lung and the PAR subtype activated by these proteases.

Protease	**Source**	**PAR subtype**
Thrombin	Blood	PAR-1, PAR-3, PAR-4
Trypsin	Epithelium	PAR-1, PAR-2, PAR-4
Mast cell tryptase	Mast cells, basophils	PAR-2
Factor Xa	Blood	PAR-1, PAR-2
Factor VIIa	Blood	PAR-2
Neutrophil proteinase 3	Neutrophils	PAR-2
Cathepsin G	Monocytes, neutrophils	PAR-4
HAT	Epithelium	PAR-2
MMP	Epithelium, alveolar	PAR-1

	macrophages	
Der p1, p3, p9	Dust mite	PAR-2
Serralysin	Bacteria	PAR-2
Pen c 13	Mold	PAR-1, PAR-2

1.3.2 Role of PARs in pathophysiology of lung tissue.

Many of the cellular effects of proteases have been shown to be mediated via activation PARs. All 4 PARs are widely distributed throughout the respiratory system and are present on nearly all cells involved in inflammatory states in human airways.

Activation of PARs modulates airway tone in vitro, but the functional response is dependent on the species examined, the cell and tissue type. For example, PAR-2 induces relaxation in isolated murine, rat and guinea pig bronchial rings and inversely, stimulates contraction in human bronchial rings . Moreover, activation of PARs on airway cells can stimulate proliferation and promote remodeling by stimulating the release of the mitogenic mediator platelet-derived growth factor (PDGF), MMP-9 or procollagen . PAR activation on fibroblasts, mast cells, eosinophils and epithelium may also stimulate the secretion of many pro-inflammatory mediators.

PARs are suggested to play an important role in inflammatory and fibroproliferative processes. Pulmonary fibrosis is characterized by rapid fibroblast proliferation and overproduction of extracellular matrix proteins. There is increasing evidence that especially PAR-1 plays a significant role in the development of proliferation through the involvement in collagen accumulation and expression of profibrotic factors .

The epithelium participates in regulation of repair processes through the secretion of extracellular matrix proteins. Moreover, the epithelium modulates airway smooth muscle tone by production of respective mediators and neurotransmitters. It has been shown *in vitro* that activation of PARs, especially PAR-2, was involved in these processes. PAR-2 mediates the release of the cytoprotective and relaxant prostanoid prostaglandin (PG) E_2, as well as the release of proinflammatory cytokines IL-6 and IL-8 in human primary epithelial cells or epithelial cell lines . PAR-2 activation induces the production of MMP-9, contributes to matrix remodeling . Epithelial PAR-2 has been shown to induce the production of eotaxin and granulocyte macrophage-colony stimulating factor (GM-CSF) which promotes eosinophil survival and recruitment .

Furthermore, PAR-2 activation in airway epithelial cells increased neutrophil adhesion to the cells and caused changes in ion transport .

PAR-2 is an extensively studied receptor in the context of participation in lung pathophysiology. However, the function of PAR-2 in lung biology is still unclear. Activation of PAR-2 has been documented also *in vivo* to induce both pro- and anti-inflammatory effects in animal models of inflammation, including studies with PAR-2-deficient mice. Activation of PAR-2 caused protective bronchial relaxation in airways, inhibited the development of eosinophilia and neutrophils influx into airways in LPS-treated or ovalbumin-sensitized mouse .

On the contrary, PAR-2 was shown to be involved in airway hyperresponsiveness and eosinophil recruitment in allergen-challenged mice .

However, the action of activated PARs may depend on the type of stimuli applied, the severity of pre-existing inflammatory status, the time point of PAR agonist administration, and finally, the types of PAR activated.

Some chronic lung diseases are frequently associated with changes in PAR protein expression as a result of modulation of gene expression by a variety of inflammatory mediators. For example, asthmatic bronchial epithelium showed significant increase in PAR-2 level, compared to the non-asthmatic tissue . In preterm infants with prolonged chronic lung injury PAR-2 immunoreactivity was significantly higher compared with newborn infants without pulmonary pathology . Pulmonary fibrosis is accompanied by increased PAR-1 on alveolar macrophages and fibroproliferative foci . Increased levels of PAR-2 mRNA were also detected in lung fibroblasts from fibrotic tissues . In alveolar macrophages from smokers PAR-1 but not PAR-2 expression is changed compared to that in healthy subjects . In animal models, LPS-induced inflammation and viral infection enhanced PAR levels and their responsiveness which is coupled to increased activation of COX and enhanced generation of bronchodilatory prostanoids .

However, there is limited information about particular mediators that are responsible for the modulation of PAR expression on airway cells. Studies on various cultured human airway cells showed different regulation of PAR expression by inflammatory mediators. In pulmonary artery endothelial cells, TNF-α induced the expression of PAR-2, but exerted no effect on the PAR-1 level . LPS and IL-1β were not able to modulate PAR-1 and PAR-2 expression in alveolar macrophages , while in smooth muscle cells IL-1β up-regulated PAR-2 . In pulmonary fibroblasts, profibrotic growth factors PDGF and TGF-β1 stimulated PAR-2 expression , the antifibrotic and

anti-inflammatory agent PGE_2 was able to down-regulate the expression of PAR-1, -2, and -3 . Interestingly, LPS and TNF-α in bronchial fibroblasts up-regulated PAR-2 expression and induced functional expression of PAR-4 .

Nevertheless, there is still limited information concerning particular factors, which are responsible for alteration of PAR levels in lung epithelial cells. Therefore the question is still open, which factors have the potential ability to enhance or diminish PAR-mediated cellular responses. Similarly, the current understanding of the effect of PAR agonists and the contribution to pro- or anti-inflammatory processes during airway disorders is incomplete. However, airway disorders, such as asthma and COPD, appear to be partially resistant to the currently available pharmacological agents. Hence, PARs might represent a useful subject for further investigation to provide a promising target for novel drugs for the treatment of various respiratory disorders .

1.4 Aims of the project and outline of the present study.

The main focus of this study was to investigate the involvement of PARs in inflammatory processes, which underlie airway disorders such as asthma.

In the human airways all four PARs (PAR-1 to -4) have been detected to be widely distributed throughout the respiratory system . The respiratory epithelium has the first contact with inhaled antigens acting not only as a physical barrier for inhaled infectious stimuli but actively participating in acute and chronic inflammatory reactions . Exposure of epithelial cells to deleterious factors, like allergens, bacteria, pollutants, and to endogenous proinflammatory factors, triggers defence mechanisms by modulation of expression and secretion of different bioactive molecules such as lipid mediators, cytokines, extracellular matrix proteins. Among many factors that are employed in these epithelial responses are PARs. Recent *in vitro* studies with cell lines clearly showed a strong impact of PAR activation in the lung epithelium on inflammatory responses and tissue . Although there are few studies giving clear evidence about the involvement of PARs in airway inflammation, their exact role in the pathophysiology of the respiratory system is still unclear. In our experimental study, investigations were conducted in vitro using lung epithelial cell lines and primary cells. Our model should mimic the inflammatory state in asthma and show the complex network between PARs, their agonists and inflammatory stimuli. This study should contribute to a better understanding of the involvement of PARs in lung disorders.

The outline of the present study is as follows (the points numbered 1) to 4) are indicated in Figure 1.3):

1) Determine whether inflammatory conditions induced by LPS, TNF-α, IL-8 and PGE_2 influence the PAR expression level.

2) Study if a persistent PAR activation and PAR activation combined with stimulation with LPS has influence on PAR expression.

3) Investigate if PAR activation stimulates production of cytokine TGF-β

4) Elucidate if PAR activation enhances IL-8 synthesis and whether LPS attenuates this process.

a) Evaluate the signaling pathway of PAR-induced IL-8 release. The focus is on three members of MAPKs, ERK1/2, JNK and p38.

i) Investigate whether PAR-3 activation also triggers IL-8 release and study whether MAPKs belong to the signaling pathway of this process.

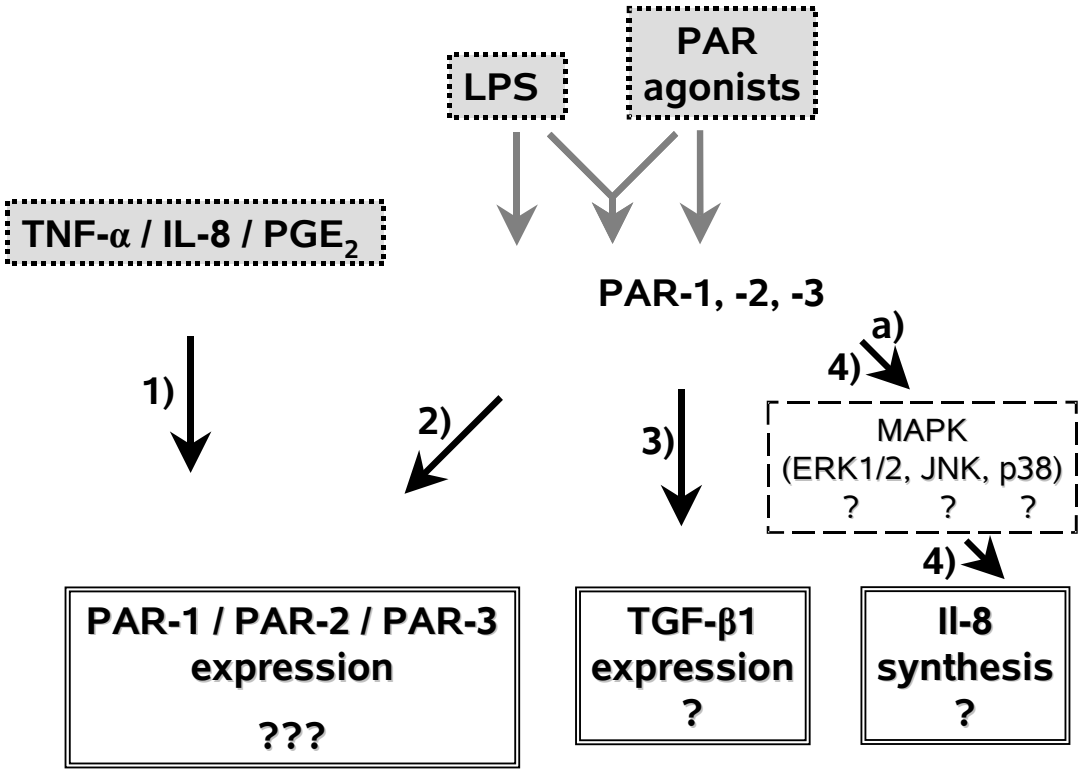

Figure 1.3: Simplified scheme for the outline of the present study. 1) to 4) are explained in the text above.

The outline of this study is shown in the scheme in Fig. 1.3. The aim of this work was to study how PAR activation alone and in combination with bacterial endotoxin LPS control the PAR expression level and production of cytokines in airway epithelium. To achieve these aims, the changes in PAR expression in lung epithelial cells exposed to inflammatory mediators as well as during persistent activation of PARs were determined. Additionally, the PAR-triggered synthesis of inflammatory mediators, such as IL-8 and TGF-β1 was explored. Pharmacological and biochemical tools, such as the use of selective inhibitors and western blot, were applied to investigate the PAR-mediated MAPK activation. An additional issue was the role and signaling mechanism of PAR-3, the most elusive receptor among PARs. HEK cells transfected with PAR-3-GFP served as experimental model for this purpose.

2 Materials and Methods

2.1 Materials

2.1.1 Chemicals and reagents

Chemicals	Manufacturer
SLIGKV (H-Ser-Leu-Ile-Gly-Lys-Val-NH_2)	Bachem, Heidelberg, Germany
GYPGQV (H-Gly-Tyr-Pro-Gly-Gln-Val-OH)	
Dulbecco's Modified Eagle's Medium (DMEM)	Biochrom, Berlin, Germany
Fetal calf serum (FCS)	
HBSS (w/o Ca^{2+} and Mg^{2+})	
Penicillin and Streptomycin	
HEPES	Biomol, Hamburg, Germany
Bio-Rad protein assay dye reagent concentrate	Bio-Rad Laboratories, München, Germany
Precision Plus Protein All Blue Standard	
TFRGAP (H-Thr-Phe-Arg-Gly-Ala-Pro-NH_2)	Biosyntan, Berlin, Germany
Ponceau S solution (0.2% in acetic acid)	Boehringer, Mannheim, Germany
Trypsin	
PD 98059	Calbiochem, La Jolla, CA, USA
SB203580	
SP600125	
U0126	
TNF-α	
IL-8	
Albumin Fraction V, Protease free	Carl Roth, Karlsruhe, Germany
Magnet assisted transfection (MATra)	IBA GmbH, Göttingen, Germany
NuPAGE® MOPS SDS Running Buffer (20x)	Invitrogen**,** Karlsruhe, Germany
NuPAGE® Transfer Buffer (20x)	
NuPAGE® LDS Sample Buffer (4x)	
SAGM™	Lonza, Verviers, Belgium
SABM™ (supplements for SAGM)	
100 bp DNA ladders	MBI Fermentas, St. Leon-Rot, Germany
TRag (Ala-pFluoro-Phe-Arg-Cha-HomoArg-Tyr-NH_2)	NeoMPS SA, Strasbourg, France
Accutase	PAA, Coelbe, Germany
TEMED	SERVA**,** Heidelberg, Germany
Triton-X-100	

Tween 20	SIGMA, Deisenhofer, Germany
Dimethyl sulfoxide (DMSO)	
β-mercaptoethanol	
Igepal CA630	
Thrombin	
Protease Inhibitor Cocktail	Roche Molecular Biochemicals, Mannheim, Germany
siRNA	Qiagen, Hilden, Germany

2.1.2 Kits

Type of kit	**Manufacturer**
BigDye Terminator Cycle Sequencing Read reaction Kit	Applied Biosystem, Foster City, CA, USA)
RNeasy Mini Kit	Qiagen, Hilden, Germany
Omniscript™ Reverse Transcription Kit	
RNase-Free DNase	
HotStarTaq™ Master Mix Kit	
MiniElute PCR Purification Kit	
iScript™cDNA Synthesis kit	Bio-Rad
iQ™SYBR® Green Supermix	
Supersignal West Pico kit	Pierce, Rockford, IL, USA
Interleukin 8 [(h)IL-8] Human, Biotrak ELISA System	Amersham Biosciences Freiburg, Germany
Transforming Growth Factor-Beta1 (TGF-β1) Human, Biotrak ELISA System	

2.1.3 Antibodies

Antibody	**Manufacturer**
mouse monoclonal anti-phospho-p44/42 MAPK (Thr202/Tyr204)	Cell Signaling Technology, Beverly, MA, USA
rabbit anti-p44/42 MAPK	
rabbit anti-phospho-JNK (Thr183/Tyr185)	
rabbit anti-JNK	
rabbit anti-phospho-p38 MAPK (Thr180/Tyr182)	
rabbit anti-p38 MAPK	
peroxidase-conjugated goat anti-mouse and anti-rabbit IgG	Dianova, Hamburg, Germany
WEDE15 (anti PAR-1)	Immunotech

Alexa Fluor®488 goat anti-mouse IgG and goat anti-rabbit IgG	Molecular Probes
H-103 (anti PAR-3)	Santa Cruz, Heidelberg, Germany
A5, polyclonal rabbit (anti PAR-2)	gift from Dr. M. Hollenberg, Calgary, Canada

2.1.4 Laboratory instruments

Instrument	**Manufacturer**
ABI PRISMTM 310 Genetic Analyzer	Applied Biosystems Division, Foster City, CA, USA
Hybond C	Amersham Biosciences Freiburg, Germany
Mighty Small II (for western blotting electrophoresis)	Amersham Pharmacia Biotech Buckinghamshire, UK
Waterbath	Bachofer, Reutlingen, Germany
T3 Thermocycler	Biometra, Göttingen, Germany
Electrophoresis power supply	Bio-Rad Laboratories, München, Germany
Gel electrophoresis system	
Semi-dry Transfer Cell	
Mini PROTEAN II (Tankblot)	
GS-800 Calibrated Densitometer	
Molecular Imager Gel Doc XR System	
Thermomixer comfort	Eppendorf
Biofuge A, 13 R, 3.2 RS (centrifuge)	Heraeus, Hamburg, Germany
LaminAir (clean bench)	
Cell culture incubator	
Refrigerator (4°C and –20°C)	Liebherr, Hamburg, Germany
Millipore purification system and ultra-pure water system	Millipore, Schwalbach, Germany
Innova 4230 Refrigerated incubator shaker	New Brunswick Scientific, Nürtingen, Germany
UV/visible Spectrophotometer	Pharmacia Biotech
Gel-blotting-papers	Schleicher & Schuell, Dassel, Germany
pH Meter (pH526)	WTW, Weilheim, Germany

2.1.5 Buffers and solvents

2.1.5.1 Cell culture medium and solutions

- **for A549 cells**- DMEM: 3.7 g/L NaHCO3, 1.0 g/L D-glucose, 1.028 g/L N-Acetyl Lalanyl-L-glutamine, 10 % FCS, 100 U/ml Penicillin, 100 µg/ml Streptomycin
- **for HEK-293 cells:** DMEM/HAM'S F12 (1:1) with 2 mM Glutamine, 10 % FCS, 100 U/ml Penicillin, 100 µg/ml Streptomycin
- **for HSAEC:** Small Airway epithelial medium (SABM) supplemented with growth factors (BPE, hydrocortisone, hEGF, epinephrine, insulin, trijodothyronine, transferrin, gentamicin/amphotericin-B, retinoic acid and BSA-FAF)
- HBSS (Hanck's balanced salt solution) without Ca^{2+} and Mg^{2+}
- Accutase
- G418 Sulphate - stock: 500 mg/ml, working concentration: 500 µg/ ml

2.1.5.2 Buffers and solutions

- NaHBS

  145 mM Na Cl, 5.4 mM KCl, 1 mM $MgCl_2$, 1.8 mM $CaCl_2$, 25 mM glucose, 20mM HEPES, pH 7.4 adjusted with Tris (hydroxymethyl) aminoethane
- 1 x PBS

  137 mM NaCl, 2.6 mM KCl, 8.1 mM Na_2PHO_4, 1.4 mM KH_2PO_4, pH 7.4
- 1 x TBS

  137 mM NaCl, 20 mMTris/HCl, pH 7.6
- 1 x TBE

  89 mM Tris, 89 mM Boric acid, 2 mM Na_2EDTA, pH 8.0
- 10 x MOPS

  0.2 M MOPS, 10 mM Na_2EDTA, 50 mM Na-Acetate, pH 7.0
- Ethidium bromide solution: 10 mg/ml
- 4 x Lysis buffer (RIPA buffer)

  50 mM Tris/HCl pH 7.4, 1 mM EDTA, 150 mM NaCl, 1% Igepal CA630, 0.25% Na-deoxycholate, 1mM Na_3VO_4, 1 mM NaF and Protease Inhibitor Cocktail
- 60 % Acrylamide/Bis-100 ml

  Acrylamid 58.4 % (w/v), 1.6 % (w/v) N,N'-Methylen-bisacrylamide
- Resolving buffer (SDS-PAGE-Laemmli)

750 mM Tris/HCl, pH 8.8

- Stacking buffer

  250 mM Tris/HCl, pH 6.8
- SDS solution: 10% (w/v) SDS in H_2O
- PER solution: 10% (w/v) Ammoniumperoxodisulfat in H_2O
- 4 x Laemmli Sample buffer

  500 mM Tris/HCl, pH 6.8, 8% SDS (w/v), 40% Glycerol, 0.005% Bromphenol blue (w/v), 20 % (v/v) β-Mercaptoethanol
- 5 x Laemmli Running buffer

  125 mM Tris, 960 mM Glycine, 0.5% SDS (w/v), pH 8.5
- 1 x Transfer buffer (for Laemmli gels with NC membrane)

  25 mM Tris, 192 mM, Glycine, 20% (v/v) Methanol
- Membrane Stripping buffer

  62.5 mM Tris, pH 6.8, 100 mM β-Mercaptoethanol, 2% SDS
- PFA 4 %

  4 g PFA, 120 mM Na-Phosphate pH 7.4, 4 g saccharose

2.2 Methods

2.2.1 RNA isolation

Total RNA was isolated from the cells with the RNeasy Kit (Qiagen Hilden). The medium was aspirated from the culture dish (6 cm) and the cells were lysed with 600 µl RLT buffer. Cells were homogenized completely by pipetting and to this homogenized suspension 600 µl 70 % ethanol were added and mixed well by pipetting for precipitating the RNA. Then 600 µl of the sample were applied to a RNAeasy mini spin column sitting in a 2-ml collection tube, and centrifuged for 1 min at 10,000 rpm. 350 µl Buffer RW1 were pipetted onto the RNeasy column, and centrifuged for 1 min at 10,000 rpm to wash lysate. Now On-column DNase digestion was performed to remove genomic DNA using the RNase-Free DNase Kit (Qiagen Hilden). 10 µl of DNase I stock solution were added (2.73 Kunitz units/µl) mixed in 70 ml Buffer RDD (DNase I incubation mix) directly onto the spin-column membrane and incubated at room temperature for 15 min. Next, 350 µl Buffer RW1 were pipetted into the column and centrifuged for 1 min at 10,000 rpm. The

RNeasy column was transferred into a new 2-ml collection tube and 500 µl Buffer RPE were pipetted onto the RNeasy column, centrifuged 1 min at 10,000 rpm and again 500 µl Buffer RPE were pipetted, centrifuged for 2 min at maximum speed to dry the RNeasy membrane. Finally, RNeasy column was transferred into a new 1.5 collection tube, and 30 µl RNeasy-free water were pipetted onto RNeasy membrane, incubated at room temperature for 10 min, and then centrifuged for 1 min at 10,000 rpm to elute. Isolated RNAs were stored at -80°C.

2.2.2 Reverse Transcription-Polymerase Chain Reaction (RT-PCR)

1 µg of total RNA was reverse-transcribed using Omniscript Reverse Transcription kit (Qiagen, Hilden). RT reaction was set as follows:

RNA	1 µg
RT Buffer (10 x)	2 µl
dNTP mix (5 mM each)	2 µl
Oligo-dT primer (0.5 µg/µl)	2 µl
Omniscript Reverse Transcriptase (4 U/µl)	1 µl
H_2O	ad 20 µl

RT was performed in T3 Thermocycler (Biometra). The reaction was incubated for 1 h at 37°C, followed by 5 min at 95°C and then rapidly cooled at 4°C.

PCR reaction was done using the HotStarTaq™ Master Mix kit (Qiagen, Hilden). The reaction mixture was pipetted as follows:

cDNA	1 µl
HotStarTaq Master Mix	25 µl
5‘ primer (10 pmol/µl)	2 µl
3‘ primer (10 pmol/µl)	2 µl
H_2O	ad 25 µl

The PCR reaction was made using the following program:

Lid temperature:	110°C		
Preheating:	On		
Initial denaturation:	95°C		15 min
35 cycles: Denaturation:	94°C		30 sec
Annealing:	variable		1 min 30 sec

Extension:	72°C	1 min
Final extension:	72°C	10 min
Pause:	4°C	

10 µl of reaction used for gel electrophoresis to check for the presence of the expected gene product.

2.2.3 Reverse transcription and real-time PCR

To reverse transcribe the isolated total RNA from the cultured cells iScript™ cDNA synthesis kit (BioRad) was used. RT reaction mixture was as follows:

RNA template	1 µg
iScript Reverse Transcriptase	1 µl
5 x iScript Reaction Mix	4 µl
Nuclease-free water	ad 20 µl

RT was done in T3 Thermocycler (Biometra). The reaction mix was incubated for 5 min at 25°C, followed by 30 min at 42 °C and 5 min at 85°C and subsequently cooled down to 4°C.

Real-time PCR is quantitative and qualitative online method, where the fluorescent emission increases when SYBR Green dye binds to the double stranded DNA. Quantification is achieved by measuring the increase in fluorescence during the exponential phase of PCR and comparing the C_t values of the samples of interest with control such as non-treated sample. Both C_t values are normalized to the hauskeeping gene GAPDH.

The specificity of the amplification was determined by generating melting curve profiles, where the total fluorescence generated by SYBR Green binding to double-stranded DNA as temperature changes is plotted in real time as a function of temperature. The melting temperature (Tm) of each product is defined as the temperature at which the corresponding peak maximum occurs. This analysis confirms the specificity of the chosen primers and reveals the presence of primer-dimers.

Real-time PCR was done using iQ™SYBR®Green Supermix (BioRad).The reaction mixture was pipetted as follows:

DNA template	1 µl
iQ SYBR Green Supermix	12.5 µl

5’ Primer (10 µM)	1 µl
3’ Primer (10 µM)	1 µl
Sterile water	ad 25 µl

The thermal cycling conditions included denaturation step at 95°C for 3 min, followed by 40 cycles at 94°C for 30 s, 60°C (PAR-1-3, IL-8, TGF-β1 and GAPDH) or 64°C (PAR-4) for 60 s, 72°C for 1 min and the final melting curve program with ramping rate of 0.5°C/s from 60°C to 95°C.

Primers were based on human PAR-1, PAR-2, PAR-3, PAR-4, IL-8, TGF-β1 sequence. At the same time, samples without templates served as negative control.

Primers sequences were used as listed below:

Primer	Sequence (5’→ 3’)	Product length (bp)
PAR-1	f: CGCCTGCTTCAGTCTGTGCGGC	405
	r: GGCCAGGTGCAGCATGTACACC	
PAR-2	f: GCCATCCTGCTAGCAGCCTCTC	341
	r: GATGACAGAGAGGAGGTCAGCC	
PAR-3	f: TTGTCAGAGTGGCATGGAA	451
	r: TGGCCCGGCACAGGACCTCTC	
PAR-4	f: CAGCGTCTACGACGAGAGCGG	423
	r: CACTGAGCCATACATGTGACCAT	
IL-8	f: CTAGGACAAGAGCCAGGAAG	237
	r: GTGTGGTCCACTCTCAATC	
TGF-β1	f: CAGAAATACAGCAACAATTCCTGG	185
	r: TTGCAGTGTGTTATCCCTGCTGTC	
GAPDH	f: TCCAAAATCAAGTGGGGCGATGCT	598
	r: ACCACCTGGTGCTCAGTGTAGCCC	

2.2.4 Agarose gel electrophoresis of DNA

To confirm the quality of DNA (PCR product, recombinant plasmid DNA, restriction analysis) 1% agarose (SIGMA) gel in 0.5 x TBE buffer was made. The gel was prestained with ethidium bromide (10 mg/ml) (SIGMA). DNA samples were prepared in 6 x loading buffer (containing bromophenol blue dye) (MBI Fermentas). Gel was run in 0.5 x TBE for 1 h at 80 V. GeneRuler 100 bp DNA Ladder (1 kb) (MBI Fermentas) was used. DNA bands were visualised under gel imaging system Molecular Imager Gel Doc XR System (Bio-Rad).

2.2.5 Agarose gel electrophoresis of RNA

Quality of isolated RNA was checked in a 1% agarose/MOPS (N-Morpholino-3-propansulphonic acid) gel. 0.1% DEPC-H_2O (diethyl pyrocarbonate water) was used for all the solutions required for RNA gel including the sample preparation. 3% Hydrogen peroxide (H_2O_2) was used for decontaminating the gel assembly. RNase-free agarose (SIGMA) gel was made in 1 x MOPS buffer. Gel was pre-stained with ethidium bromide (10 mg/ml). 200 ng of RNA were used with 6 x Loading buffer. Gel was run in 1 x MOPS buffer for 1 h at 80 V. 18S and 28S RNA bands were visualised under gel imaging system Molecular Imager Gel Doc XR System (Bio-Rad)

2.2.6 DNA Sequencing

For sequencing reaction, either 100 ng of cleaned PCR DNA or 1 µg of recombinant plasmid DNA used with 2 µl of respective primer (10 µM) and 4 µl Big dye (contains DNA polymerase, fluorescent dye-labelled dNTPs, buffer) (Applied Biosystems, Warrington, UK) were mixed with H_2O to a final volume of 20 µl. The PCR conditions were:

Denaturation: 98°C for 2 min

25 cycles:	Denaturation:	96°C for 30 sec
	Annealing:	55°C for 30 sec
	Extension:	60°C for 4 min + 25 sec increament/cycle
	Pause:	4°C

Sequencing PCR product was precipitated with sodium acetate and 70% ethanol and then resuspended in 25 µl of Template Suppression Reagent (TSR) buffer (ABI PRISM, Applied Biosystems Division, Foster City, CA, USA), denatured for 2 min at 95°C and then kept on ice for 2 min. The sequence of nucleotides was determined by a ABI PRISM™ 310 Genetic Analyzer.

2.2.7 Quantification of nucleic acids

The quantity of isolated DNA and RNA was measured by the UV absorption ratio 260 nm/280 nm in quartz cuvette (5.00 mm thickness) using an Ultrospec 2000 UV/visible spectrophotometer (Pharmacia Biotech, Freiburg, Germany).

2.2.8 Cloning

2.2.8.1 Generation of DNA insert by PCR

To clone a particular DNA fragment into plasmid vector for generating a recombinant plasmid, PCR was done to amplify the full coding sequence of the gene. PAR-3 fragment was amplified with PCR (30 cycles: 30 sec at 94°C, 1 min at 51°C, 2 min at 72°C and 10 min at 72°C) using a primer pair flanking the entire coding region (designed on published human PAR-3 sequence in the Genbank; Accession number: U92971) and XhoI / HindIII restriction sites (underlined):

Sense: 5'-GTCATCCTCGAGAAAATGAAAGCCCTC-3'

Antisense: 5'-ATTTCACTAAAGTCTTTTTTGTAAGGTAAGC-3'

For cloning the full cDNA, the stop codon was mutated in the 3'primer when cloned into a vector with a 3' detection tag. 1 µl of cDNA used for generating the required cDNA fragment with 2 µl of each primer (10 µM) using the Hotstar Taq Master Mix kit. The amplified PCR product (length 1140 bp) was loaded on the agarose, cut out from the gel, purified with Concert Rapid Gel Extraction Kit (Gibco BRL) and digested with XhoI /HindIII enzymes; cleaned again to remove digestion buffer with Concert Rapid PCR purification kit (Gibco BRL), quantified and ligated into pEGFP-N1 vector (BD Biosciences Clontech, Germany). The DNA specificity was confirmed by sequencing.

2.2.8.2 Plasmid isolation from bacteria (mini-preparation)

Plasmid DNA from transformed bacteria was harvested using the Invisorb Spin Plasmid Mini Kit (Invitek, Berlin). E. coli culture (single colony) was grown under appropriate antibiotic selection (here: kanamycin) in 3 ml LB media overnight at 37°C with shaking at 250 rpm. Overnight grown culture was centrifuged, supernatant was removed and pellet was resuspended in 200 µl of Solution I by vortexing. Next, 250 µl of Solution II were added, mixed carefully followed by application of 250 µl of Solution III mixing and centrifugation step. The clarified supernatant was decanted into the Spin Filter; 200 µl of Binding Solution were added to the filled Spin Filter and centrifuged. 750 µl of Wash Buffer PL were added, centrifuged 2 times for complete removal of residual Wash Buffer PL. The Spin Filter was placed into a new Receiver Tube and allowed the Spin Filter to air dry for 1 min for complete removal of ethanol in Wash Buffer. Then Elution Buffer was added directly onto the membrane of Spin Filter,

incubated at room temperature for 10 min. and finally centrifuged to recover the plasmid DNA.

2.2.8.3 Plasmid DNA isolation from bacteria (midi-preparation)

Plasmid DNA from transformed bacteria was harvested using the HiSpeed Plasmid Midi Kit (Qiagen, Hilden). 50 ml of overnight grown transformed bacteria culture was centrifuged and bacterial pellet was resuspended in 4 ml of Buffer P1 containing RNase A. 4 ml of Buffer P2 were added, mixed and incubated at room temperature for 5 min. Then 4 ml of chilled Buffer P3 were added, mixed immediately but gently and poured into the barrel of the QIAfilter Midi Cartridge; incubated at room temperature for 10 min to allow precipitation of protein and genomic DNA at the top of the solution. In the mean time 4 ml of Buffer QBT were applied to equilibrated a Qiagen-tip 500 and allowed the column to empty by gravity flow. Then the cap was removed from the QIAfilter outlet nozzle and inserted the plunger into the cartridge and the cell lysate was filtered. The Qiagen-tip was washed with 2 x 10 ml Buffer QC and placed in a fresh falcon tube. Plasmid DNA was eluted with 5 ml of Buffer QF, precipitated with 3.5 ml of Isopropanol (room temperature) and centrifuged immediately for 30 min at 5000 rpm. Supernatant was discarded and DNA pellet was washed with 2 ml of 70% ethanol and centrifuged for 10 min at 5000 rpm. Again supernatant was discarded carefully and pellet was allowed to air-dry. Dried DNA pellet was redissolved in TE.

2.2.8.4 Isolation of DNA fragment from agarose gel

To isolate DNA fragment (PCR product) from agarose gel, Concert Rapid Gel Extraction Kit (Gibco BRL) was used. The area containing the DNA fragment was cut from the gel and 30 µl of Gel solubilization buffer (L1) for every 10 mg of gel was added. The gel slices were dissolved in buffer at 50°C and placed into a 2.0 ml cartridge. Next, centrifuged for 1 min at maximum speed; discarded the flow-through; 500 µl of Solubilization buffer (L1) were added and centrifuged again; the flow-through was discarded; 700 µl of Wash buffer (L2) (containing ethanol) were added and incubated for 5 min at room temperature and finally centrifuged at maximum speed to remove residual wash buffer The cartridge was placed into a 1.5 ml recovery tube, pre-warmed TE buffer (70°C) was added, incubated for 10 min at room temperature and then centrifuged for 2 min at 12,000 rpm.

2.2.8.5 Cleaning of DNA fragment

DNA fragments after PCR amplification and restriction digestion were cleaned using the Concert Rapid PCR Purification kit (Gibco BRL). The Binding Solution (H1) was added to the amplification reaction in ratio 4:1 and sample mix was applied into the cartridge in wash tube and centrifuged. The next steps were: washing with 700 µl of Wash Buffer (H2) (containing ethanol) and multiple centrifugations to remove the residual wash buffer. Then the cartridge was placed into a 1.5 ml recovery tube; pre-warmed TE buffer (70°C) was added, incubated for 10 min at room temperature and then centrifuged.

2.2.8.6 Hydrolysis of DNA with restriction endonucleases

DNA digestion was performed as follows:

DNA	5 µg
Enzyme 1 (10 U/µl) (Xho)	2 µl
Enzyme 2 (10 U/µl) (Hind III)	2 µl
Buffer (10x) (Y+/Tango)	2 x
H_2O	ad 30 µl

Incubation time: 10-12 h at 37°C

After restriction, reaction mix was purified using Concert Rapid PCR Extraction kit (Gibco BRL). DNA was quantified as described above.

2.2.8.7 Ligation of plasmid and DNA

To generate recombinant plasmid, digested plasmid (pEGFP-N1) was ligated with the DNA insert (PAR-3) using the T4 DNA Ligase (Gibco BRL).

Plasmid vector (EGFP-N1)	1 x
DNA insert (hPAR-3)	3 x
T4 DNA Ligase (1 U/µl)	1 µl
Ligase buffer (5x)	4 µl (1x)
H_2O	ad 20 µl

Ligation was done in (T3) Thermocycler (Biometra) using following reaction conditions:

8 h	16°C
4 h	22°C
2 h	37°C
Pause	4°C

Ligation mixture was then used to transform bacteria to generate recombinant plasmid.

2.2.8.8 Transformation of E. coli by heat-shock method ($CaCl_2$ based)

For transformation of E. coli, DH5α strain was used. Cells were grown in 5 ml LB media overnight at 37°C with shaking at 250 rpm. 1 ml of overnight bacterial culture was then transferred to 100 ml of fresh LB media and continued to grow at 37°C with shaking till the cells reached their logarithmic phase i.e., OD 600= 0.3-0.4 (3-4 hours). Then the bacterial suspension was centrifuged at 6000 rpm in SS 34 Rotor in Sorvall centrifuge (pre-cooled) for 5 min at 4°C. Supernatant was discarded and cell pellet was resuspended in 10 ml of ice-cold 100 mM $CaCl_2$ solution. The cell suspension was then incubated on ice in cold room (4°C) for 1 h and centrifuged for 5 min at 6000 rpm at 4 °C. Supernatant was discarded carefully and pellet was resuspended in 1 ml of ice-cold 100 mM $CaCl_2$ containing 30% glycerol. From this competent cell suspension aliquots of 200 µl were frozen in liquid nitrogen and stored at -80°C.

To transform bacteria, 200 µl of $CaCl_2$ competent cells were thawed on ice. To the cells 100 µl of cold TCM buffer were added and either 10-20 ng DNA of super-coiled plasmid or 20 µl of ligation mix. Next transformation reaction mix was incubated on ice for 20 min and then for 90 sec at 42°C (heat –shock) and then immediately incubated on ice for 1 min. 700 µl of LB media (pre-warmed at 37°C and without any antibiotic) were added to transformation mix and incubated for 30-60 min with shaking at 37°C. 100 µl of the transformation mixture in case of super-coiled DNA plated on the LB-agar plate containing suitable antibiotic. For ligation transformation, reaction mix was centrifuged briefly, supernatant discarded and pellet resuspended in the residual volume and plated on LB-agar containing suitable antibiotic. LB-agar plates incubated at 37°C.

2.2.9 Cell culture

The medium for culturing of cells was sterile and ready to use (Biochrom). Cells were incubated in cell culture incubator (Heraeus) in a humidified atmosphere of 95% air, 5% CO_2 at 37°C. A549 cells (ATCC, Wesel, Germany) were cultured in DMEM (Dulbecco minimum essential medium) and HEK-293 cells (ATCC, Wesel, Germany) in DMEM/HAM'S F12 (1:1) supplemented with heat inactivated 10% FCS (fetal calf serum), 100 U/ml penicillin and 100 µg/ml streptomycin (Biochrom). Primary human small airway epithelial cells (HSAEC) (Cambrex, Walkersville) were grown in Small Airway Cell Basal Medium (SABM) supplemented with growth factors and antibiotics according to the manufacturer's instructions. HBE cells (provided by Prof. Dr. L. Pott,

Inst. für Physiologie, Ruhr-Universität Bochum, Germany) were cultured in DMEM Ham's F-12 (1:1) culture medium supplemented with gentamicin (50 µg/ml), kanamycin (50 µg/ml), ITS (10 µg/ml), hydrocortisone (1 µM), pituitary extract (3.75 µg/ml), EGF (25 ng/ml), T3 (30 nM), cholera toxin (10 ng/ml). Culture medium was changed every 2-3 days. For cells passage A549, HSAE and HBE cells were washed with HBSS and then incubated with Accutase (PAA) for 3 min at 37°C to detach the cell from the dish bottom. Accutase was used to minimize proteolytic activation of PARs. HEK-293 cells were washed and resuspended with HBSS.

2.2.9.1 Lipotransfection

To express a fusion protein in mammalian expression system, recombinant plasmid was transfected into mammalian HEK-293 cell lines using the Liposomal transfection reagent DOTAP (Roche Diagnostic). Plasmid DNA was isolated using the Invisorb mini plasmid kit (Invitek, Berlin) to obtain clean DNA. Cells were grown 60-80% confluent. In one tube 5 µg of DNA were diluted up to 50 µl with 20 mM HEPES, in another tube 30 µl DOTAP were mixed with 70 µl of 20 mM HEPES. Then DNA-HEPES solution was mixed with DOTAP-HEPES solution and incubated for 30 min at room temperature. The culture media was replaced with fresh medium without serum and antibiotic. Transfection mix containing DNA-DOTAP-HEPES was pipetted carefully into the dish. Cells were incubated in the transfection media for 12 h and then full medium containing serum and antibiotic was given to cells. The cells were visualised under the fluorescent microscope to confirm the expression of fusion protein in case of vector containing GFP tag (GFP fusion protein showed green fluorescence). To maintain stable transfected cells, selection antibiotic G418 Sulphate antibiotic (kanamycin and neomycin derivative) (Calbiochem) was applied.

2.2.9.2 Magnet assisted Transfection (MATra)

The cells were transfected with siRNA using Magnet Assisted Transfection for adherent cells (MATra-A) reagent. Cells were grown 50-60% confluency on 21.5 cm^2 dish. 100 nM siRNA was diluted in 400 µl serum-free medium and mixed with 6 µl MATra-A Reagent and incubated at RT 20-30 min. Beads-mixture was applied to the cells with 3.5 ml medium without serum. The cells were placed immediately on the Magnet Plate. After incubation for 15 min, Magnet Plate was removed and medium changed to fresh one.

siRNA was synthesized by Qiagen (Hilden, Germany). The sequences of human PAR-1 siRNA were as follows: sense 5'-GGGACUGCUGGGAGGUUAA-3'; antisense 5'-UUAACCUCCCAGCAGUCCC-3' and the DNA target sequence: AAGGGACTGCTGGGAGGTTAA. As control siRNA served AllStars negative control siRNA.

2.2.9.3 Freezing and thawing of cells

Cells were frozen in DMSO and FCS for long storage when not required in the culture. Briefly, cells resuspended in 0.5 ml medium were frozen in cryo tube together with 50 µl DMSO (sterile) and 450 µl FCS (fetal calf serum) at –20°C for 24h.Then shifted to –80°C for long storage or liquid nitrogen.

Cryo-preserved cells were quickly thawed in 37°C and cell suspension was dispensed into 9 ml of complete cell culture medium, centrifuged at 1000 rpm for 3 min at room temperature. Cell pellet was resuspended in appropriate medium and transferred into culture dish.

2.2.10 Protein chemistry

2.2.10.1Cell lysate

Serum-starved cells were treated with agonists for the respective time needed. After stimulation, cells were rinsed with ice-cold phosphate-buffered saline (PBS) and lysed in 1 ml of modified RIPA Buffer. Cell lysate was gently rotated for 30 min at 4°C and centrifuged at 14,000 g for 15 min at 4°C. Supernatant was transferred into a fresh tube and pellet discarded. The protein concentration was determined by the Bradford method using bovine serum albumin as standard. Lysates were stored at –80°C.

2.2.10.2SDS-PAGE and immunoblotting

The cell lysate was prepared as described above. Samples containing equal amounts of protein were precipitated with ice cold acetone/methanol solution (1:1), denatured in Laemmli sample buffer system, loaded to SDS-PAGE gels and electrophoresed for 1.30 min at 120 V. Samples were transferred to nitrocellulose membrane (0.2 µm) using semi-dry transfer system (Biorad) at constant voltage (10 V) and 200 mA for 60 min at room temperature. Membranes were stained for protein bands with 0.2% Ponceau S and then blocked in 3% BSA (bovine serum albumin) for 1 hour.

Membranes were incubated overnight at 4°C with phospho-p44/42 MAPK (1:2000), phosho-JNK (1:2000), phosho-p38 MAPK (1:1000), washed three times in TBST-Tween (0.1%) (30 min total), followed by incubation with horseradish peroxidase-conjugated anti-rabbit IgG or anti-mouse IgG (1:10,000) (Dianova, Hamburg) for 60 min at 25°C. Washing step was repeated. Bands were visualized by enhanced chemiluminescence (Amersham Biosciences). To reprobe the membrane with second primary antibody the membranes were washed in TBS-Tween (0.1%), incubated in stripping buffer for 30 min at 55°C, washed extensively in TBS-Tween, blocked in 3% BSA and finally re-probed with anti-p44/42 MAPK (1:1000), JNK (1:1000), p38 MAPK (1:1000) antibody. Washing step was repeated in TBS-Tween (0.1%) (30 min total), followed by incubation with secondary antibody peroxidase-conjugated anti-rabbit IgG or anti-mouse IgG (1:10,000) (Dianova, Hamburg) for 60 min. at 25°C. Quantification of the bands densities was carried out using a GS-800 calibrated densitometer and Quantity One software (Bio-Rad).

2.2.11 IL-8 protein determination

According to the manufacturer's protocol, extracellular IL-8 protein was measured using IL-8 ELISA kit. Briefly, serum-starved A549 cells were stimulated with TRag, thrombin, PAR-2 AP alone or together with LPS for 24 h. HEK-293 used in our studies were treated with TRag or thrombin for 6 h. Then supernatants were collected for ELISA analysis. The levels of IL-8 were assayed at an optical density (OD) of 450 nm. For inhibitor studies, cells were pretreated with the inhibitors for 30 min prior to stimulation with agonists.

2.2.12 Immunocytochemistry

A549 cells cultured on coverglass were washed three times with cold PBS, incubated with primary antibodies against PAR-1, PAR-3 (20 µg/ml) or with rabbit antiserum against PAR-2 (dilution 1:50) at 4°C for 1 h, washed three times in PBS and incubated with secondary antibodies conjugated to Alexa Fluor ® 488 (5-10 µg/ml) at 4°C for 1 h. Controls were made by omitting the primary antibodies. The cells were visualized with a LSM510 meta confocal laser scanning microscope (Carl Zeiss, Germany).

2.2.13 Cytosolic Ca^{2+} measurements

The cells grown on a coverslip were removed from culture dish and placed in 1 ml HEPES-buffered saline (HBS) for 30 min at 37°C, supplemented with 2 µM Fura-2-AM

(dissolved in DMSO). Loaded cells were transferred into a perfusion chamber with bath volume of about 0.2 ml and mounted on an inverted microscope (Zeiss, Axiovert 135). During the experiments the cells were continuously superfused with buffer heated to 37°C. Single cell fluorescence measurement of $[Ca^{2+}]_i$ were performed using an imaging system from TILL Photonics GmbH. Regions of interest were selected before the experiment started. Cells were excited alternatively at 340 nm and 380 nm for 30-100 ms at each wavelength with a rate of 0.33 Hz and the resultant emission was collected above 510 nm. Images were stored on a personal computer and subsequently the changes in fluorescence ratio (F_{340}/F_{380}) were determined from selected regions of interest covering single cell.

The general principles of the measurement are based on the fact, that there are two forms of Fura-2 in equilibrium solution: Ca^{2+}-free and Ca^{2+}-binding Fura-2. Although showing great similarity in emission spectra, they are different in their excitation spectra: if the Ca^{2+}-Fura-2 complex is excited at 340 nm, the increasing of free Ca^{2+} concentration leads to an increased fluorescence at 510 nm. If the Ca^{2+}-Fura-2 complex is excited at 380 nm, increasing Ca^{2+} concentration leads to a decreased fluorescence at 510 nm. Therefore the ratio of fluorescence at the two wavelengths is directly related to $[Ca^{2+}]_i$.

2.2.14 Confocal imaging

Images were taken on a Zeiss inverted LSM510 meta laser scanning confocal microscope equipped with a Plan-Apochromat x63 objective. The GFP was excited using a 488 nm argon/krypton laser, and the emitted fluorescence was detected with a 505-530 band pass filter. Images were processed with Zeiss confocal microscopy software, release 3.2.

2.2.15 Analysis of fluorescence intensities

Fluorescence intensities of confocal images were analyzed using the Zeiss LSM 510meta software histo macro. Region of interests (closed free-shape curves surrounding ca. 60 μm^2) were set on the membrane of single cells and the average fluorescence intensity in the ROI was determined. The intensity values for the treated cells were normalized to untreated cells, which were set as 100%.

2.2.16 Statistics

Statistical evaluation was done using the Student's t-test, and ANOVA with Dunnett post test (compare all columns vs control column) and $P<0.05$ was considered significant. Data are given as mean values ± standard error of the mean (SEM).

3 Results

3.1 Expression of the PARs in A549 cells and other lung epithelial cells.

3.1.1 Detection of PARs by RT-PCR.

The gene expression of four subtypes of PARs was investigated by RT-PCR analysis using total RNA from A549 cells. Specific primers were used to amplify PAR-1, PAR-2, PAR-3 and PAR-4 mRNA. Simultaneous detection of GAPDH was used as an internal control of RT-PCR analysis. The use of intron-flanking primers excluded the possibility of genomic DNA amplification. As shown in Figure 3.1A, RT-PCR analysis revealed the presence of mRNA transcripts for PAR-1, PAR-2 and PAR-3 in A549 cells, giving PCR products of 405 bp, 341 bp and 451 bp long, respectively. A PCR fragment corresponding to PAR-4 (423 bp) was not detected. However, the possible appearance of the PAR-4 PCR signal was unambiguously confirmed using a plasmid containing the full length DNA of human PAR-4. In two other airway epithelial cells, human bronchial epithelial cells (HBE) and human small airway epithelial cells (HSAEC) we could determine the presence of PAR-1 and PAR-2 transcripts.

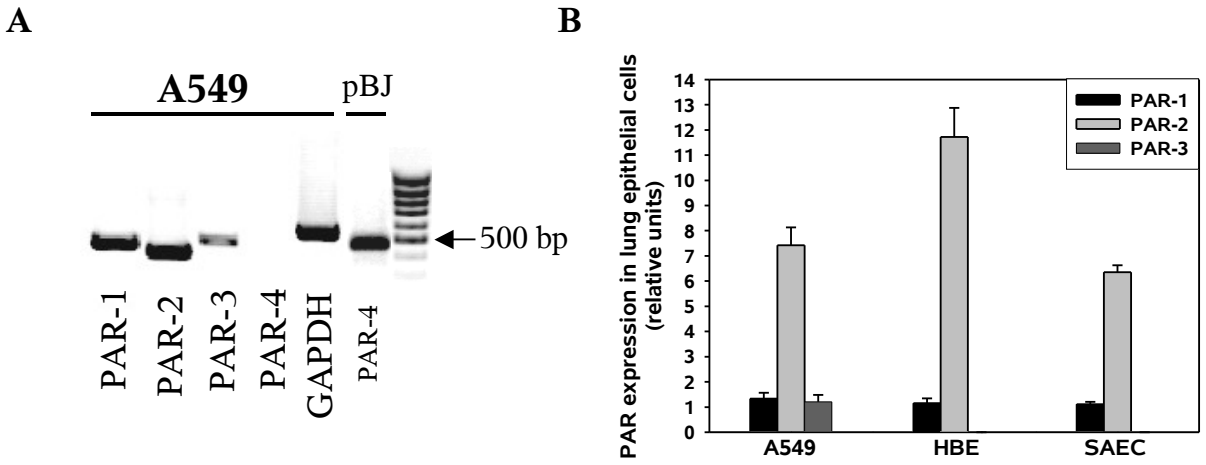

Figure 3.1: RT-PCR detection of PAR-1-4 in A549 cells in comparison with HBE cells and SAEC. A: RT-PCR analysis of PARs in A549 cells. Amplified PCR product was loaded on 1% agarose gel prestained with ethidium bromide (10 mg/ml). **B:** Quantification of PAR expression levels in A549, HBE and HSAE cells by real-time PCR. Measurements were normalized to the GAPDH mRNA level. The values given are means ± SE of three independent measurements. PAR expression levels are expressed relative to the PAR-1 mRNA expression in A549 cells, which was chosen as a reference value of 1.

With the help of real-time PCR, the PAR mRNA level in all three epithelial cells, A549, HBE and HSAEC, could be determined (Fig. 3.1B). Quantification of the relative abundance of PARs showed the predominance of PAR-2 mRNA in all cells tested. In

A549, HBE cells and HSAEC PAR-2 expression levels were 7, 12 and 6 times higher than the respective PAR-1 transcript level. PAR-3 expression level in A549 cells was comparable to the PAR-1 transcript level, whereas in HBE and HASEC it was not significantly above the threshold value. Similar to A549, also HBE cells and HSAEC expressed no PAR-4. Relative amounts of PAR transcripts were calculated by normalization to the housekeeping gene GAPDH.

3.1.2 Detection and localization of PARs by immunocytochemistry.

To confirm the expression of PARs in airway epithelial cells on protein level and to determine receptor localization, immunostainig of the cells was performed using antibodies against N-terminal parts of PAR-1, PAR-2 and PAR-3. Figure 3.2 shows the representative pictures for PAR-1, PAR-2, and PAR-3 where fluorescence staining is clearly visible on the cell plasma membrane.

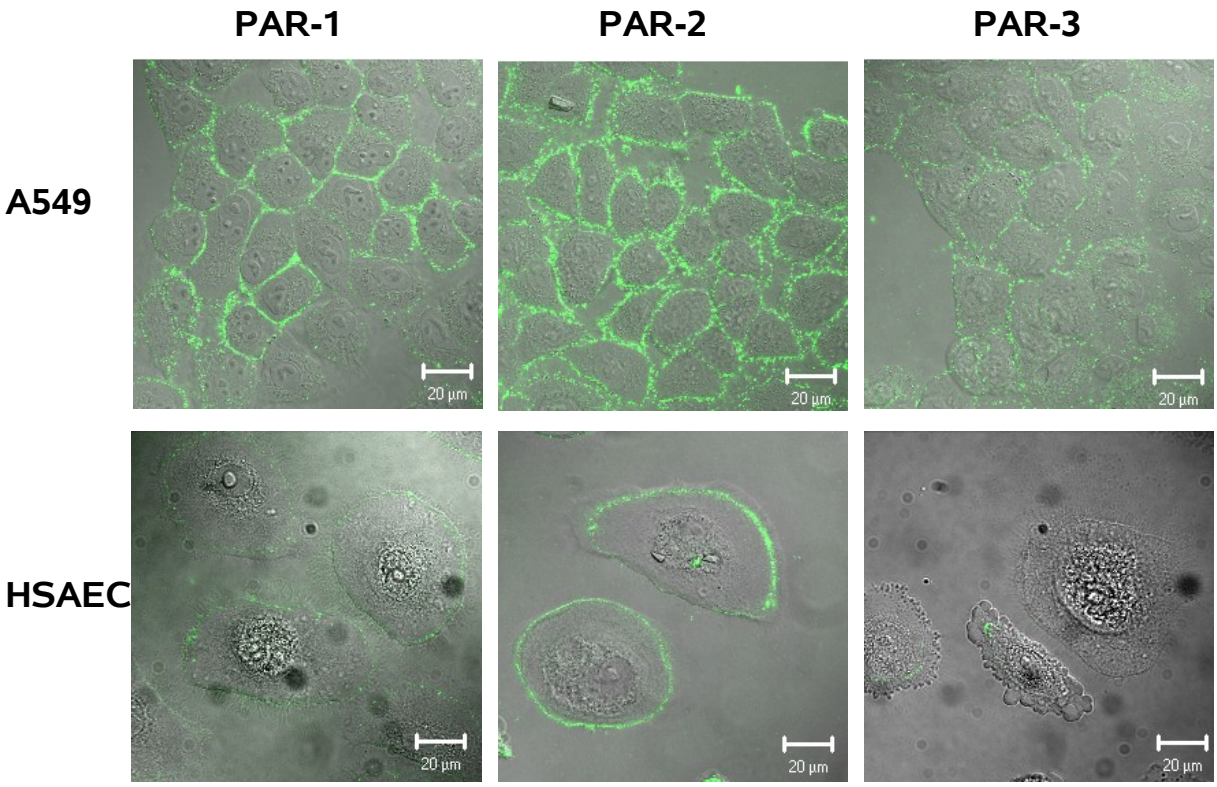

Figure 3.2: PAR localization in human airway epithelial cells. PAR detection and localization was determined by immunofluorescent staining. A549 cells (upper panel) and HSAEC (lower panel) were incubated with antibodies directed against PAR-1, PAR-2 and PAR-3. PAR localization was visualized by staining with secondary antibodies conjugated with the fluorescent dye Alexa Fluor ® 488. Images are representative for three different experiments.

Immunostaining with antibodies against N-terminal parts of PAR-1, PAR-2 and PAR-3 confirmed the presence of these three PAR proteins on the plasma membrane of

A549 cells (Fig. 3.2, upper panels) and PAR-1 and PAR-2 in HSAEC (Fig. 3.2, lower panels), and in HBE cells (data not shown). The fluorescence staining for PAR-1 was always weaker than that for PAR-2 and was hardly detectable on some portions of the cells. This is consistent with the low transcript level of PAR-1. The negative controls in this study, where we used only secondary antibody, yielded no detectable labeling (data not shown).

3.1.3 PAR agonist-mediated mobilization of Ca^{2+} in A549 cells.

PARs are G protein-coupled receptors and hence mobilize intracellular Ca^{2+}. To provide evidence for functional expression of PARs on A549 cells we examined the effect of PAR agonists on intracellular calcium concentration, $[Ca^{2+}]_i$. As shown in Figure 3.3, short-term application of the synthetic PAR-1-activating peptide, TRag (Ala-pFluoro-Phe-Arg-Cha-HomoArg-Tyr-NH_2) (5 µM) or the PAR-1 and PAR-3 agonist thrombin (5 U/ml) induced a comparable transient increase of $[Ca^{2+}]_i$ in the A549 cell line (Fig. 3.3A, C) and primary HSAEC (Fig. 3.3B, D), and comparably in the HBE cell line (data not shown). All three cell lines demonstrated high heterogeneity in terms of Ca^{2+} response to TRag even within the same experiment. The PAR-1 activating peptide induced a $[Ca^{2+}]_i$ elevation only in a small number of cells while the majority of the cells remained unresponsive. Moreover, only at concentrations of 5 µM and higher, TRag produced a Ca^{2+} response in epithelial cells. This can be due to the low density of PAR-1 on the cell surface that was shown immunocytochemically (Fig. 3.2) and which might be not sufficient for stable Ca^{2+} signaling. Similarly to TRag, thrombin induced a heterogeneous Ca^{2+} response in HSAEC, whereas in A549 cells an elevation of $[Ca^{2+}]_i$ was observed for all cells. This may be due, in A549 cells, to the expression of another thrombin receptor, PAR-3. A transient elevation of $[Ca^{2+}]_i$ was achieved also after application of the synthetic PAR-2-activating peptide SLIGKV (200 µM) (Fig. 3.3E, F). In contrast to PAR-1 AP, PAR-2 AP always induced stable Ca^{2+} responses in all epithelial cells tested. This reflects the high level of PAR-2 expression. Application of the synthetic PAR-3 peptide (TRFGAP-NH_2) and PAR-4 peptide (GYPGQV) did not induce any effect in all three cell line even when used up to 500 µM (data not shown). However, it is important to note, that the effectiveness and specificity of the PAR-3 peptide is still controversial . Taken together, we can conclude that PAR-1 and PAR-2 are functionally expressed in lung epithelial cell lines A549, HBE and primary HSAEC and PAR-2 is the main functional receptor in terms of Ca^{2+} signaling.

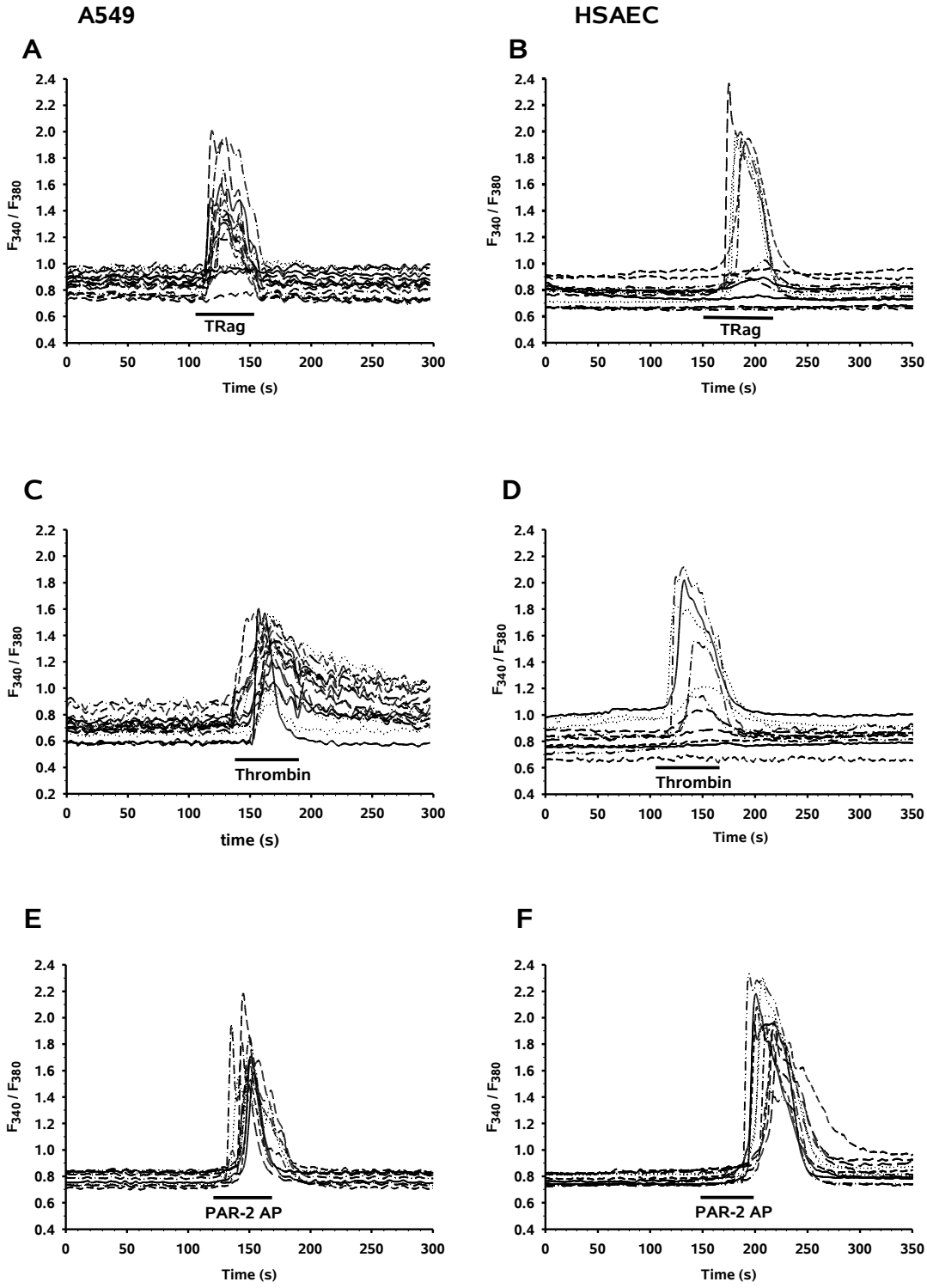

Figure 3.3: Rise of intracellular calcium concentration ($[Ca^{2+}]_i$) in human airway epithelial cells induced by PAR agonists. Ca^{2+} responses elicited in A549 cells **(A, C, E)** and primary HSAEC **(B, D, F)** by the PAR agonists TRag, thrombin and PAR-2 AP. The fura-2 AM-loaded cells were exposed to 5 µM TRag, 5 U/ml thrombin or 200 µM PAR-2 AP for 60 s, as shown by the horizontal bar. The increase in $[Ca^{2+}]_i$ is indicated by the change in the measured fluorescence ratio (F_{340}/F_{380} nm). The traces give responses of individual cells from one experiment. The pictures are representative for at least three different experiments.

3.2 Evaluation of PARs activation by trypsin isoforms in airway epithelial cells.

Previous results have described that bovine pancreatic trypsin caused $[Ca^{2+}]_i$ signaling in particular through the activation of PAR-2 in the epithelial cell lines . To determine whether human trypsin isoforms could also activate PAR-2, we tested the ability of all three human trypsin isoforms, cationic, anionic trypsin and mesotrypsin, to cause $[Ca^{2+}]_i$ elevation in A549 lung epithelial cells. The cells were exposed to recombinant trypsins for 60 s, which is sufficient time to produce the peak amplitude of Ca^{2+} responses for any given concentration of PAR agonists (as it was shown in Fig. 3.3).

The purity and homogeneity of the samples of recombinant human cationic trypsinogen (PRSS1), anionic trypsinogen (PRSS2) and mesotrypsinogen was confirmed as described before . The activity of the three trypsin isoforms was comparable when measured on turnover of the fluorogenic substrate Boc-Glu-Ala-Arg-7-amido-4-methylcoumarin.

Figure 3.4 represents typical Ca^{2+} responses in A549 cells elicited by the same concentration (10 nM) of cationic trypsin (A), anionic trypsin (B) and mesotrypsin (C). These data are also representative for HBE cells (data not shown). These cells produced similar Ca^{2+} responses as the A549 cells. Cationic and anionic trypsins caused $[Ca^{2+}]_i$ elevation comparable to that produced by the application of commercial bovine trypsin, whereas mesotrypsin was completely ineffective. Concentrations up to 400 nM mesotrypsin which is approximately 4-fold higher than the saturating concentration of trypsin for PAR-2 activation in human lung epithelial cells were not able to elicit $[Ca^{2+}]_i$ signaling. Additional pulses of commercial bovine trypsin, given 3 min after the mesotrypsin applications were applied to find out whether mesotrypsin is able to influence the PAR responsiveness. The amplitude of the subsequent Ca^{2+} responses to bovine trypsin was not affected, suggesting that mesotrypsin was ineffective with respect to both PAR activation and PAR receptor disabling. Thus, it is possible that mesotrypsin, in contrast to cationic and anionic trypsin isoforms, cannot activate or disable PARs in human epithelial cells.

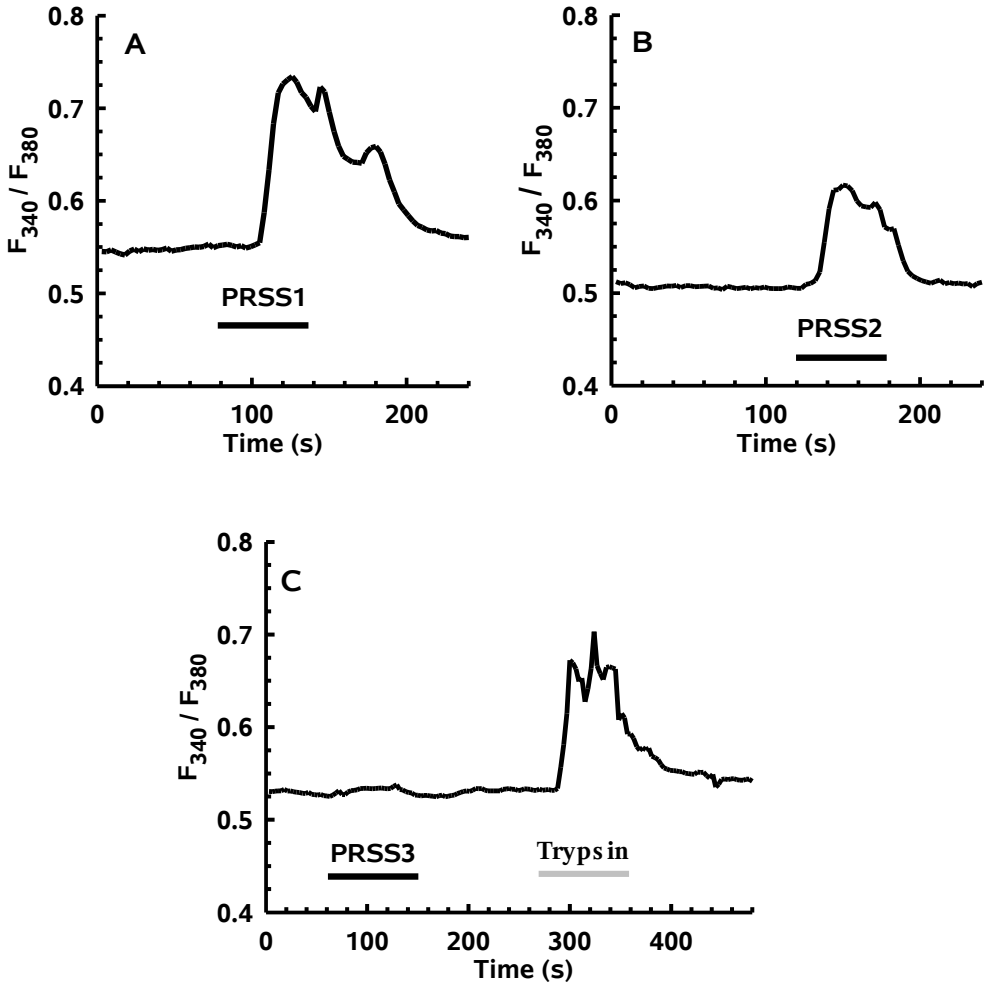

Figure 3.4: Rise of intracellular calcium concentration ($[Ca^{2+}]_i$) in A549 cells induced by different isoforms of human recombinant trypsin. The fura-2 AM-loaded cells were exposed to 10 nM cationic trypsin (PRSS1) (A), 10 nM anionic trypsin (PRSS2) (B), 10 nM mesotrypsin (PRSS3) followed by 10 nM bovine trypsin (C) for 60 s, as indicated by the horizontal line, and the changes in fluorescence ($\Delta F_{340\ nm}/F_{380\ nm}$) were detected. The traces are the mean of minimally 25 single cells measured in one experiment and are representative for at least three different experiments.

HBE cells were used to characterize the ability of the respective trypsin isoforms to induce Ca^{2+} responses. The data for the concentration dependence of the response amplitude (peak change of the ratio above basal level) allowed to determine that the effectiveness of cationic trypsin was similar to that of commercial bovine trypsin. The latter had already been characterized before in HBE cells . As shown in Figure 3.5, anionic trypsin was 20-30% less effective than cationic one. Analysis of the concentration-effect curves revealed similar parameters for both trypsin isoforms, an EC_{50} value of about 5 nM and 6 nM for cationic and anionic trypsin, respectively. The response maximum was obtained at about 10 nM.

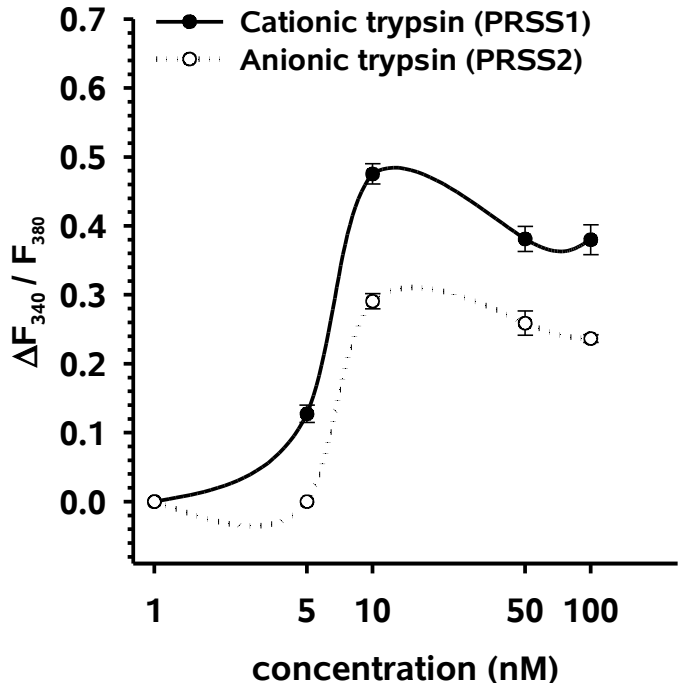

Figure 3.5: Concentration-effect curves for recombinant human trypsin isoforms inducing $[Ca^{2+}]_i$ rise in human HBE cells. The fura-2-AM loaded cells were stimulated with varying concentrations of the cationic or anionic trypsin and the change in fluorescence ($\Delta F_{340\ nm}/F_{380\ nm}$) was detected. Data represent the mean ±s.e. from 70 single cells obtained in at least three separate experiments. SE from a minimum of 25 single cells measured in at least 3 different experiments (in some cases the error bars are smaller in size than the symbols used).

The next aim was to prove that the recombinant human trypsin isoforms cause $[Ca^{2+}]_i$ signaling in particular through the activation of PAR-2 in the epithelial cells. This was established in the epithelial cell lines with bovine pancreatic trypsin before . For this purpose we tested whether the Ca^{2+} responses produced by the trypsin isoforms were influenced by PAR-2 desensitization. We achieve this by PAR-2 activation with its specific agonist, PAR-2 AP. The results are shown in Figure 3.6. The quantitative analysis of the responses produced by cationic and anionic trypsin is shown by the two first grey bars, marked as “contr”, with the respective patterns. The responses due to stimulation with both trypsin isoforms as a second pulse, following the exposure of the cells to PAR-2 AP (response marked as black bars) is presented as a group of three bars in the middle and on the right. The cytosolic Ca^{2+} release produced by cationic or anionic trypsins after treatment of the HBE cells with high concentrations of PAR-2 AP was significantly decreased as compared to the control measurement. After PAR-2 desensitization with 600 μM PAR-2 AP, the effect of both cationic and anionic trypsins was reduced up to 4-5 times.

These data confirm that cationic and anionic trypsin cause $[Ca^{2+}]_i$ elevation in human lung epithelial cells mainly through PAR-2 activation.

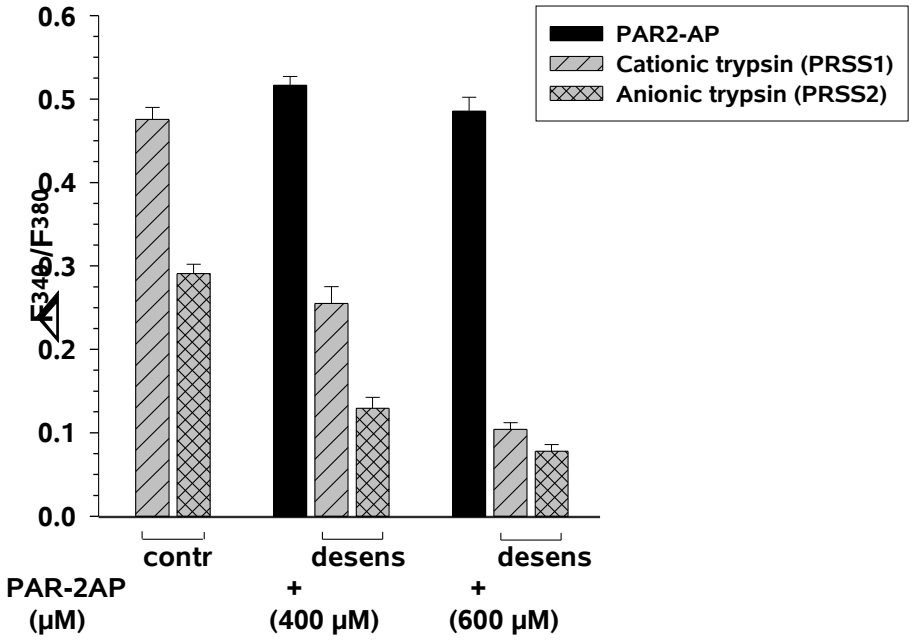

Figure 3.6: Effect of PAR-2 desensitization induced by PAR2-AP on cationic and anionic trypsin isoforms-mediated Ca^{2+} responses in HBE cells. Control cells were not exposed to the peptide before the protease addition (left group of columns). HBE cells were treated with 400 or 600 µM PAR-2 AP (black bars) followed by the application of 10 nM of cationic or anionic trypsins. The amplitude values of the Ca^{2+} responses are given as means ± SE from a minimum of 50 single cells measured in at least 3 different experiments.

3.3 Modulation of PAR expression and synthesis of cytokines by exposure of the cells to inflammatory mediators and / or PAR activation.

3.3.1 Effect of inflammatory mediators on the expression of PARs, IL-8 and TGF-β1 in A549 cells.

To examine the influence of different inflammatory mediators on the PAR expression, the cells were incubated with proinflammatory agents LPS, TNF-α, and IL-8 for 4 h and 24 h and then the mRNA level for each PAR was determined by real-time PCR analysis. As it is shown in Figure 3.7A, exposure of A549 cells to LPS (10 µg/ml) for 4 h induced significant up-regulation of PAR-2 expression, about 1.8-fold above control ($P<0.01$). After 24 h of incubation the value returned to basal level. LPS did not influence PAR-1 and PAR-3 expression levels. TNF-α (20 ng/ml) induced up-regulation of PAR-1, PAR-2 and PAR-3 transcript levels only after the long-term stimulation of 24 h (1.6, 1.7, and 1.4 fold, respectively (Fig. 3.7B). Unlike LPS and TNF-α, IL-8 (2 ng/ml) induced only slight down-regulation of the three PARs by 25-30% with a significant

effect for PAR-2 mRNA. This effect developed only after long-term stimulation for 24 h and appeared only when the low concentration (2 ng/ml) was tested (Fig. 3.7C). Higher concentrations (20 and 200 ng/ml) exhibited no effect (data not shown).

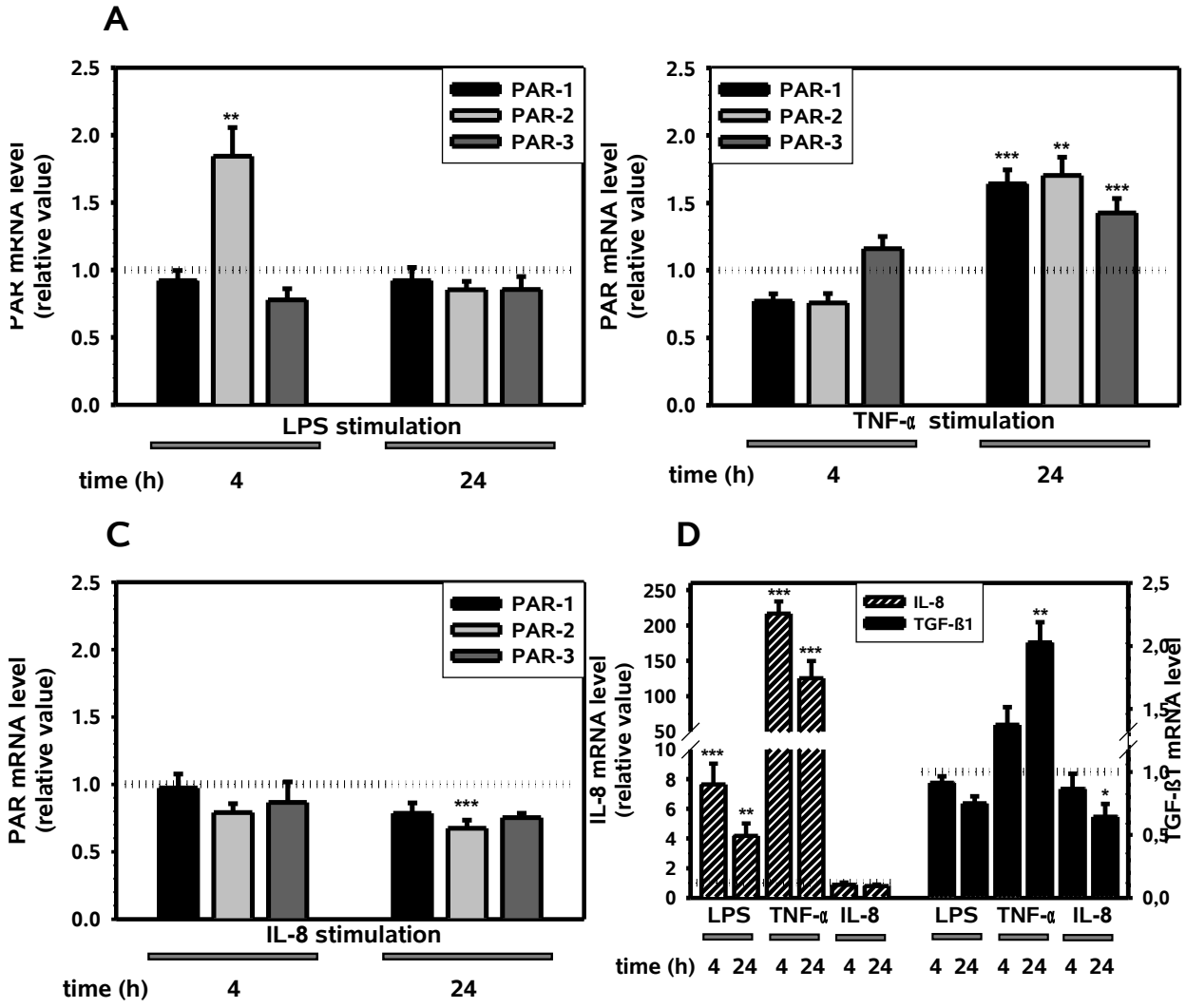

Figure 3.7: Effect of LPS, TNF-α and IL-8 on the expression of PARs, IL-8 and TGF-β1 in A549 epithelial cells. Changes in PAR mRNA levels after incubation with 10 µg/ml LPS (A), 20 ng/ml TNF-α (B) or 2 ng/ml IL-8 (C) as well as corresponding changes in IL-8 and TGF-β1 mRNA levels (D) for the time periods indicated below the graphs were estimated by real-time PCR. Modulation of mRNA expression was calculated using GAPDH as a reference gene. Data are means ± SE of three independent experiments. Dotted line at "1" indicates control level. Grey bars point on used agonist. $^{***}p<0.001$, $^{**}p<0.01$, $^{*}p<0.05$ as compared with the untreated cells.

To ascertain the action of these inflammatory mediators, we also measured changes in the expression of the proinflammatory chemokine IL-8 and the immunomodulatory agent TGF-β1 (Fig. 3.7D). TNF-α induced a robust increase (200-fold) of the IL-8 transcript level as early as 4 h after addition of the agent, and this effect was retained up to 24 h. This finding is consistent with a previous report . Compared to TNF-α, LPS

induced smaller, but significant up-regulation of IL-8 expression (7.5 fold), whereas IL-8 did not affect the expression of its own gene. Expression of TGF-β1 was not changed upon LPS stimulation of A549 cells, while TNF-α induced a significant (2-fold) up-regulation. IL-8 had no effect at 4 h and slightly down-regulated the TGF-β1 expression after 24 h of stimulation.

When A549 cells were stimulated with the anti-inflammatory agent PGE_2 (500 nM), a biphasic effect of PGE_2 on PAR expression levels could be observed during the period of incubation (Fig. 3.8A).

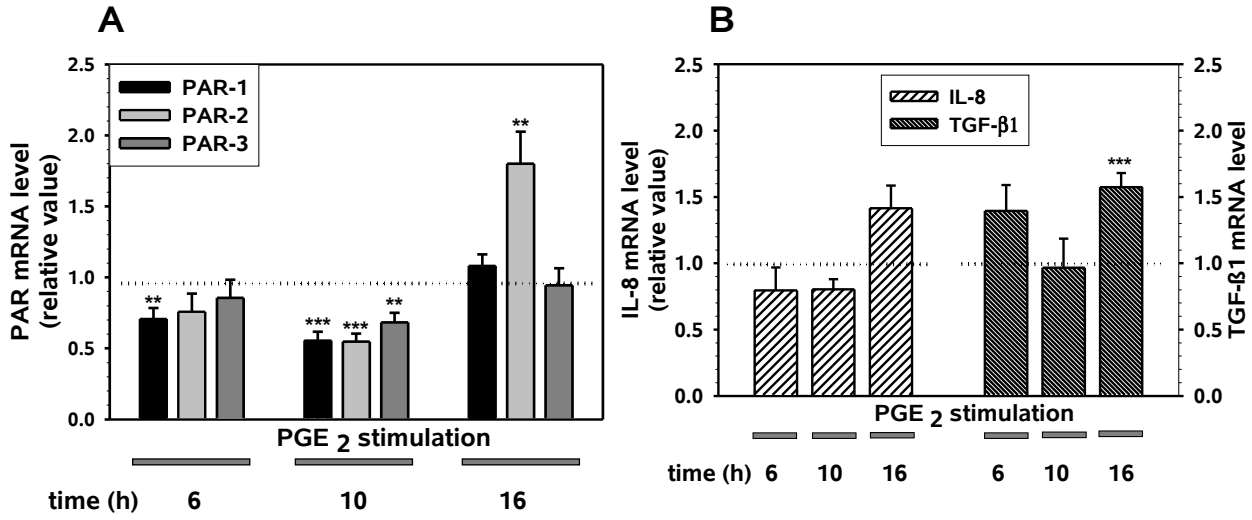

Figure 3.8: Effect of PGE_2 on the expression of PARs, IL-8 and TGF-β1 in A549 epithelial cells. Changes in PAR, IL-8 and TGF-β1 mRNA levels after incubation with 500 nM PGE_2 after 6, 10 and 16 hours was estimated by real-time PCR. Modulation of mRNA expression was calculated using GAPDH as a reference gene. Data are means ± SE of three independent experiments. Dotted line at "1" indicates control level. Grey bars below the graphs indicate the agonist used. $^{***}p<0.001$, $^{**}p<0.01$, as compared with the untreated cells.

PAR-1 to -3 mRNA levels were down-regulated significantly by 40-50% after 10 h of incubation with PGE_2, while 16 h stimulation with this prostanoid caused significant ($P<0.01$) up-regulation of the PAR-2 mRNA level (1.8-fold). Short-term (3 h) and long-term (24 h) stimulations with PGE_2 did not alter the PAR expression levels (data no shown). PGE_2 did not affect the expression level of IL-8 during the complete period of incubation, whereas it slightly increased the TGF-β1 mRNA level, but only after 16 h of incubation (Fig. 3.8B).

3.3.2 Modulation of PAR, IL-8 and TGF-β1 expression by continuous PAR activation in A549 cells.

Next, the effect of continuous PAR activation on PAR expression was examined. Stimulation with the PAR-1 agonist TRag (5 µM) for 4 h did not affect PAR-1 expression

but slightly up-regulated the PAR-2 level by 1.5-fold (Fig. 3.9A). Longer stimulation (24 h) resulted in significant up-regulation of PAR-1 and PAR-2 mRNA, by 1.5- and 2-fold, respectively ($P<0.01$). Surprisingly, thrombin (5 U/ml), also a PAR-1 agonist, reproduced the effect of TRag only in case of PAR-2 after 24 h of incubation.

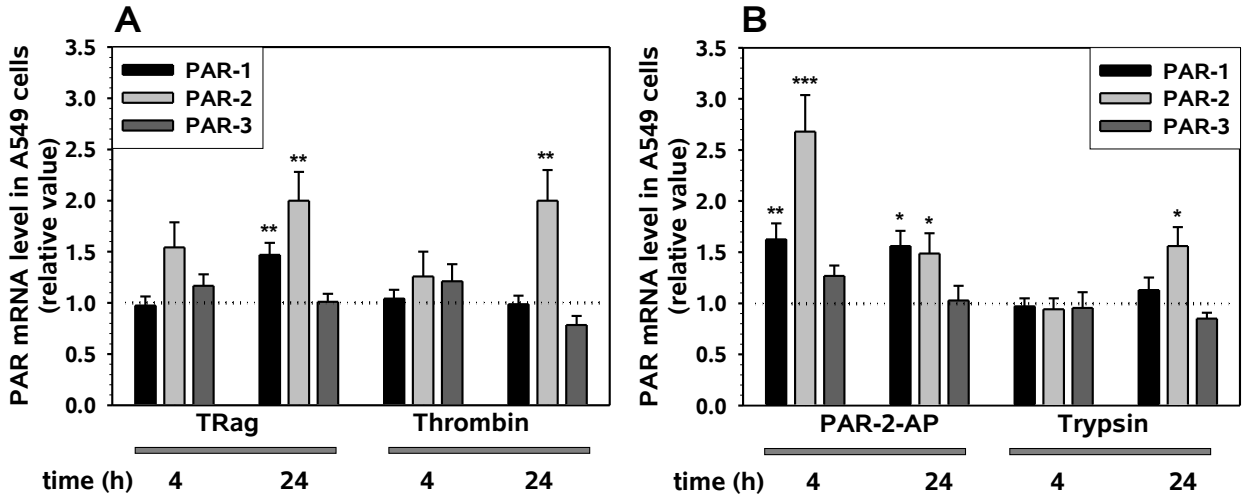

Figure 3.9: Modulation of PAR expression by PAR agonists in A549 cells. Changes in PAR mRNA level after treatment with PAR-1 agonists (5 µM TRag or 5 U/ml thrombin) (*A*) or with PAR-2 agonists (200 µM PAR-2 AP or 10 nM trypsin) (B) for times indicated were estimated by real-time PCR. Modulation of mRNA expression was calculated using GAPDH as a reference gene. Data are means ± SE of three independent experiments. Dotted line at "1" indicates control level. Grey bars point on used agonist. $^{***}p<0.001$, $^{**}p<0.01$, $^{*}p<0.05$ as compared with the untreated cells.

Activation of PAR-2 by PAR-2 AP for 4 h up-regulated PAR-1 and PAR-2 mRNA levels (Fig. 3.9B). The PAR-2 level was influenced more than that of PAR-1 (2.8 vs. 1.8 fold, $P<0.01$). After 24 h of stimulation with PAR-2 AP, the transcript level for PAR-1 remained elevated while that of PAR-2 tended to decline, but was still significantly higher than the control level ($P<0.05$). Trypsin induced only PAR-1 mRNA up-regulation after 24 h of stimulation. All the agonists tested did not affect the PAR-3 expression level.

Taken together, in A549 cells, PAR-2 is the most strongly affected receptor in terms of regulation of its expression after activation of the various PARs. To support this observation, the studies of PAR-2 mRNA expression changes were extended to HBE cells. As shown in Figure 3.10A, like in A549 cells, stimulation of HBE cells with the PAR-1 agonists TRag and thrombin induced slight up-regulation of the PAR-2 level. Activation of PAR-2 using activating peptide significantly increased its own mRNA level after 4 h as well as after 24 h of exposure (Fig. 3.10B).

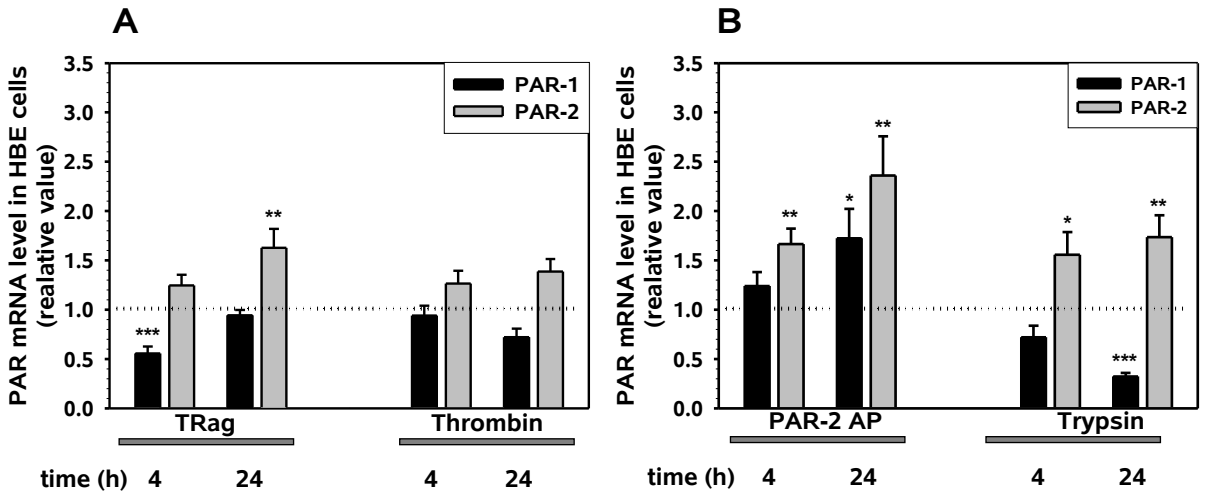

Figure 3.10: Modulation of PAR-2 expression by PAR agonists in HBE cells. Changes in PAR mRNA level after treatment with PAR-1 agonists (5 µM TRag or 5 U/ml thrombin) (*A*) or with PAR-2 agonists (200 µM PAR-2 AP or 10 nM trypsin) (B) for times indicated were estimated by real-time PCR. Modulation of mRNA expression was calculated using GAPDH as a reference gene. Data are means ± SE of three independent experiments. Dotted line at "1" indicates control level. Grey bars point on used agonist. $^{***}p<0.001$, $^{**}p<0.01$, $^{*}p<0.05$ as compared with the untreated cells.

In HSAEC, stimulation with TRag and thrombin did not exhibit significant effects on PAR mRNA level. Only exposure of the cells to PAR-2 AP induced up-regulation of PAR-2 mRNA level up to 1.7-fold (data not shown).

In summary, PAR-1 and PAR-2 activation on epithelial cells induced up-regulation of PAR-1 and more prominently PAR-2 expression. The PAR-2 activator showed higher effects than the PAR-1 activators.

3.3.3 The influence of concomitant stimulation with PAR agonists and LPS on PAR expression in A549 cells.

Next, we studied how PAR expression might be affected by simultaneous treatment of A549 cells with both, the inflammatory mediator LPS and PAR agonists. This combination of stimuli may reflect the pathological situation *in vivo* when both, proinflammatory mediators, e.g. from pathogens, and PAR-activating proteases are present in the airways at elevated levels. Incubation of A549 cells with LPS together with the PAR-1 agonist (TRag) for 4 and 24 h diminished or completely abolished the up-

regulation of PAR-1 and PAR-2 (Fig. 3.11A, B), induced by the stimulation only with TRag, as shown above in Figure 3.10A.

Addition of thrombin together with LPS caused an effect similar to that induced by TRag together with LPS. Application of PAR-2 AP in combination with LPS completely abolished the up-regulation of PAR-1, which was induced when PAR-2 AP was applied alone (Fig. 3.11A).

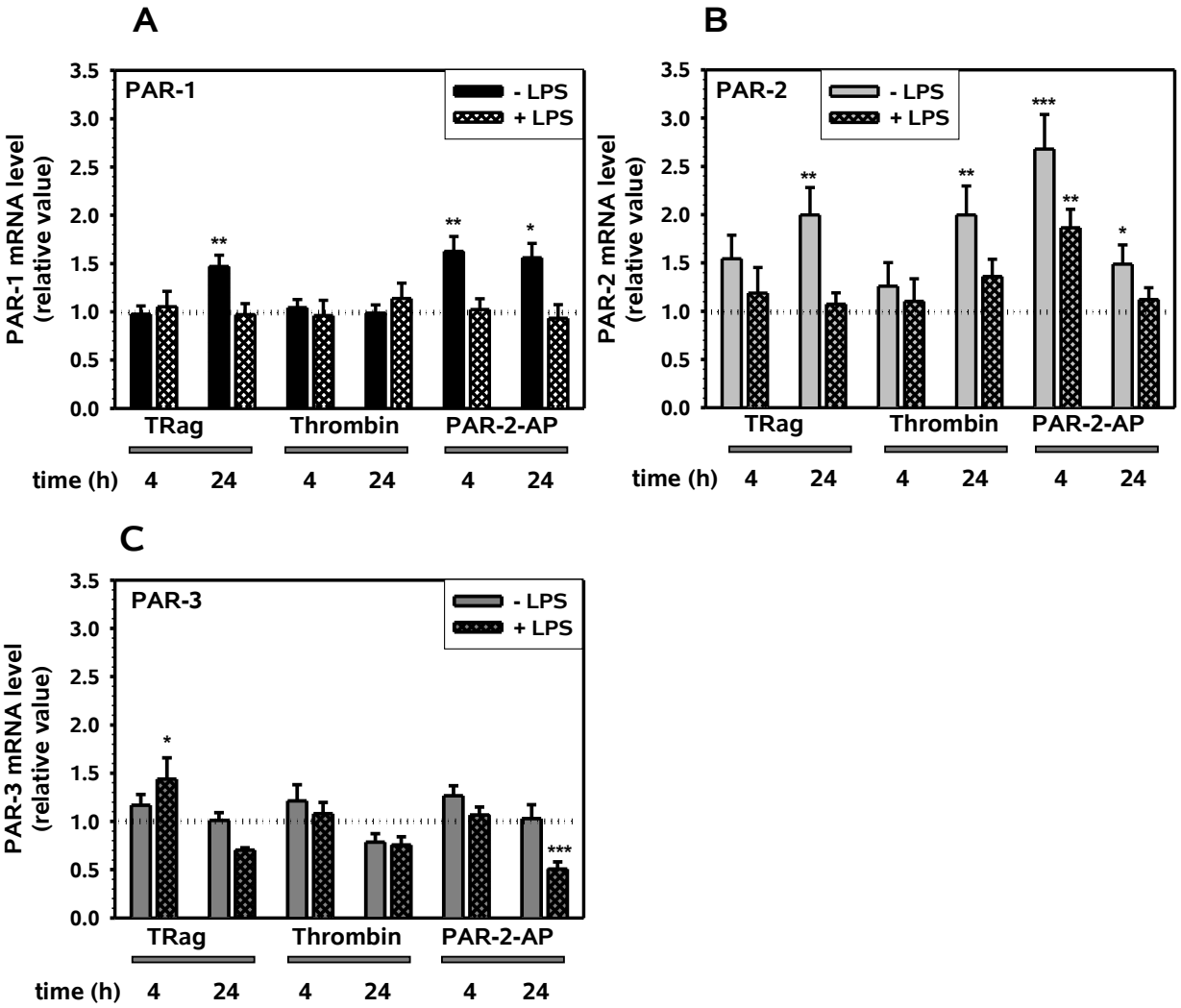

Figure 3.11: The influence of simultaneous action of PAR agonists and LPS on PAR expression. Changes in PAR-1 (A), PAR-2 (B), and PAR-3 (C) mRNA after simultaneous stimulation with PAR agonist together with LPS were estimated by real-time PCR. The cells were incubated with LPS (10 µg/ml) simultaneously with TRag (5 µM), thrombin (5 U/ml) or PAR-2 AP (200 µM) for the different times indicated. Modulation of mRNA expression was calculated using GAPDH as a reference gene. Data are means ± SE of three independent experiments. Dotted line at "1" indicates control level. Grey bars below the graphs indicate the agonist used. $^{***}p<0.001$, $^{**}p<0.01$, $^{*}p<0.05$ as compared with the untreated cells.

However, differently to PAR-1, the PAR-2 expression level after 4 h of concomitant stimulation of the cells with LPS and PAR-2 AP remained elevated (Fig. 3.11B).

Interestingly, prolonged (24 h) simultaneous treatment of A549 cells with LPS and the PAR agonists resulted in down-regulation of the PAR-3 mRNA level. The decrease was up to 2 times ($P<0.001$ for the combination of PAR-2-AP and LPS) (Fig. 3.11C).

We attempted to measure changes of PAR-2 protein level on the cell surface using immunocytochemical analysis. We stimulated epithelial cells with either LPS or PAR-2 AP or with their combination for 4 h and waited for an additional 2 h incubation period after withdrawal of the stimuli. Then we observed an increase by 30% in the fluorescence signal intensity of the PAR-2 (data not shown). These results correlate with the data obtained by RT-PCR shown in Fig. 3.7A and 3.11B.

These data again underpin the importance of PAR-2. The most affected receptor, in terms of regulation of its expression after activation of the PARs and simultaneous exposure to the inflammatory mediator LPS, is PAR-2.

3.3.4 Modulation of IL-8 synthesis in airway epithelial cells by PAR activation with simultaneous exposure to LPS.

In parallel with the determination of changes in PAR expression after persistent PAR activation in A549 cells, we tested the ability of the PAR agonists to induce the synthesis of IL-8. The exposure of the A549 cells to the specific PAR-1-activating peptide TRag did not change the IL-8 mRNA level significantly. However, stimulation with thrombin up-regulated the IL-8 mRNA level in A549 cells after 4 h up to 3.5 fold ($P<0.01$). This effect persisted for 24 h of incubation ($P<0.001$). Activation of PAR-2 by the specific peptide PAR-2 AP increased the IL-8 mRNA level after 4 h by 14-fold ($P<0.01$). After 24 h stimulation the effect was attenuated but still significant (2.4-fold ($P<0.01$)) (Fig. 3.12A). To verify the PAR agonist-induced IL-8 up-regulation on protein level, the secreted IL-8 in cell culture supernatants was determined by ELISA. Similar to the mRNA level described above, IL-8 secretion was induced by PAR agonists in A549 cells (Fig. 3.12B). However, when the cells were stimulated with TRag we could detect almost no change in IL-8 protein level after 4 h and 24 h of stimulation, compared to untreated cells. Only thrombin induced approx. 3-fold increase in IL-8 secretion. As expected, PAR-2 AP stimulation resulted in increase 11- and 20-times of IL-8 concentration in the culture medium after 4 h and 24 h of incubation, respectively ($P<0.01$). The most potent agent to stimulate the IL-8 transcription was PAR-2 AP.

We also investigated the effect of simultaneous treatment with LPS and PAR agonists on the expression and synthesis of IL-8. LPS alone induced significant 7.6- and

4- fold up-regulation of the chemokine expression after 4 and 24 hours, respectively. The IL-8 expression was enhanced up to 30 times ($P<0.01$) after 4 h of stimulation with LPS together with PAR-1 and -2 agonists (TRag, thrombin, PAR-2 AP). However, after 24 h of co-stimulation with LPS and PAR agonists, the expression level of IL-8 decreased significantly compared to the short-term stimulation for 4 h, but still remained significantly higher than the control level, as shown in Figure 3.12A.

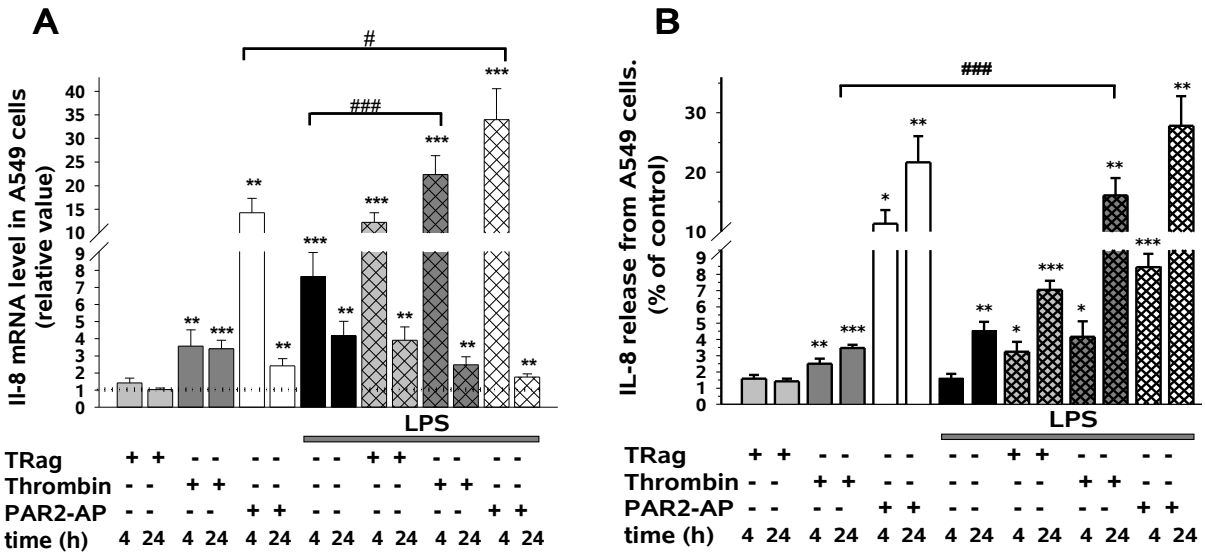

Figure 3.12: Induction of IL-8 synthesis by PAR agonists alone or in combination with LPS in A549 cells. Changes in IL-8 mRNA level after 4 and 24 hours of incubation were estimated by real-time PCR Modulation of mRNA expression was calculated using GAPDH as a reference gene (A). IL-8 secreted into the medium was quantified by ELISA (B). The cells were incubated with TRag (5 µM), thrombin (5 U/ml) or PAR-2 AP (200 µM) alone or together with LPS (10 µg/ml). Data are means ± SE of three independent experiments. Dotted line at "1" indicates control level. Grey bar below the graphs indicate applied LPS. $^{***}p<0.001$, $^{**}p<0.01$, $^{*}p<0.05$ as compared with the untreated cells. $^{###}p<0.001$, $^{#}p<0.05$ as compared with the cells treated with only one agonist.

The potentiation of the IL-8 expression after the challenge of the A549 cells with LPS together with thrombin and PAR-2 agonist also led to amplified IL-8 secretion (Fig. 3.12B). The effects of the agonists on the mRNA level described above were seen similarly on protein level. Concomitant exposure of the cells to thrombin or PAR-2 AP together with LPS induced a 16- or 27-times elevated amount of IL-8 release. Thus, in A549 cells we observed an amplifying effect of PAR-2 AP or thrombin together with LPS on IL-8 synthesis, compared to the effects of each stimulus alone.

We confirmed the modulation of IL-8 production by PAR agonists using primary HSAEC. Stimulation of these cells with the PAR-1-activating peptide TRag did not induce IL-8 mRNA synthesis and protein release from these cells (Fig. 3.13A, B). This

was detected by real-time PCR and ELISA, respectively. Thus, consistently in both lung epithelial cell lines, A549 and HSAEC, PAR-1 was not able to induce IL-8 production. Stimulation of HSAEC with thrombin resulted in an increase of the IL-8 transcript level and in protein release (Fig. 3.13A, B).

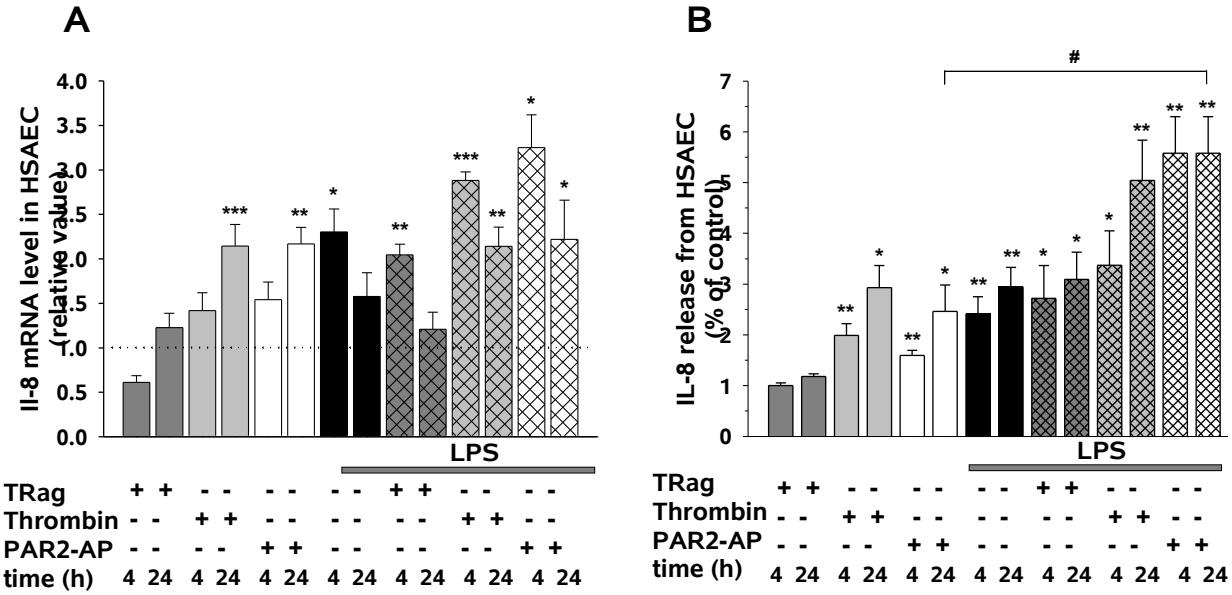

Figure 3.13: Induction of IL-8 synthesis by PAR agonists alone or in combination with LPS in HSAEC. Changes in IL-8 mRNA level after 4 and 24 hours of incubation were estimated by real-time PCR Modulation of mRNA expression was calculated using GAPDH as a reference gene (A). IL-8 secreted into the medium was quantified by ELISA (B). The cells were incubated with TRag (5 µM), thrombin (5 U/ml) or PAR-2 AP (200 µM) alone or together with LPS (10 µg/ ml). Data are means ± SE of three independent experiments. Dotted line at "1" indicates control level. Grey bar below the graphs indicate applied LPS. $^{***}p<0.001$, $^{**}p<0.01$, $^{*}p<0.05$ as compared with the untreated cells. $^{\#}p<0.05$ as compared with the cells treated with only one agonist.

In HSAEC the IL-8 expression was increased by 1.6 fold after 4 h stimulation, and was further significantly increased after 24 h stimulation (2.2 fold) (Fig. 3.13A). The delayed response of HSAEC to PAR-2 agonist might be a characteristic feature of primary cells, which was also documented in another work . The effect of the PAR-2 agonist was seen similarly on the protein level of IL-8. PAR-2 AP stimulation resulted in significant increase of IL-8 concentration in the culture medium (2.0-fold) (Fig. 3.13B). In A549 cells the amount of cytokine released was higher than in HSAEC.

In the present work, we found that in A549 cells as well as in primary HSAEC activation of PAR-2, but not PAR-1, resulted in the production of the proinflammatory chemokine IL-8.

Further, we investigated the effect of simultaneous treatment with LPS and PAR agonists on the IL-8 production by HSAEC. LPS alone induced significant up-regulation

of the chemokine expression in HSAEC (2.3 fold). Challenging the HSAEC for 4 h with PAR-2 AP or thrombin in the presence of LPS amplified the IL-8 expression (Fig. 3.13A). Like in A549 cells, the IL-8 expression in HSAEC reached the highest level after combined stimulation with PAR-2 AP and LPS, compared to the co-stimulation with LPS and thrombin or with each stimulus alone. Co-stimulation with LPS and TRag did not alter IL-8 expression level compared to the effect of LPS alone in these cells.

As expected from the effects on the IL-8 mRNA level, the release of IL-8 into the culture medium after 24 h of incubation of HSAEC with the PAR agonists in the presence of LPS was potentiated (Fig. 3.13B). Again, the co-stimulation with LPS and thrombin or PAR-2 AP resulted in greater IL-8 protein production from A549 cells than from HSAEC. That is similar to the effects of these stimuli on the IL-8 mRNA level.

To summarize this part, TRag did not influence the effect of LPS on IL-8 release in both A549 and HSAE cells. Similar to the effects observed on transcript levels, the highest protein release was achieved when PAR-2 was activated with PAR-2 AP together with concomitant stimulation with LPS. That emphasizes again the importance of epithelial PAR-2 receptor in airway pathophysiology.

Table 3.1 summarizes the potentiating effects on IL-8 release of the combined stimulation of A549 cells and HSAEC with LPS and PAR-2 AP or thrombin. The effect of simultaneous treatment of A549 cells with LPS and thrombin was 4.9 times higher than that induced by thrombin alone and 3.2 times higher than that achieved by LPS alone. In HSAEC the IL-8 concentration in the cell culture medium was potentiated 1.7 times after stimulation with thrombin together with LPS, compared to the effects of each stimulus alone. After the combined stimulation of A549 cells with PAR-2 AP and LPS, the IL-8 protein level was 1.6-times higher than after stimulation by PAR-2 AP alone and 5.5-times higher than after stimulation by LPS alone. In HSAEC IL-8 concentration was potentiated 2.3 and 1.9 times compared to that induced by PAR-2 AP or LPS, respectively.

PAR agonist	Potentiation of PAR agonist-induced effect by LPS (n-fold)		Potentiation of LPS-induced effect by PAR-agonist (n-fold)	
	A549 cells	**HSAEC**	**A549 cells**	**HSAEC**
Thrombin	**4.9**	**1.7**	**3.2**	**1.7**
PAR-2 AP	**1.6**	**2.3**	**5.5**	**1.9**

Table 3.1: Potentiating effect on IL-8 protein release, induced by simultaneous incubation of A549 cells and HSAEC with PAR agonists and LPS. The potentiation effect is shown as n-fold increased IL-8 concentration in the cell culture medium after 24 h simultaneous application of the PAR agonists (thrombin or PAR-2 AP) together with LPS, relatively to IL-8 concentration after stimulation with the PAR agonists alone, and LPS alone, respectively.

3.3.5 The influence of PAR activation and concomitant stimulation with LPS on TGF-β1 expression in A549 cells.

We also investigated the TGF-β1 mRNA levels after PAR activation and simultaneous exposure of the cells to LPS. TGF-β1 expression was up-regulated upon PAR activation using all PAR agonists. The PAR-2 activating peptide was the most potent agent. It induced a 2-fold increase in TGF-β1 transcript.

After simultaneous stimulation with LPS and PAR-2 AP, the TGF-β1 mRNA level was up-regulated only after 4 h by 1.6-fold ($P<0.01$), and was slightly increased after application of TRag and LPS. Compared to untreated cells, the TGF-β1 mRNA level was not altered after 4 h of stimulation with thrombin together with LPS. After 24 h of co-incubation with the PAR agonists and LPS, the TGF-β1 mRNA level was comparable to the control level or even slightly lower than the control level (Fig. 3.14).

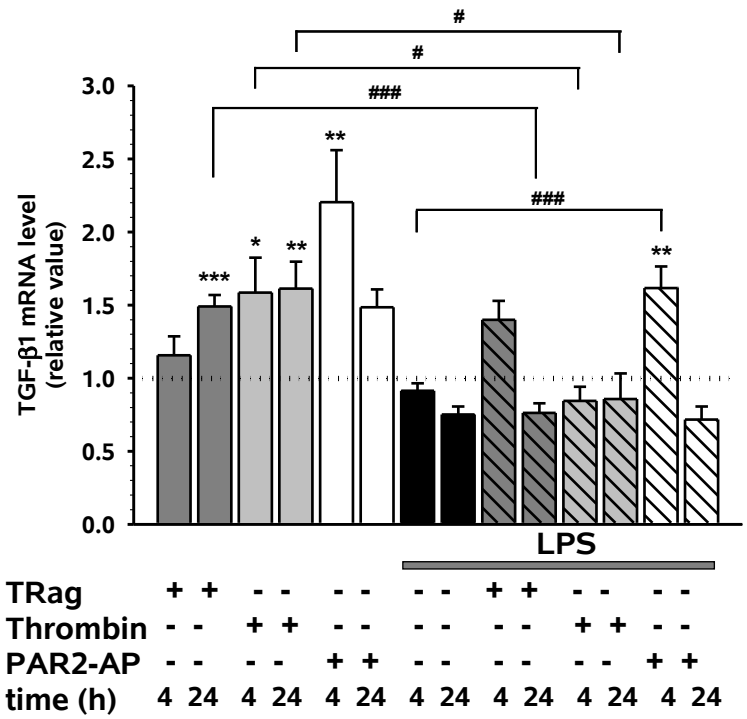

Figure 3.14: The influence of PAR agonists alone and in combination with LPS on TGF-β1 expression in A549 cells. Changes in TGF-β1 mRNA level after 4 and 24 hours of incubation were estimated by real-time PCR. Modulation of mRNA expression was calculated using GAPDH as a reference gene. Data are means ± SE of three independent experiments. Dotted line at "1" indicates control level. Grey bars below the graphs indicate the agonist used. $^{***}p<0.001$, $^{**}p<0.01$, $^{*}p<0.05$ as compared with the untreated cells.

The detection of the TGF-β1 release by A549 cells (measured by ELISA after 4 h and 24 h of incubation) confirmed that PAR activation leads to a slight increase of TGF-β1 secretion (60-100% above control) (data not shown).

3.4 Role of MAPKs in PAR-mediated IL-8 release from A549 cells.

3.4.1 Influence of thrombin, PAR-2 AP and LPS on MAPK phosphorylation in A549 cells.

MAPK play an important role in various cells participating in different immune responses. The responses reach from the initiation of the immune response to inducing cell death . However, only little is known about the involvement of MAPKs in PAR-mediated IL-8 synthesis in airway cells. This following study by Western blot analysis addresses the question of whether PAR agonists and LPS (alone and in combination) lead to activation of MAPKs in A549 cells. Figure 3.15 demonstrates that incubation of the A549 cells with thrombin (5 U/ml) and PAR-2 AP (200 µM) induced phosphorylation of

JNK and ERK1/2. Stimulation with LPS did not influence the levels of ERK1/2 and JNK phosphorylation up to 60 min, despite its ability to induce IL-8 production.

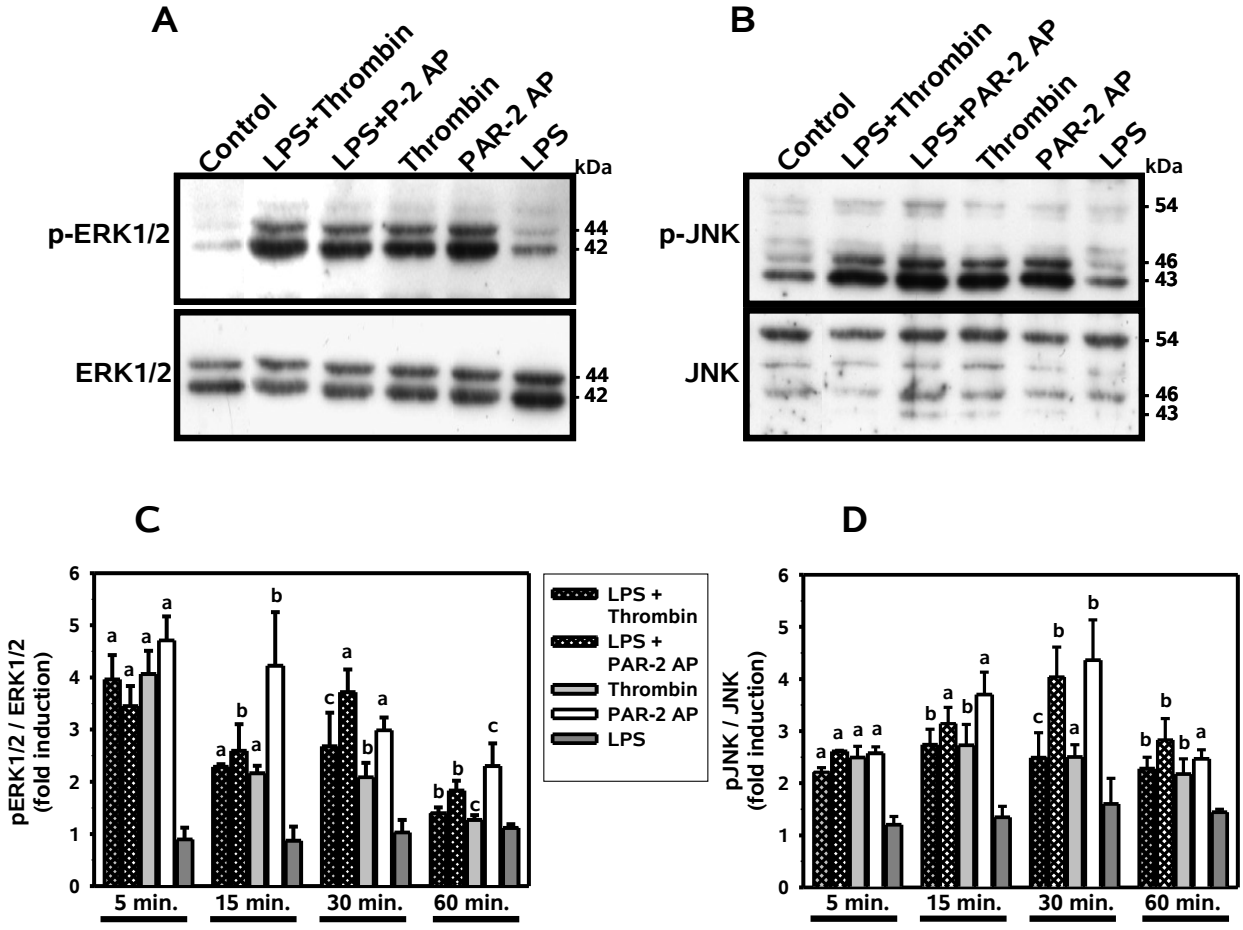

Figure 3.15: Activation of ERK1/2 and JNK by PAR agonists. Serum-starved A549 cells were exposed to thrombin (5 U/ml) or PAR-2 AP (200 µM) alone or together with LPS (10 µg/ml) for 5, 15, 30 and 60 min. Representative blots from one experiment are shown (A and B). The cells were incubated for 5 min with medium alone (Control) or with thrombin and LPS (LPS +Thrombin), PAR-2 AP and LPS (LPS+PAR-2 AP), thrombin (Thrombin), PAR-2 AP (PAR-2 AP), or LPS (LPS). Phosphorylation of ERK1/2 and JNK were analyzed by Western blotting using the anti-phospho-ERK1/2 and anti-phospho-JNK antibodies (upper panels). Equal amounts of protein loading were confirmed using the specific antibodies for total ERK1/2 and JNK (lower panels). The bands were quantified by densitometry and normalized by referring to the corresponding total amounts (C, D). JNK phosphorylation was quantified by taking the 46 kDA isoform band densitometry and normalized by referring to the corresponding total amount of 46 kDA JNK isoform. Data are shown as -fold induction compared to control (untreated cells) and represent the means ± SE of at least three independent experiments; $^{a}p<0.001$, $^{b}p<0.01$, $^{c}p<0.05$ as compared with the untreated cells. Horizontal lines indicate time periods of cell stimulation.

Phosphorylation of ERK1/2 after stimulation with either thrombin or PAR-2 AP was maximal at 5 min (400% of control) and then gradually declined, almost reaching the

basal level by 60 min of incubation (Fig. 3.15C). When A549 cells were stimulated with thrombin or PAR-2 AP together with LPS, the degree of phosphorylation was comparable to that obtained with thrombin or PAR-2 agonist alone. Stimulation with PAR-2 AP alone or together with LPS induced ERK1/2 phosphorylation which was slightly stronger than that caused by thrombin or thrombin with LPS.

JNK phosphorylation was smaller than that of ERK1/2 (200%) and persisted for at least 1 h (Fig. 3.15D). The effect of thrombin (alone and in combination with LPS) was retained up to 60 min, whereas stimulation with PAR-2 AP (alone or with LPS) induced maximal phosphorylation level at 30 min.

3.4.2 Inhibition of ERK1/2 or of JNK decreases the production of IL-8 in response to thrombin and PAR-2 AP, either alone or together with LPS.

Using specific pharmacological inhibitors of the MAPK cascade, the involvement of the MAPK family in PAR-mediated IL-8 release in A549 cells was investigated (Fig. 3.16). A blockade of p38 MAPK by SB203580 (10 µM) failed to affect the secretion of IL-8, which was induced by stimulation with thrombin, and PAR-2 AP, either alone or in combination with LPS.

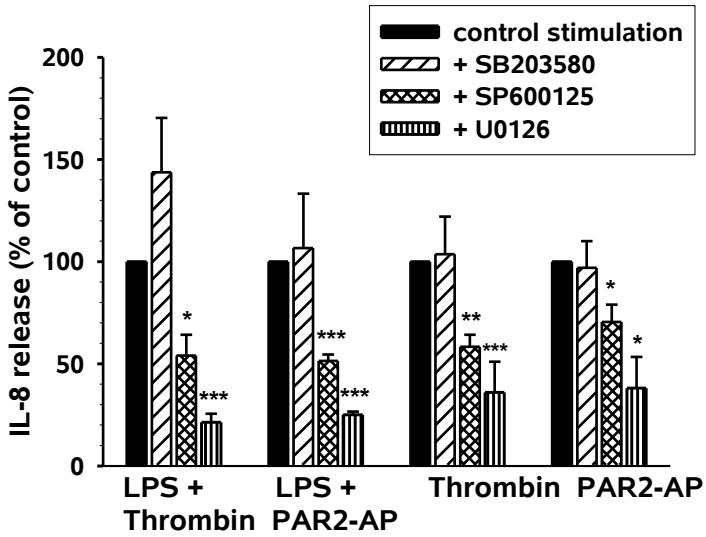

Figure 3.16: Effect of MAPK inhibitors on PAR induced IL-8 release in A549 cells. Serum-starved cells were pretreated with either p38 MAPK inhibitor SB203580 (10 µM), JNK inhibitor SP600125 (10 µM) or ERK1/2 inhibitor U0126 (20 µM) for 30 min, followed by incubation with medium or thrombin (5 U/ml), PAR-2 AP (200 µM), alone or in combination with LPS (10 µg/ml) for the next 24 h. An ELISA was used to quantify the amount of released IL-8. The results are means ± SE of three independent experiments. ; $^{***}p<0.001$, $^{**}p<0.01$, $^{*}p<0.05$ as compared with the cells exposed to only agonists (without inhibitor).

Pretreatment of the cells with the JNK inhibitor SP600125 (10 µM) reduced the IL-8 release after incubation with thrombin or PAR-2 AP by 30 and 40%, respectively. SP600125 abolished by 50% the cytokine release induced by the combined stimulation of the cells with PAR agonists together with LPS. A MEK1/2 inhibitor, U0126 (20 µM), showed an 80% reduction of the IL-8 production, which was caused by combined incubation with thrombin or PAR-2 AP together with LPS. The thrombin- or PAR-2 AP-induced IL-8 secretion was inhibited by U0126 by 60%. These results are consistent with the ERK and JNK phosphorylation data shown above in Figure 3.15.

3.5 PAR-3 signaling

From the experiments presented above PAR-3 attracted our special attention. Firstly, the PAR-3 mRNA level was down-regulated after prolonged incubation of A549 cells with PAR agonists together with LPS. Secondly, stimulation of the A549 cells with thrombin but not with PAR-1-activating peptide increased production of the pro-inflammatory cytokine IL-8. These interesting observations led us to assume that PAR-3, the most elusive receptor within the PAR family, plays a role in inflammatory reactions and is directly involved in IL-8 production.

In order to assess our hypothesis about an important function of PAR-3, we engineered exogenous human PAR-3 expression. The full-length human PAR-3 was cloned by PCR amplification into the pEGFP-N1 vector (see Materials & Methods). Further, this GFP-tagged PAR-3 was stably transfected using Lipotransfection into human embryonic kidney cells (HEK-293). The obtained HEK-PAR3-GFP cell line was used in further experiments. As a reference served HEK-293 cells transfected with pEGFP-N1 plasmid DNA (HEK-GFP) and HEK-293 wildtype cells (HEK-WT).

Quantification of relative expression of PAR-3 in HEK-PAR3-GFP showed significant expression of PAR-3. It was about 100-fold compared with the endogenous PAR-1 expression level. PAR-3 was not expressed by HEK-WT and HEK-GFP cells (Fig. 3.17A). Transfection of the cells had no influence on the PAR-1 mRNA level. The PAR-3-GFP fusion protein was found to be localized on the plasma membrane due to the green fluorescence of GFP, and there was very little cytoplasmic distribution (Fig.3.17B). GFP in HEK-GFP cells was visible in the whole cell without staining of particular organelles.

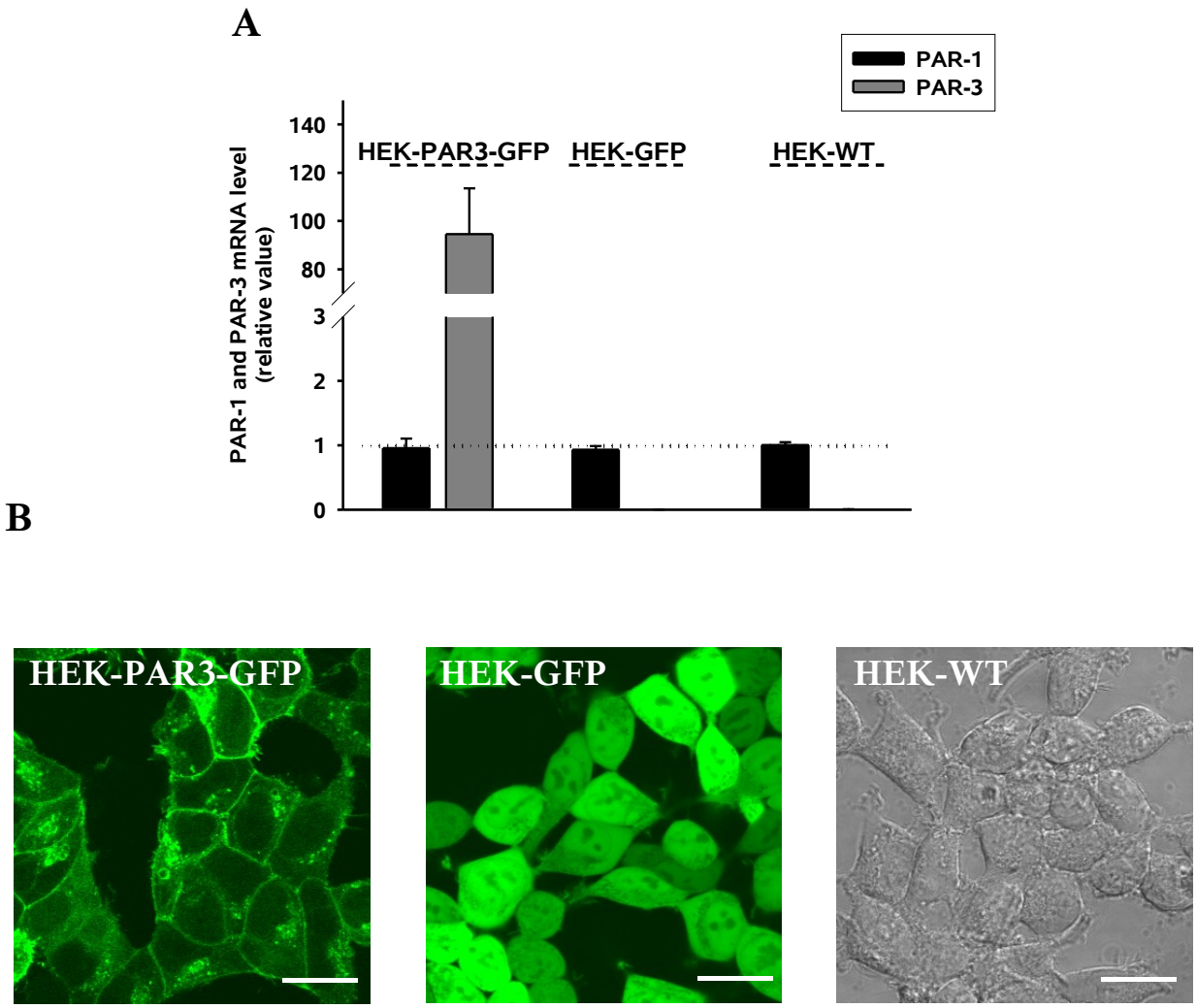

Figure 3.17: Detection and localization of PAR-3 in PAR-3-transfected HEK-293 cells. A: RT-PCR analysis of PAR-1 and PAR-3 in PAR-3-GFP- or GFP-transfected HEK and wild-type HEK cells: Total RNA was isolated and used for real-time PCR. Modulation of mRNA expression was calculated using GAPDH as a reference gene. Data are means ± SE of three independent experiments. Dotted line at "1" indicates control level. PAR expression levels are expressed relative to the PAR-1 mRNA expression in HEK-WT cells, which was arbitrarily chosen as a reference value of 1. N.D. stands for not detected. **B:** PAR-3-GFP and GFP were detected by GFP fluorescence using LSM510 confocal laser scanning microscope (Carl Zeiss, Germany). Images are representative for three different experiments.

To confirm the functional expression of PAR-3, we used thrombin, which is the only PAR-3 agonist known till now. We tested the induction of an increase in $[Ca^{2+}]_i$. Since HEK-293 cells endogenously express another thrombin receptor, namely PAR-1, HEK-GFP cells were used in parallel for proper evaluation of our experimental concept.

The concentration-response curves were obtained by analyzing the thrombin-induced Ca^{2+} mobilization for both cell lines as represented in Figure 3.18. The application of thrombin to HEK-PAR3-GFP cells resulted in significantly higher (appprox. 3 times) amplitude of Ca^{2+} responses than in HEK-GFP cells. The maximal response was achieved at a concentration of 10 U/ml thrombin for both cell types. This clearly indicates that PAR-3 used in our studies is functionally expressed and mediates cellular Ca^{2+} signaling, upon stimulation with thrombin.

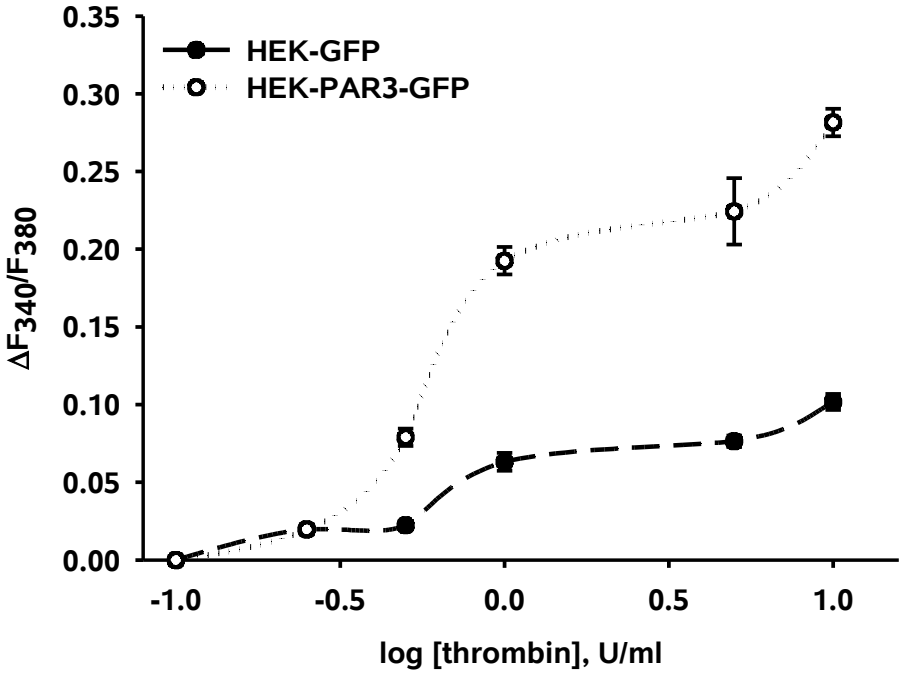

Figure 3.18: Concentration–response curves for thrombin in inducing $[Ca^{2+}]_i$ rise in HEK-293 cells stably expressing the PAR-3 receptor GFP fusion protein and only GFP protein. The fura-2-AM-loaded cells were stimulated with varying concentrations of thrombin, and the change in fluorescence ($\Delta F_{340\ nm}/F_{380\ nm}$) was detected. Data represent the mean ± s.e.m. from 70 to 150 single cells, which were measured in at least three separate experiments (in some cases the error bars are smaller in size than the symbols used).

Next, we wanted to clarify whether the expression of PAR-3 is modulated by thrombin. Since both PAR-1 and PAR-3 are thrombin receptors, it is of interest to elucidate the possible differences in thrombin-mediated changes of the transcript levels of these two receptors. With the help of real-time PCR we assessed the alteration of the

expression of the endogenous PAR-1 and the overexpressed PAR-3, after exposure of the cells to thrombin (10 U/ml).

Activation of the HEK-PAR3-GFP cells with thrombin for 3 h or 6 h had no effect on the PAR-1 mRNA level. However, the PAR-3 mRNA expression was significantly up-regulated (Fig. 3.19). Similarly, in control cells, HEK-GFP and HEK-WT, the PAR-1 mRNA level was also not influenced by the exposure of the cells to thrombin.

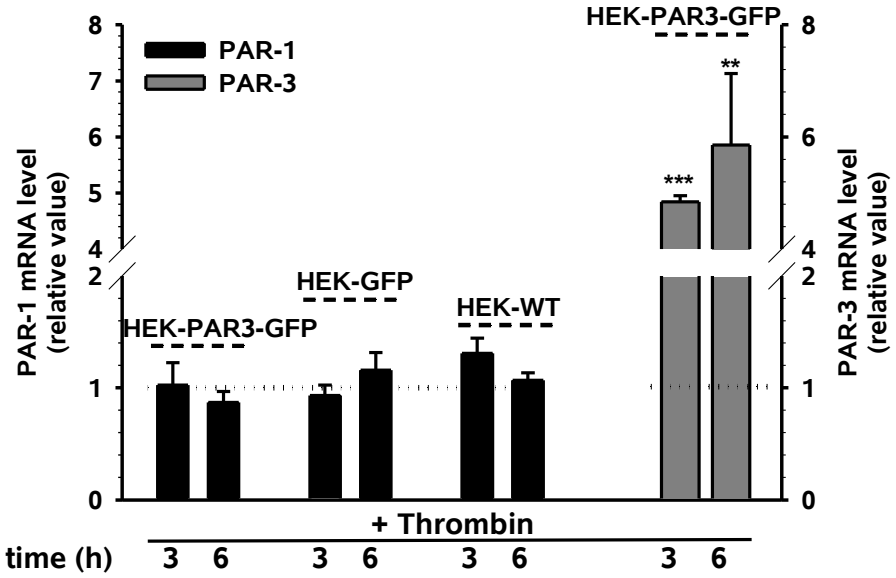

Figure 3.19: Effect of thrombin on the expression level of PAR-1 in HEK-PAR3-GFP, HEK-GFP and HEK-WT cells and PAR-3 level in HEK-PAR3-GFP cells. Changes in PAR-1 (black bars) and PAR-3 (grey bars) mRNA level after incubation with 10 U/ml thrombin for 3 h or 6 h. Total RNA was isolated and used for real-time PCR. Modulation of mRNA expression was calculated using GAPDH as a reference gene. Data are means ± SE of three independent experiments. Dotted line at "1" indicates control level. $^{***}p<0.001$, $^{**}p<0.01$ as compared with the respective untreated cells.

To address the question of whether PAR-3 activation can lead to other cellular responses, we studied the effect of thrombin on IL-8 production in HEK cells stably expressing PAR-3. IL-8 synthesis was greatly enhanced in HEK-293 cells overexpressing PAR-3 upon stimulation with thrombin both on mRNA and protein level. The increase was up to 30- and 25-fold, respectively (Fig. 3.20). The IL-8 production by HEK-WT and HEK-GFP was not influenced by exposure to thrombin demonstrating that PAR-3-deficient cells do not respond to thrombin to release IL-8.

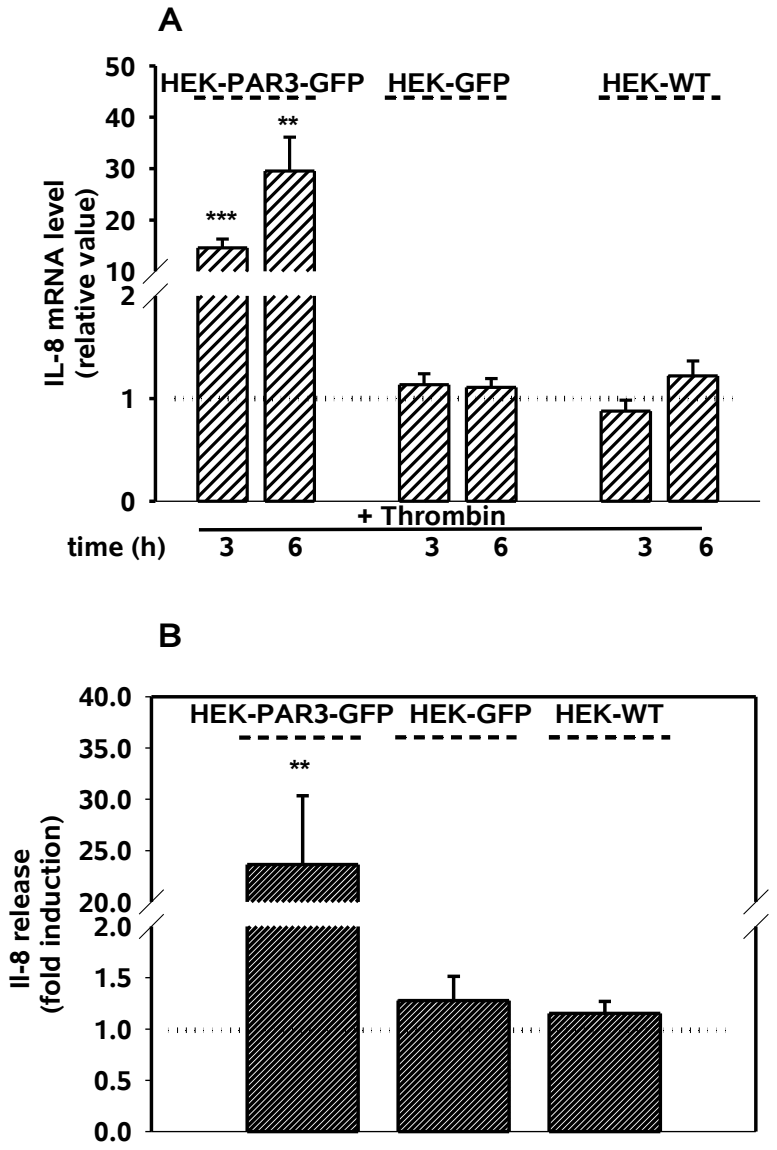

Figure 3.20: Effect of thrombin on the expression of IL-8 mRNA level and on protein secretion in HEK-PAR3-GFP cells. The HEK-PAR3-GFP, HEK-GFP and HEK-WT cells were incubated with 10 U/ml thrombin. **A:** Changes in IL-8 mRNA level after 3 and 6 hours of stimulation were estimated by real-time PCR. Modulation of mRNA expression was calculated using GAPDH as a reference gene. **B:** Secreted IL-8 in the medium after 6 hours of incubation quantified by ELISA. Data are means ± SE of three independent experiments. Dotted line at "1" indicates control level. $^{***}p<0.001$, $^{**}p<0.01$ as compared with the respective untreated cells.

To exclude the possibility that the thrombin-mediated IL-8 release is due to activation of PAR-1 or that PAR-3 participates in a dual receptor system as a thrombin cofactor for PAR-1 activation, we performed gene silencing of PAR-1, using target sequence-specific small interfering RNA (siRNA). HEK-PAR3-GFP cells were co-transfected with 100 nM of PAR-1 siRNA or with AllStars negative control siRNA.

Transfection with PAR-1 siRNA for 48 h resulted in highly suppressed (about 80%) PAR-1 transcript level. The control siRNA did not interfere with PAR-1 mRNA expression (Fig. 3.21A).

Additionally, the $[Ca^{2+}]_i$ rise after PAR-1 activation was verified. Specific activation of PAR-1 with TRag induced a significantly lower $[Ca^{2+}]_i$ response in cells transfected with PAR-1 siRNA than in untransfected cells or in cells transfected with control siRNA (Fig. 3.21B). Therefore, we can conclude that PAR-1 siRNA significantly decreases both PAR-1 expression and the function in terms of Ca^{2+} signaling.

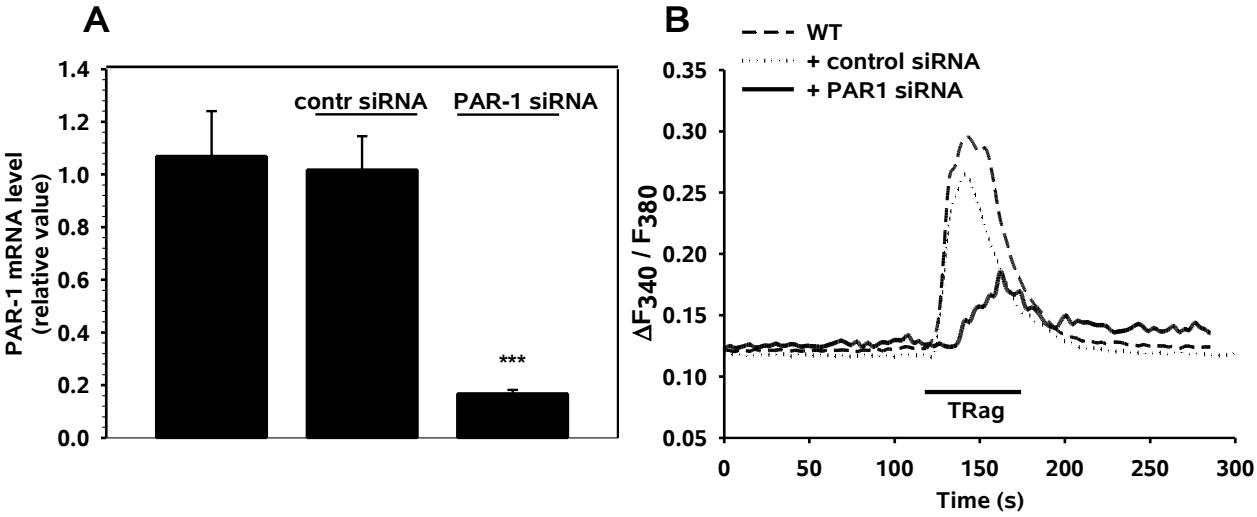

Figure 3.21: Suppression of PAR-1 expression by siRNA. HEK-PAR3-GFP cells were transiently transfected with either PAR-1 siRNA or control siRNA. Quantification of PAR-1 expression was assessed by real-time PCR **(A)**. Measurements were normalized to the GAPDH mRNA level. The values given are means ± SE of three independent measurements. PAR-1 expression level is expressed relative to the PAR-1 mRNA expression in cells transfected with control siRNA, which was arbitrarily chosen as a reference value of 1. $[Ca^{2+}]_i$ rise in HEK-PAR3-GFP induced by PAR-1 activating peptide (TRag) **(B)**. The fura-2-AM loaded HEK-PAR3-GFP cells and HEK-PAR3GFP cells co-transfected with PAR1 siRNA or control siRNA were exposed to TRag (10 µM) and the changes in fluorescence ($\Delta F_{340\ nm}/F_{380\ nm}$) were detected. The traces are the mean of minimally 25 single cells measured in one experiment and are representative for at least three different experiments

Furthermore, siRNA-transfected HEK-PAR3-GFP cells were incubated for 6 h with 10 µM TRag or 10 U/ml thrombin. The PAR-1 mRNA level in cells treated with control siRNA decreased slightly after stimulation with TRag and thrombin. However, the PAR-3 mRNA level was up-regulated significantly, about 3-fold, upon treatment with thrombin in both cells, transfected with PAR-1 siRNA and control siRNA. This is comparable to the results presented above with HEK-PAR3-GFP (Fig. 3.19).

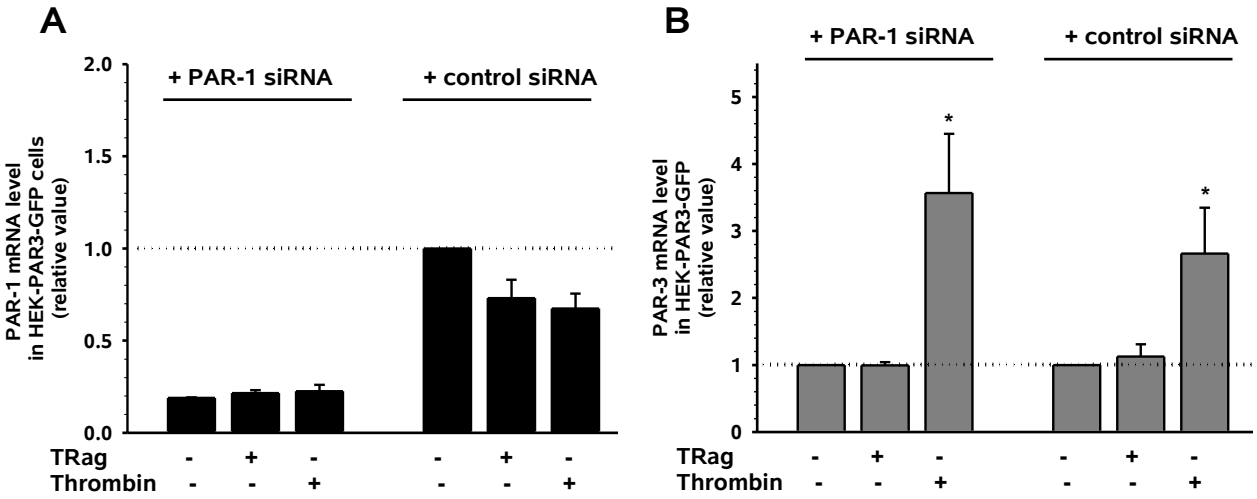

Figure 3.22: Effect of TRag and thrombin on the expression levels of PAR-1 and PAR-3 in HEK-PAR3-GFP cells transfected either with PAR-1 siRNA or control siRNA. Changes in PAR-1 mRNA level **(A)** and in PAR-3 mRNA level **(B)** after incubation with 10 µM TRag or 10 U/ml Thrombin for 6 h were estimated by real-time PCR. Modulation of mRNA expression was calculated using GAPDH as a reference gene. Data are means ± SE of three independent experiments. Dotted line at "1" indicates control level. $^{***}p<0.001$, $^{*}p<0.05$ as compared with the untreated cells.

These results provide convincing evidence that thrombin-induced up-regulation of PAR-3 expression is independent from PAR-1 activation.

Similarly, as shown in Fig. 3.23A, treatment with thrombin, but not with TRag, significantly elevated the synthesis of IL-8 mRNA by 20- and 22-fold ($P<0.05$) in HEK-PAR3-GFP cells transfected with PAR-1 siRNA and in cells transfected with control siRNA, respectively. Consequently, thrombin induced a significant increase of IL-8 in the cell culture supernatant of these cells (13- and 17-fold, respectively) (Fig. 3.23B). This highly enhanced amount of IL-8 released from the HEK cells expressing PAR-3 upon exposure to thrombin did not differ significantly between cells transfected with PAR-1 siRNA and control siRNA

Therefore, it can be concluded that suppression of endogenous PAR-1 expression in HEK-PAR3-GFP cells had no significant influence on the synthesis and protein secretion of IL-8 induced by thrombin. This indicates that PAR-3-mediated IL-8 production is not dependent on PAR-1 co-expression.

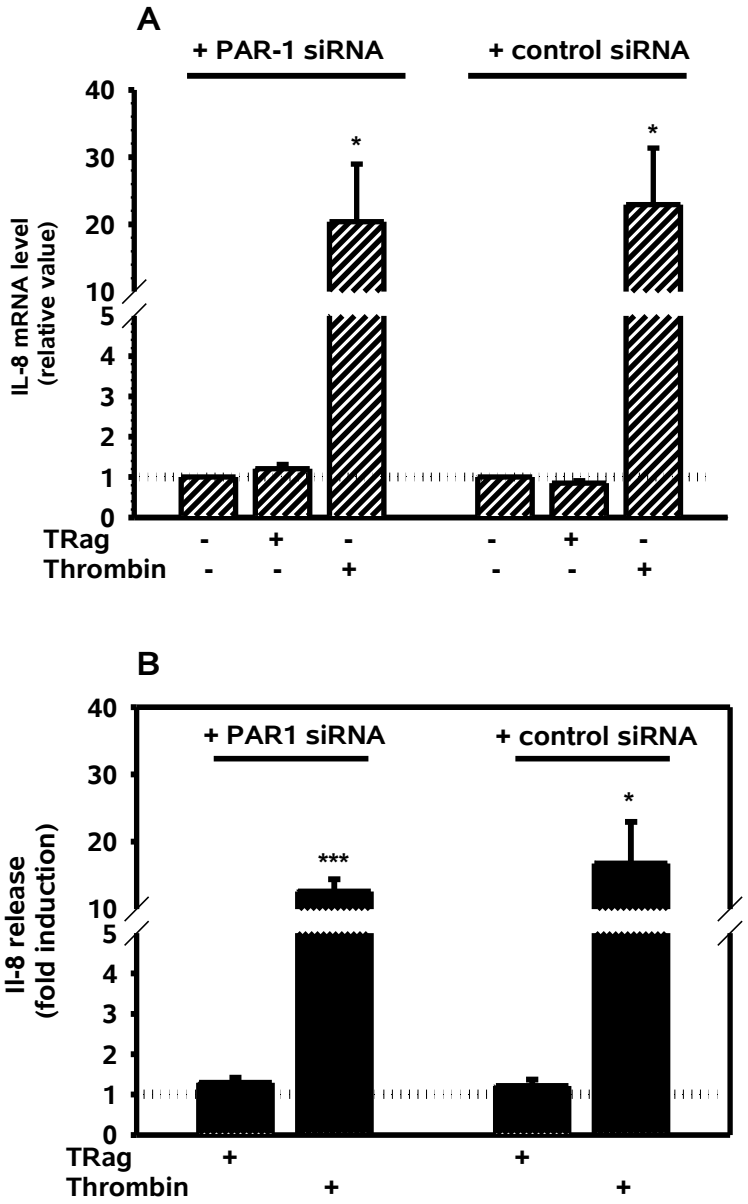

Figure 3.23: Effect of TRag and thrombin on the expression of IL-8 mRNA level and protein secretion in HEK-PAR3-GFP cells transfected with PAR1 siRNA. Changes in IL-8 mRNA level by real-time PCR **(A)** protein secretion by ELISA **(B)** after incubation of HEK-PAR3-GFP cells transfected either with PAR1 siRNA or control siRNA with 10 µM TRag or10 U/ml thrombin for 6 h. Total RNA was isolated and used for real-time PCR. Modulation of mRNA expression was calculated using GAPDH as a reference gene. Data are means ± SE of three independent experiments. Dotted line at „1" indicates control level. $^{***}p<0.001$, $^{*}p<0.05$ as compared with the respective untreated cells.

It has been shown that PAR-1 and PAR-2 can affect cellular functions through different signal transduction pathways, including the MAPK pathway. Furthermore, MAPK cascades are involved in PAR-1 and PAR-2-induced IL-8 production . However, until now, there is no data available showing the participation of MAPKs in PAR-3 signaling. In this work, the involvement of MAPKs, ERK1/2, JNK and p38 MAPK, in

PAR-3-mediated production of IL-8 was investigated using specific inhibitors. The HEK-293 cells overexpressing PAR-3 were pre-incubated with 10 µM of the p38 MAPK inhibitor SB203580, 10 µM of the JNK inhibitor SP600125 and 20 µM of the ERK1/2 inhibitor U0126, followed by the stimulation with 10 U/ml thrombin. As shown in Figure 3.24, a blockade of JNK and ERK1/2 reduced the IL-8 secretion induced by thrombin by about 40% and by 77%, respectively. Pretreatment of the cells with the p38 MAPK inhibitor did not significantly affect the IL-8 production.

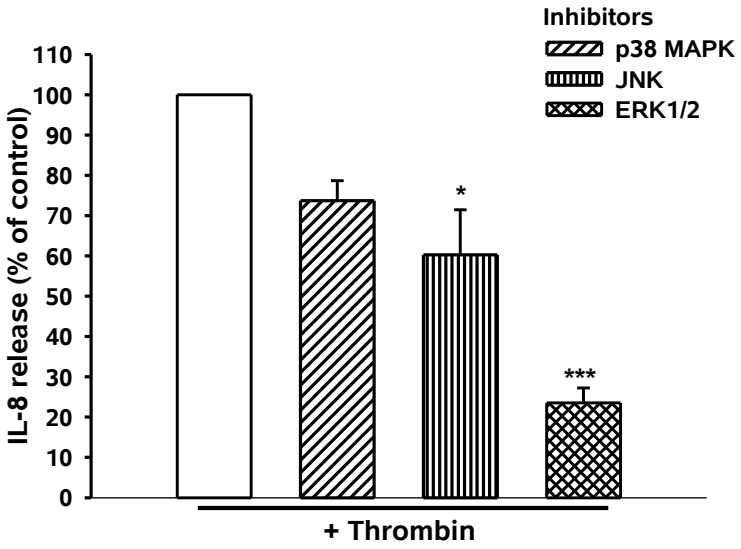

Figure 3.24: Effect of MAPK inhibitors on thrombin-induced IL-8 release in HEK-PAR3-GFP cells. Serum-starved cells were pretreated with either the p38 MAPK inhibitor SB203580 (10 µM), the JNK inhibitor SP600125 (10 µM) or the ERK1/2 inhibitor U0126 (20 µM) for 30 min, followed by incubation with 10 U/ml thrombin for 6 h. An ELISA was used to quantify the amount of IL-8 released. The results are means ± SE of three independent experiments. $^{***}p<0.001$, $^{*}p<0.05$ as compared with the cells treated with thrombin only.

By Western blot analysis we confirmed that thrombin activates ERK1/2 in HEK-PAR3-GFP cells. Figure 3.25 demonstrates that incubation of these cells with thrombin (10 U/ml) highly induced the time-dependent phosphorylation of ERK1/2 (up to 26-times) in HEK-PAR3-GFP cells, expressing endogenous PAR-1. Also in the cells transfected with PAR-1 siRNA there was an increase of up to 21-times above the control level. Only, after 5 min of incubation with thrombin, there seemed to be a difference in phosphorylation levels between HEK-PAR3-GFP cells and the cells with silenced PAR-1. The ERK1/2 activation was 50% higher in HEK-PAR3-GFP cells expressing endogenous PAR-1 than in cells co-transfected with PAR-1 siRNA. After 10 min of incubation the ERK1/2 phosphorylation in these two cell lines reached a similar level. These results are

presented in Figure 3.25A as time-course showing representative blots, which are quantified in Figure 3.25B.

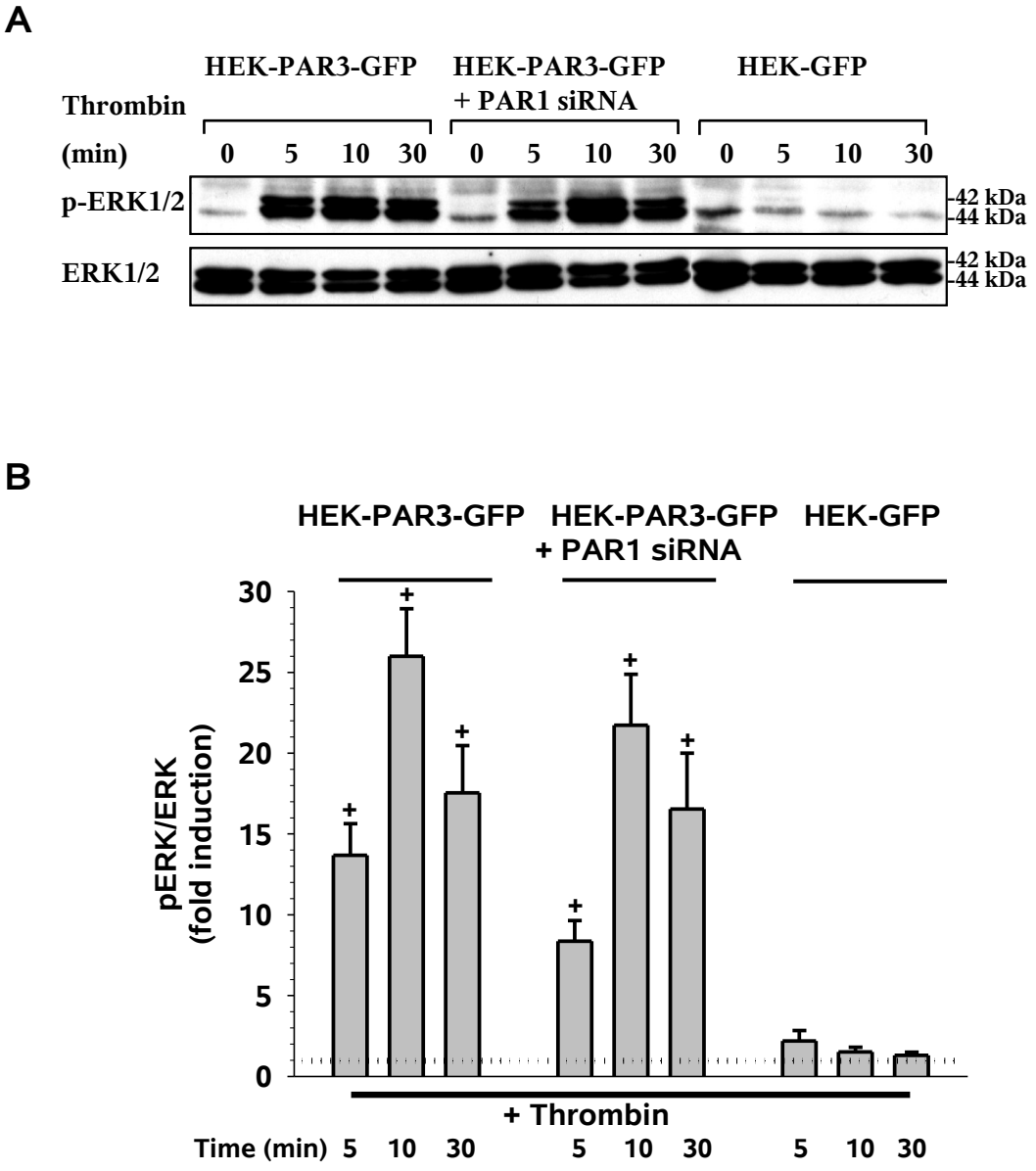

Figure 3.25: Activation of ERK1/2 by thrombin in HEK-PAR3-GFP, HEK-PAR3-GFP deficient in PAR-1 and HEK-GFP cells. Serum-starved cells were exposed to thrombin (10 U/ml) for 5, 10 and 30 min. Phosphorylation of ERK1/2 was analyzed by Western blotting using the anti-phospho-ERK1/2 antibodies. Equal amounts of protein loading were confirmed with the antibodies specific for total ERK1/2. The bands were quantified by densitometry and normalized by referring to the corresponding total amount of ERK1/2. Cells without treatment with thrombin served as control (100%), indicated by dotted line at "1". The results are means ± SE of three independent experiments. $^{+}$ $p<0.001$ as compared to the cells without treatment with thrombin.

JNK phosphorylation was considerably smaller than that of ERK1/2 and reached a maximal level of 200% of control value in HEK-PAR3-GFP cells after thrombin treatment (Fig.3.26).

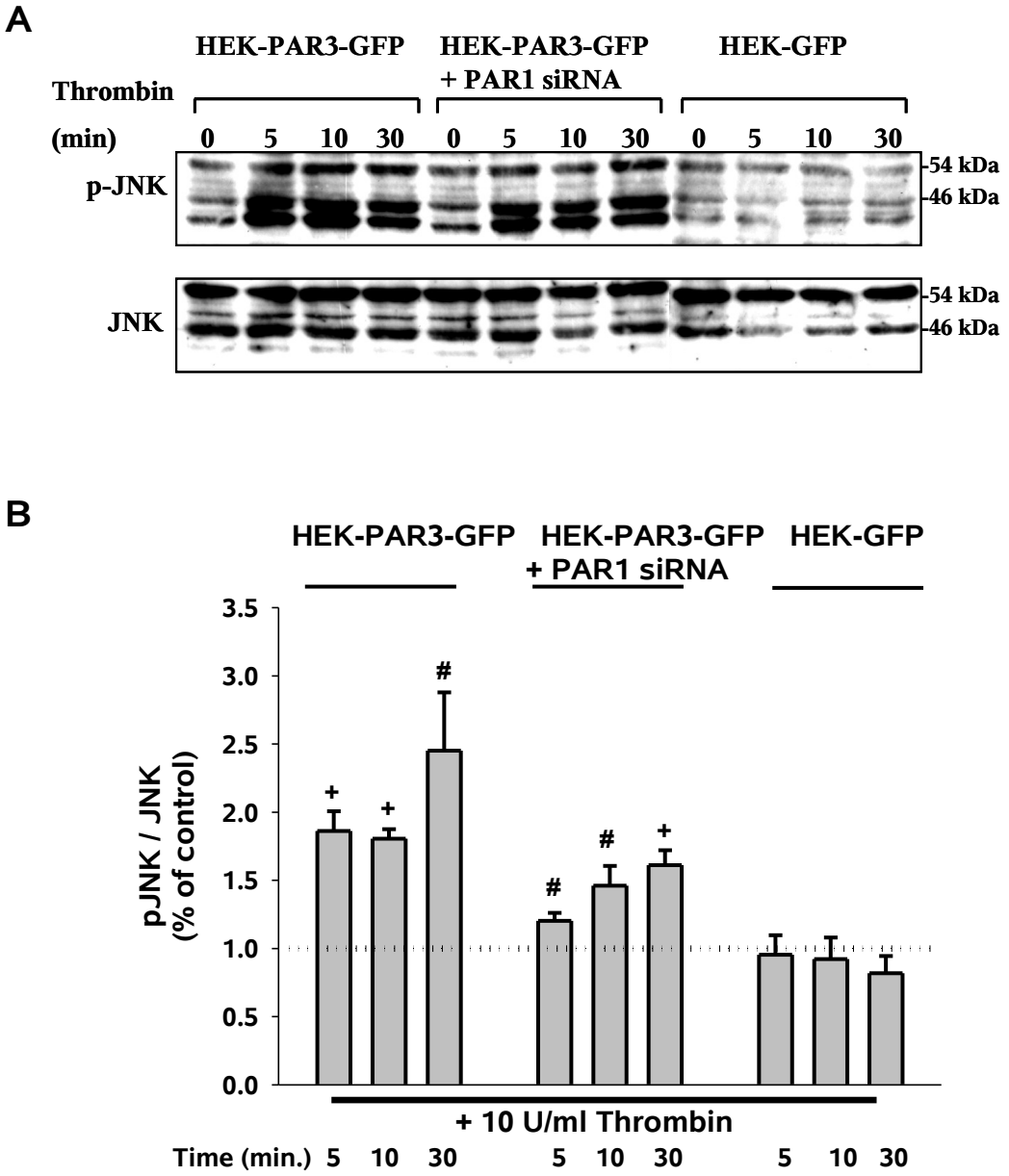

Figure 3.26: Activation of JNK by thrombin in HEK-PAR3-GFP, HEK-PAR3-GFP deficient in PAR-1 and HEK-GFP cells. Serum-starved cells were exposed to thrombin (10 U/ml) for 5, 10 and 30 min. Phosphorylation of JNK was analyzed by Western blotting using the anti-phospho-JNK antibodies. Equal amounts of protein loading were confirmed with the antibodies specific for total JNK. The bands were quantified by densitometry and normalized by referring to the corresponding total amount of JNK. Cells without treatment with thrombin served as control (100%), indicated by dotted line at "1". The results are means ± SE of three independent experiments. $^{+}p < 0.001$, $^{\#}p < 0.005$ as compared to the cells without treatment with thrombin.

In the HEK-PAR3-GFP cells transfected with PAR-1 siRNA, this effect was reduced by about 40-80%.

p38 MAPK was not activated by exposure to thrombin in HEK-293 cells expressing PAR-3 (data not shown).

4 Discussion

4.1 Functional expression of PARs in airway epithelial cells.

The results presented here demonstrate that A549, HBE and primary HSAE cells, lung epithelial cells, express two PAR subtypes, PAR-1 and PAR-2. A549 cells additionally express PAR-3 that was confirmed by RT-PCR and immunocytochemistry. Functional expression of these PARs in all lung epithelial cells investigated was confirmed by monitoring the changes of $[Ca^{2+}]_i$ induced by PAR-1 and -2 activating peptides as well as by stimulation with thrombin and trypsin. All methods used, RT-PCR, immunocytochemistry and measurement of $[Ca^{2+}]_i$ indicate predominance of PAR-2 mRNA and protein expression and function. The detection of PAR-4 by RT-PCR and Ca^{2+} mobilization studies gave negative results, so we can accept that PAR-4 was not expressed by any of the cells. In conclusion, PAR-2 is the main functionally expressed PAR receptor on lung epithelial cells.

4.2 Evaluation of PAR activation by trypsin isoforms in airway epithelial cells.

The further aim of this study was to extend the knowledge about trypsin-mediated PAR activation on human lung epithelial cells by investigating the ability of different human trypsin isoforms to activate PARs.

The measurements of $[Ca^{2+}]_i$ were performed in the human epithelial A549 and HBE cell lines. The results clearly demonstrate that mesotrypsin failed to produce Ca^{2+} responses in epithelial cells even at high concentrations, whereas cationic and anionic trypsins showed typical activity, comparable to that of bovine trypsin in epithelial cells.

The ability of the cationic and anionic trypsin isoforms to activate Ca^{2+} signaling in lung epithelial cells directly through the interaction with PAR-2 was confirmed in desensitization assays in HBE cells. However, mesotrypsin does not seem to be a potent activator of PAR-2. This finding is somehow in contradiction to studies of the Bunnet group . They have found that trypsin IV can evoke a Ca^{2+} response via PAR-2 and PAR-4 in cells overexpressing these receptors. Similarly, epithelial cells, like A549 cells, besides endogenous PAR-2 also express enteropeptidase that cleaves trypsinogen IV released by the cells. That consequently causes PAR-2 and PAR-4 activation. The reason for these discrepancies can be the fact that this group applied in their investigations enteropeptidase-activated conditioned medium from CHO-Igκ-TIV cells that may contain other substances that display proteolytic activity. We used purified, active recombinant trypsin. Furthermore, the recent report from the same research group demonstrates on

transfected cells that human trypsin IV activates PAR-1 and PAR-2 with similar potencies . It seems that the capacity of mesotrypsin/trypsin IV to activate PARs may depend on the preparation of the enzyme, and cell type- and species-specific PAR expression. It has to be also mentioned that trypsinogen IV is an alternatively spliced form of mesotrypsinogen and the amino acid sequences of the N-terminus encoded by the alternative exon 1 are completely different. Therefore trypsin IV lacks a recognizable signal sequence .

Originally, trypsinogen IV was found to be expressed in the human brain . It was shown that trypsinogen IV expression leads in mouse neurons to a massive increase of glial fibrillar acidic protein expression in astrocytes as well as to the lack of amyloid deposits in trypsinogen IV transgenic mice . Mesotrypsin/trypsin IV causes PAR-dependent oedema with granulocyte infiltration and induces hyperalgesia to thermal and mechanical stimuli in mice paw . Thus, mesotrypsin/trypsin IV contributes to neurogenic inflammation and pain. These results together with mesotrypsin's resistance to polypeptide trypsin inhibitors, which are present in the brain , suggest a special physiological role of this trypsin isoform in the human brain. However, it is still controversial, which PAR is activated by mesotrypsin/trypsin IV. To explore the ability of mesotrypsin to activate PARs in brain tissue, human astrocytoma 1321N1 cells expressing functional PAR-1, PAR-3 and no PAR-2 were used. The functionality of PAR-1 was confirmed by measurement of TRag-induced $[Ca^{2+}]_i$ rise, whereas PAR-2 AP was completely ineffective. Astrocytoma cells demonstrated lower susceptibility to be activated by bovine trypsin as compared to the epithelial cells. The lower potency of both cationic and anionic trypsin isoforms as compared to that in HBE cells was evident from the analysis of the concentration response curves. The EC_{50} value of these isoforms in 1321N1 cells was determined to be 20 nM and 10 nM, respectively. Similar to the epithelial cells, cationic trypsin-produced effects in 1321N1 cells were more pronounced than those by anionic trypsin. Interestingly, in contrast to the epithelial cell lines, mesotrypsin was definitely effective in 1321N1 cells, although with an EC_{50} value of 60 nM, which is 3-5-fold higher than that of cationic and anionic trypsin.

Taking into account the ability of trypsin to activate both PAR-1 and PAR-2 and the absence of PAR-2 in 1321N1 cells, we can suggest that trypsin initiates the signaling in the human astrocytoma cells through PAR-1. This was confirmed by the results of desensitization assays in 1321N1 cells in which responses to trypsin isoforms were significantly diminished after PAR-1 desensitization with TRag. Stimulation of PAR-1 in 1321N1 cells by 10 μM of the receptor-specific agonist peptide TRag before the

applications of cationic and anionic trypsin as well as mesotrypsin resulted in approximately 50% decrease of Ca^{2+} responses produced by these trypsin isoforms. These are clear evidences demonstrating that all three trypsin isoforms mediate their effects in the cells through PAR-1 as well.

Like in epithelial cells, anionic and cationic trypsin isoforms displayed an activity in 1321N1 cells similar to that of commercial trypsin. In contrast to epithelial cells, high concentrations of mesotrypsin produced significant Ca^{2+} responses in astrocytoma cells, suggesting that mesotrypsin can be considered as a potent activator of PAR-1 in brain cells. Supporting evidence was shown by another study from our laboratory . Data obtained during these investigations revealed that, similarly to the human system, mesotrypsin activates PAR-1 also in rat astrocytes, however with much higher effectiveness. This indicates a physiological role of mesotrypsin with regard to the Ca^{2+} response in brain cells.

Such differences between cells from different tissue origin can be due to specific properties of the receptor in the particular tissue. At present several possibilities can be suggested concerning the state of PARs: either tissue- and species-specific mutations or glycosylation pattern, which were both shown to be able to influence receptor activation .

In summary, it can be concluded that PAR-2 is a substrate for both cationic and anionic trypsin isoforms in human epithelial cells. Different from these two isoforms, mesotrypsin demonstrates distinct properties and activates neither PAR-1 nor PAR-2 in human epithelial cells. Interestingly, according to our results on human astrocytoma cells and the data on rat astrocytes, this trypsin isoform may be a potential activator of PAR-1 in the brain participating in protection / degeneration processes in brain tissue. However, in the lung epithelial cell, in contrast to cationic and anionic trypsin, mesotrypsin does not seem to play a physiological role.

4.3 Inflammatory mediators LPS, TNF-α, IL-8 and PGE_2 regulate PAR expression in A549 cells.

Pulmonary epithelial cells are the first line of host defence against inhaled pathogens. However, there is increasing evidence that the airway epithelium is not only a passive barrier against microbial components but is also an active player in the innate immune response of the lung and in the development of chronic inflammation.

The respiratory epithelium can generate various immune mediators, such as cytokines, chemokines, and anti-microbial peptides (e.g. defensins) and regulate the activation and recruitment of phagocytes and lymphocytes. Particularly chronic inflammatory diseases, such as asthma, are associated with epithelial damage and alteration of the epithelial phenotype. The cells persistently express abnormally high levels of bioactive molecules and surface receptors and thus are able to maintain the ongoing inflammation. PARs are involved in the regulation of epithelial responses to injury.

However, there is still limited information concerning the question which particular factors can modulate PAR expression on airway cells. Therefore, the investigation of the effect of inflammatory mediators and persistent PAR activation by their agonists provide important evidence for the involvement of PARs in many pathological conditions.

Bacteria colonize the airways inducing inflammation and release of numerous potent inflammatory molecules, including endotoxin, peptidoglycan fragments, outer membrane lipoproteins, lipoteichoic acid, microbial toxins . LPS, a cell wall component of gram-negative bacteria, is a common occupational air contaminant, which causes both acute and chronic airflow obstruction, airway inflammation and airway remodeling. Respiratory epithelial cells along with alveolar macrophages are a target for this endotoxin. Inhaled LPS forms complexes with LPS-binding protein, interacts with CD14 that initiates cell signaling via Toll-like receptor 4 associated with the accessory molecule MD-2. This leads to signaling cascades that finally result in the biosynthesis of pro-inflammatory cytokines . Another inflammatory mediator, TNF-α, an early proinflammatory cytokine, which can be released by blood monocytes and alveolar macrophages after LPS stimulation, has many proinflammatory effects in common with LPS, resulting in the pathogenesis of lung injury.

Epithelial cells, upon activation by either LPS or TNF-α release different chemokines, cytokines, defensins and adhesion molecules. Besides the release of the inflammatory agents from the cells, LPS and TNF-α can modulate cellular responsiveness to subsequent stimuli via alteration of expression of cell-surface receptors .

In the present study, we showed that although both agents, LPS and TNF-α, can up-regulate PAR expression in A549 cells, they display different time dependence and selectivity towards particular PAR subtypes. LPS affected exclusively PAR-2 that was observed only after short-term stimulation. A similar selectivity of LPS towards up-regulation of PAR-2 was seen for endothelial cells . The effect of TNF-α occurred after prolonged incubation and influenced the expression of all three PARs in A549 cells.

Interestingly, another proinflammatory cytokine, IL-8, which is also rapidly produced by immune cells and by epithelial cells themselves after LPS challenge, had an effect opposite to that of TNF-α. After long-term stimulation, IL-8 slightly down-regulated the PAR expression, especially PAR-2.

Under normal conditions, the epithelial cells produce proinflammatory chemokines and anti-inflammatory molecules, e.g. surfactant proteins, in a highly balanced manner, and the cell response to the exposure of inhaled LPS is dampened. Considering the expression of CXCR1 and 2, receptors for IL-8, on airway epithelial cells , the IL-8/CXCR1,2 axis may contribute to dampening cellular inflammatory responses in autocrine fashion under healthy conditions. In support of this, we observed that low (picomolar) concentrations of IL-8 that reflects the chemokine concentrations determined in BALF of healthy subjects , but not higher (nanomolar) IL-8 concentrations, down-regulated the expression of PAR-2 on airway epithelial cells (data not shown).

Therefore, it can be assumed that under physiological conditions the regulation of the level of PAR-2 is under the control of a negative feedback mechanism. Only when the burst of inflammatory reactions cannot be controlled and suppressed any more, PAR-2 participates actively in the development of proinflammatory responses.

Moreover, PAR-2, among all three PARs, was essentially influenced by PGE_2. Considering the fact that activation of epithelial PAR-2 induces the release of PGE_2 , down-regulation of PAR-2 by PGE_2 observed in our studies further supports the hypothesis about the presence of the PAR-2-PGE_2-prostanoid receptor EP axis in airway epithelium . Moreover, it has been postulated that the interplay between PAR-2, PGE_2 and its receptor predominantly produces anti-inflammatory effects within the lung.

Furthermore, a correlation between the modulation of PAR-2 mRNA synthesis and changes in IL-8 and TGF-β1 expression upon stimulation with inflammatory agents was observed. It means that the up-regulation of PAR-2 transcripts after stimulation with LPS or TNF-α was accompanied by increase in IL-8 expression level. Similarly, exposure to TNF-α and PGE_2 induced increase in PAR-2 and TGF-β1 transcript. On the contrary, the

down-regulation of PAR-2 expression induced by 24-h-exposure of the cells to IL-8 was observed together with reduced IL-8 mRNA level. Similarly, PGE_2 over 10 h induced slight down-regulation of PAR-2 as well as IL-8 expression.

Therefore, it can be speculated that PAR-2 belongs to the inflammatory network in lung and actively participates in regulation of ongoing inflammation and attraction of neutrophils.

4.4 Continuous PAR activation and simultaneous exposure to endotoxin modulate PAR expression in airway epithelial cells.

Both acute lung injury and chronic lung diseases, such as asthma, are accompanied by increased activity of the coagulant proteases, as a result of vascular leakage, and proteases from immune cells. Among those proteases are thrombin , tryptase , human airway trypsin-like protease (HAT) that possess the ability to activate PARs. However, it is not clear whether PAR activation can modulate PAR expression and susceptibility on airway cells. Therefore, it is important to evaluate the feedback influence of persisting PAR activation on PAR expression.

In the present study we showed that continuous activation of both PAR-1 and PAR-2 caused up-regulation of expression of these receptors in A549 cells, while PAR-3 expression was not influenced. This effect was seen for up to 24 h of incubation. Moreover, activation of PAR-2 resulted in higher up-regulation of the receptors than activation of PAR-1. The high susceptibility of PAR-2 to persistent PAR activation was confirmed also with primary HASEC and HBE cells. In HSAEC, activation of PAR-2 induced increased transcript levels of PAR-2, whereas PAR-1 agonist exhibited no effect on PAR expression level. In HBE cells, activation of both receptors PAR-1 and PAR-2 induced up-regulation of PAR-2 mRNA level. Studies on the consequences of simultaneous occurrence of PAR activation and bacterial pathogen invasion represent an important issue for the better understanding of lung infectious and inflammatory diseases. Therefore we assessed the interaction between PAR agonists and LPS. The combination of PAR-1 or PAR-2 agonists with LPS abrogated the effects on PAR-1 expression during all periods of incubation. At the same time, the PAR-2 expression level remained up-regulated after short stimulation only with the combination of LPS and PAR-2 AP. Thus, the elevation of expression of PAR-2 occurs to a higher extent than that of the other PARs and it persists even under those conditions, which decrease the expression of PAR-1. This is in line with the observations made in animal models of lung injury which showed that

rat bronchi after LPS treatment exhibited increased levels of PAR-2 on the epithelium and, as a consequence, increased responsiveness to PAR-2 activation . Taken together, these data underline the importance of epithelial PAR-2 and PAR-2 activators during acute and chronic inflammation.

Interestingly, prolonged incubation with PAR agonists together with LPS resulted in down-regulation of the PAR-3 level. This implies that PAR-3 can play a role in the development of inflammation in the human lung.

The control of PAR-1, -2 and -3 expression exerted by PAR activation by PAR-1 AP or PAR-2 AP and exposure to LPS, which we observed in epithelial cells is schematically summarized in Figure 4.1.

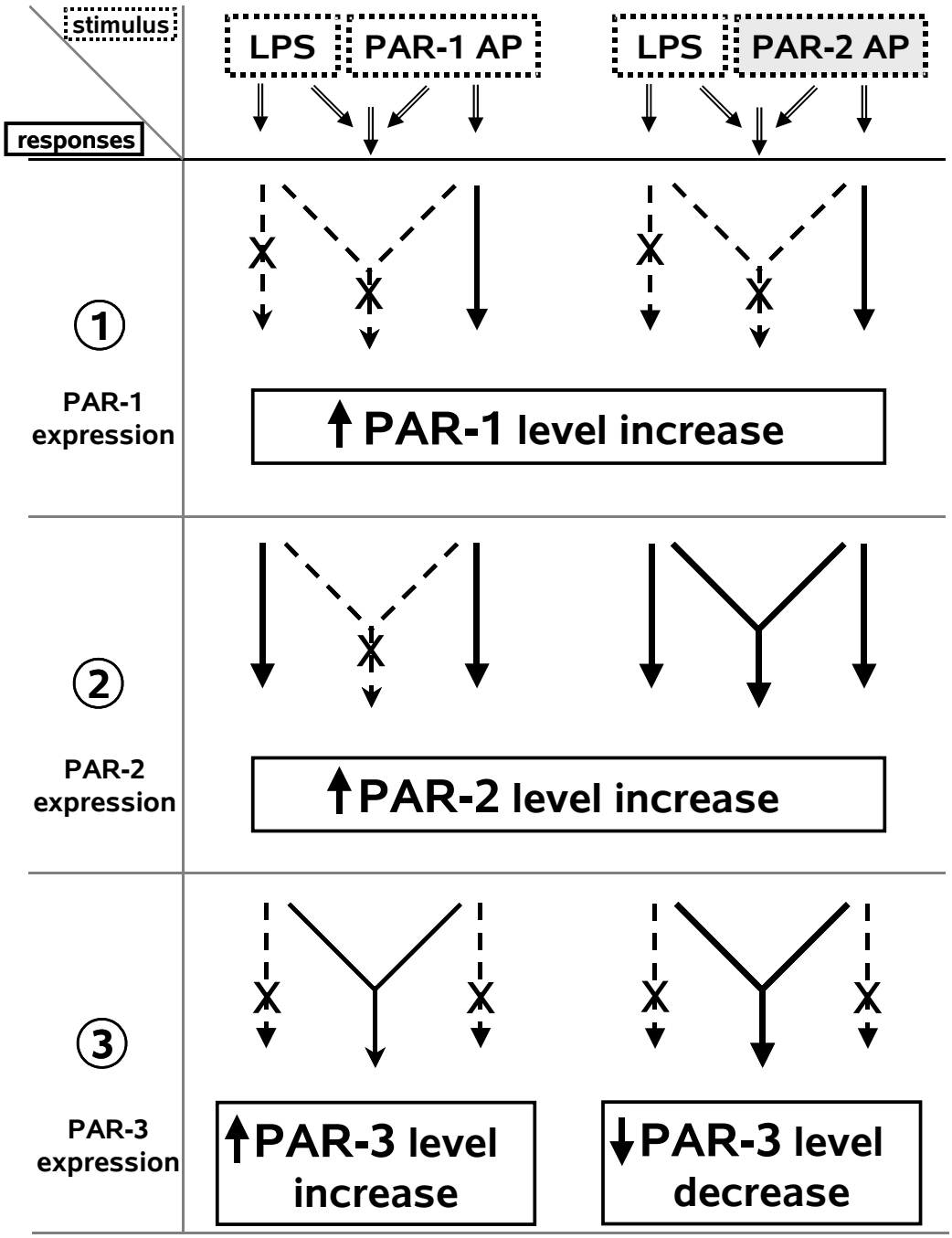

Figure 4.1: Scheme summarizing the effects of the exposure of lung epithelial cells to PAR agonists and LPS on PAR expression level. Application of PAR agonists and LPS as a single stimulus as well as the combined application are marked on top of the scheme in boxes within dotted frames. The effects of the stimulation of the cells with these agonists, given as **"Response 1"** (PAR-1 expression), **"Response 2"** (PAR-2 expression) and **"Response 3"** (PAR-3 expression) are presented below. The thickness of the arrows illustrates the strength of the response. The dashed arrows with a cross portray the lack of influence of the respective agonist.

However, it should be noted that pathological situations *in vivo* are characterized by the action of multiple factors. Each of them can potentiate or abolish the effects of others. Therefore, the receptor expression level is a result of complex interactions.

4.5 PAR activation stimulates and potentiates the LPS-induced IL-8 production.

In the present study, using primary airway epithelial cells (HASEC) and an epithelial cell line (A549), we found that PAR-2 agonists and LPS substantially potentiated each other's effects on the mRNA synthesis and release of IL-8 from the cells. We can conclude that epithelial PAR-2 synergistically with LPS intensifies neutrophil recruitment during bacterial infection. In agreement with this, PAR-2-deficient mice compared to wild-type animals showed lowered leukocyte rolling and reduced content of myeloperoxidase, a neutrophil marker. This was seen after surgical trauma and LPS-induced damage, respectively .

Asthmatic conditions and viral infection sensitize airways to noxious agents and are characterized by airway hyper-responsiveness. Disbalanced overproduction of proinflammatory mediators exacerbates the inflammatory airway status. The potentiation of IL-8 release by simultaneous PAR-2 activation and LPS exposure, as observed in this work, intensifies neutrophil recruitment, which is an example of cooperative action of inflammatory mediators acting in chronic inflammatory airway diseases. This supports the observations of others reporting a proinflammatory role of PAR-2 in airways . The participation of PAR-2 in the amplification of inflammatory signaling underlines the enormous importance of this receptor in lung pathophysiology.

Investigations presented above show that the persistent activation of PAR-2 by its agonists for which elevated levels have been observed in lung disorders, causes up-regulation of its own expression level. This might further increase the susceptibility and responsiveness to following activation of this receptor. The consequence of all these events is a substantial enhancement of IL-8 production. An alternative explanation for the potentiating effect of PAR-2 on the LPS-induced release of IL-8 can be the fact that LPS as well as PAR-2 activation independently induce expression of an additional portion of PAR-2 and thus enhance the responsiveness to PAR agonists. This participation of PAR-2 in a positive feedback loop that amplifies inflammatory signaling, underlines the enormous importance of this receptor in the lung pathophysiology.

We can also speculate that the potentiation of IL-8 production, observed in our work, which was induced by the combination of PAR-2 AP and LPS, is also due to increased transcriptional activity of factors responsible for IL-8 transcription. IL-8 transcription can be regulated by several transcription factors, including AP-1, NF-κB, AP-2, and NF-1L-6 **(**. PAR-2 activation in airway epithelial cells can induce AP-1 and NF-κB transcriptional activity . The same transcription factors can be activated upon LPS

exposure . We propose that simultaneous application of PAR-2 agonist and LPS to epithelial cells synergistically increases transcriptional activity of AP-1 and NF-κB and their binding to the IL-8 promoter.

It should be mentioned that only PAR-2, but not PAR-1, activation by specific activating peptides leads to release of IL-8 and is able to potentiate the LPS-induced chemokine release from both primary epithelial cells and cell lines, what is schematically summarized in Figure 4.2.

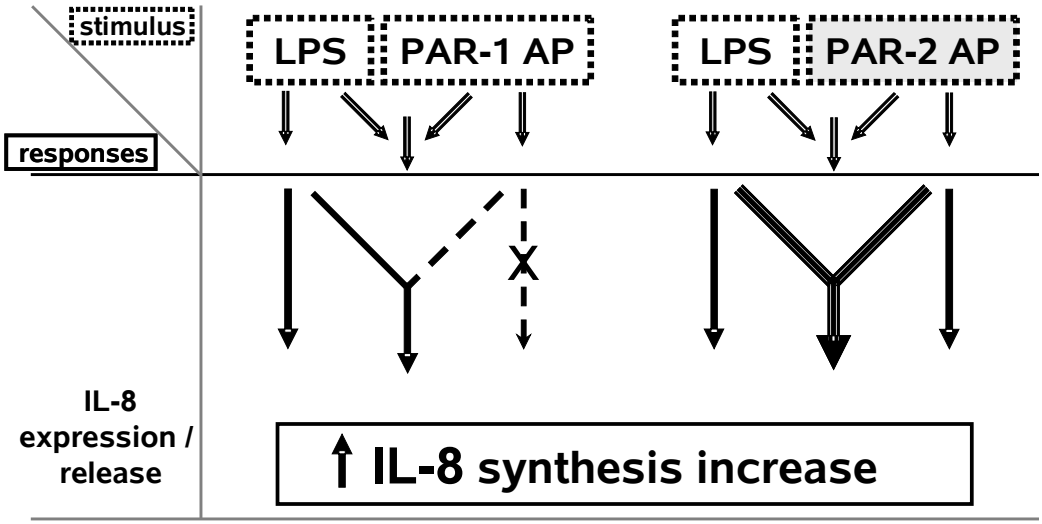

Figure 4.2: Scheme summarizing the effects of the exposure of lung epithelial cells to PAR agonists and LPS on IL-8 production. Application of PAR agonists and LPS as a single stimulus as well as the combined application are marked on top of the scheme in boxes within dotted frames. The effect of the stimulation of the cells with these agonists is given as **"Response"** (IL-8 synthesis). The thickness of the arrows illustrates the strength of the response. The dashed arrows with a cross portray the lack of influence of the respective agonist.

The observed effect of thrombin on IL-8 release, which was observed in A549 cells and HSAEC can be due to activation of other receptors for thrombin than PAR-1, e.g. PAR-3.

However, each member of the PAR family possesses a different selectivity towards agonists. PARs can induce different responses, depending on the agonist and cell type. Several recent reports have shown that different PAR subtypes can elicit cellular responses, which are unique for this PAR. For example, in A549 cells PAR-2, but not PAR-1, activation resulted in PGE_2 release and increased neutrophil adhesion to the cells in spite of the functional presence of PAR-1 . Activation of PAR-2 in normal bronchial epithelial cells causes changes in ion transport, while PAR-1 activation was ineffective in

this respect . These observations can serve as an example for demonstrating distinct roles of PARs in lung epithelium.

4.6 Inflammatory mediators and PAR activation induce TGF-β1 production.

The next part of this work aimed to assess the influence of PAR activation and LPS stimulation on TGF-β1 synthesis and release from lung epithelial cells. The present study shows for the first time enhancement of TGF-β1 mRNA expression in A549 cells upon PAR-1 and PAR-2 activation in A549 cells. This is consistent with the data obtained in human proximal tubule cells showing that PAR agonists are able to induce TGF-β1 release . Unlike PAR agonists, the bacterial component LPS displayed no effect on the TGF-β1 mRNA level, that is in line with a previous report . Moreover, in our study LPS suppressed the ability of PAR agonists to induce transcription of TGF-β1 in epithelial cells.

Interestingly, a correlation between modulation of TGF-β1 mRNA and PAR-2 mRNA synthesis was observed. TGF-β1 mRNA level was similarly modified as the PAR-2 mRNA level. Activation of PARs in A549 resulted in up-regulation of PAR-2 and TGF-β1 mRNA. Furthermore, application of LPS, in addition to PAR activation, attenuated the increase in the transcription level of PAR-2 as well as that of TGF-β1. This similarity possibly reveals a coupled action of PARs and TGF-β1 in the development of inflammatory and immunomodulatory effects in pathological conditions in the lung.

4.7 PAR-mediated signaling pathway in respiratory epithelium. Distinct role of MAPKs in PAR-induced IL-8 release.

There are multiple intracellular signaling pathways mediating the down-stream effects of GPCRs. Among them, mitogen-activated protein kinases (MAPKs) that belong to a family of serine/threonine kinases are important components of signal transduction pathways stimulated by GPCRs. They participate in diverse cellular events, including cell differentiation, movement and division. MAPK play also an important role in different immune responses in various cells, from the initiation of the immune response to inducing cell death . Signals of the members of the MAPK are transmitted by phosphorylation by their immediate upstream MEK and following translocation to the nucleus, where they phosphorylate transcription factors, thereby regulating the expression of genes. The MAPK family comprises five modules, which can signal independently from each other. The best characterized members are the extracellular signal-regulated kinase 1 and 2

(ERK1/2), c-Jun N-terminal kinase (JNK) and p38 MAPK. The ERK1/2-activated cascade preferentially regulates cell growth and differentiation, whereas JNK and p38 MAPK participate in cascades that function mainly in stress responses, like inflammation and apoptosis .

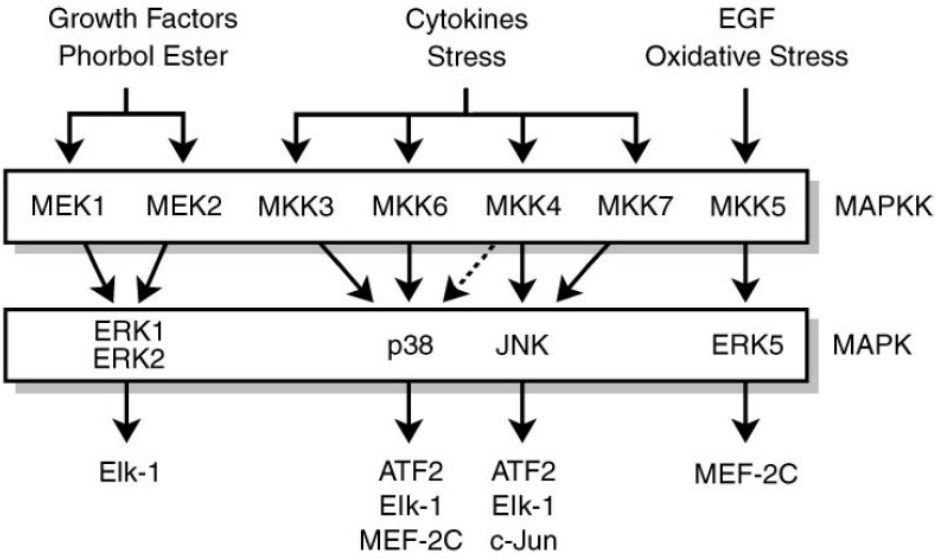

Figure 4.3: A schematic overview of mammalian MAPK modules (Schaeffer and Weber, 1999).

In this study the involvement of MAPKs in the IL-8 release induced by LPS and PAR agonists was investigated. The MAPKs have been shown to regulate the IL-8 expression and secretion induced by various inflammatory mediators in lung epithelial cells . The involvement of particular MAPK (ERK1/2, JNK or p38) in IL-8 release depends on the type of stimulus. In the present investigation, we have found that LPS-induced IL-8 release from A549 cells does not require the activity of MAPKs. None of the MAPKs was phosphorylated after stimulation with LPS. However, by phosphorylation analysis and inhibitor studies we showed that both PAR-2 AP- and thrombin-induced IL-8 release was dependent on ERK1/2 and JNK signaling (Fig.4.4). p38 MAPK was not involved in this process.

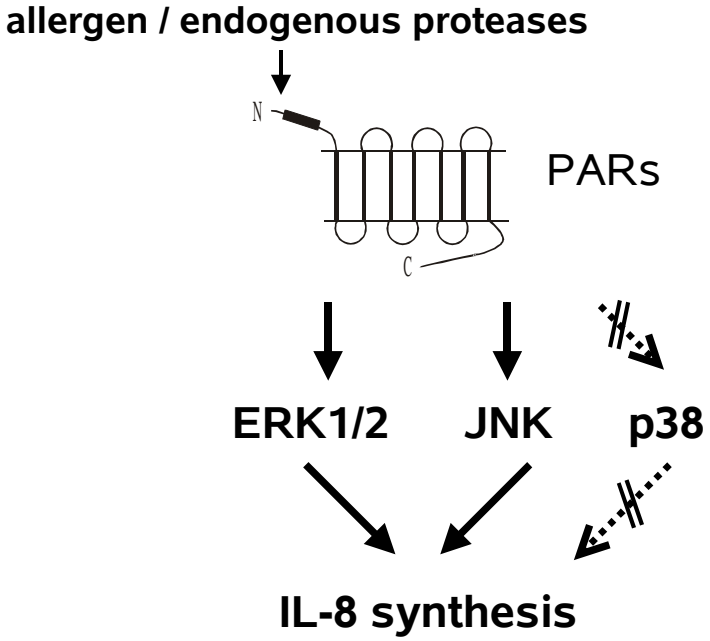

Figure 4.4: Activation of PARs in airway epithelial cells induces IL-8 release via ERK1/2 and JNK. During lung inflammation and injury, besides the presence of exogenous proteases from airborne allergens, there is elevated level of serine proteases from the coagulation system and released from the cells of the immune system. Subsequently, PARs are activated by these proteases inducing IL-8 release via activation of ERK1/2 and JNK but not activation of p38 MAPK.

Our data on PAR-2 activation by its specific activating peptide are in good agreement with recently published results on IL-8 release induced by PAR-2 activation by a protease from house dust mite, Der p3 . Interestingly, in that work the involvement of p38 but not JNK in the IL-8 release induced by PAR-2 AP was shown.

In our work, we found that simultaneous stimulation of A549 cells with LPS and PAR-2 AP or thrombin did not modify the phosphorylation levels of MAPKs compared to the effect of the PAR agonists alone. Pharmacological inhibitors of the MAPK signaling pathway showed the same inhibitory capacity in terms of IL-8 release for each stimulus alone and for the combination of stimuli. The inhibitor of MEK1/2, U0126, and the inhibitor of JNK, SP600125, both abolished the effects of thrombin and PAR-2 AP in A549 cells. Therefore, we conclude that the MAPK pathway is not involved in the potentiating effect of LPS and PAR agonist in IL-8 production. However, activation of ERK1/2 and JNK contribute to the signaling pathway in PAR-mediated IL-8 secretion in A549 cells, as shown in Figure 4.4.

4.7.1 Role of PAR-3 in IL-8 production and the signaling pathway involved in this process.

The intriguing question raised during our observation was the possible contribution of PAR-3 in thrombin-mediated IL-8 release from epithelial cells.

The patho-physiological roles of human PAR-3 are still largely unknown. Therefore the aim of this study was to verify whether PAR-3 participates in inflammatory reactions, similarly to other PARs, by mediating interleukin-8 production. Furthermore, the important question to be answered was whether human PAR-3 can signal autonomously or only in cooperation with another thrombin receptor. Finally, is should be answered if MAPKs are involved in PAR-3 signaling.

In our studies, the HEK-293 cells transfected with the PAR-3-GFP served as experimental model to investigate the issue mentioned above. The PAR-3-GFP construct showed clearly a significant rise in Ca^{2+} response compared to those cells transfected only with GFP. These data confirm that the PAR-3 used in our system was functional. Indeed, PAR-3 can be activated by thrombin, thereby triggering increase in $[Ca^{2+}]_i$. Our findings are in line with data obtained from PAR-3-expressing COS-7 cells and Xenopus oocytes, where thrombin induced phosphoinositide hydrolysis and ^{45}Ca release, respectively . However in other systems, expressing endogenous PAR-3, thrombin did not trigger PAR-3 signaling. The group of Hollenberg reported the inability of thrombin to induce Ca^{2+} mobilization after desensitization of PAR-1 with its specific agonist in cells expressing PAR-3, i.e. Jurkat and HEK-293 cells . Similar results were obtained in human brain microvascular endothelial and in human umbilical vein endothelial cells (HUVEC) . This inconsistency in the calcium signaling between endogenous und exogenous PAR-3 may be due to the respective expression level of the receptor.

Further, the results presented here demonstrate that thrombin mediates IL-8 production in HEK-293 cells stably expressing PAR-3. The cytokines are the main effector substances of the inflammatory and immune response. Many common human diseases are characterized by a dysregulation of the balance between pro- and anti-inflammatory cytokines. Therefore, this ability of PAR-3 to mediate the increased IL-8 release allows us to assume that human PAR-3 is an important player in the inflammatory state.

Concerning the issue whether PAR-3 is able to mediate autonomously intracellular signaling, it has to be mentioned, that PAR-4 was not expressed in HEK-293 cells, both wildtype cells and cells transfected with PAR-3 receptor. This we conclude from PAR-4

detection by RT-PCR and measurements of $[Ca^{2+}]_i$, which both gave negative results. Therefore it can be concluded that, differently from the mouse system, where PAR-3 acts as a cofactor for PAR-4 activation, in humans PAR-3 can generate an intracellular signal independent from PAR-4. Additionally, our investigations on PAR-1-deficient cells suggest that also the presence of PAR-1 is not necessary for PAR-3-mediated production of IL-8. The silencing of the PAR-1 expression in HEK-PAR3-GFP cells had no significant influence on IL-8 production upon thrombin stimulation. Moreover, the application of TRag, the PAR-1-activating peptide, did not trigger the IL-8 synthesis in HEK-PAR3-GFP cells co-transfected with control siRNA, which thus express functional PAR-1. That finding underlines that PAR-1 was not involved in the IL-8 synthesis and that PAR-3 mediates, independently from PAR-1, IL-8 release in HEK-PAR3-GFP cells upon exposure to thrombin.

A similar effect of thrombin was seen in lung epithelial A549 cells that endogenously express PAR-3. These cells responded to this protease with enhanced IL-8 release. On the contrary, HBE cells that lack PAR-3 expression failed to respond to thrombin with increasing IL-8 production. Although both cell lines express PAR-1, PAR-1 activation by its activating peptide was not able to induce IL-8 synthesis. These finding can give supportive evidence that endogenous PAR-3 is susceptible to thrombin, which causes IL-8 production.

However, it has to be mentioned that in other systems such as human dermal fibroblasts or human luteinized granulosa cells (LGC), thrombin stimulation resulted in increased IL-8 release via PAR-1 activation, which was proven using the PAR-1 agonist . It can be suggested that this PAR-1-mediated IL-8 synthesis might be due to the high expression level of PAR-1 in these cells. Since both cells expressed besides PAR-1, also PAR-3, the second alternative might be that when endogenously expressed, both receptors form in some part heterodimers, according to a recent report . With high expression levels of PAR-1, the possibility to form heterodimers with PAR-3 is increased. It seems possible that mainly the PAR1/PAR3 heterodimers, but not PAR1 alone, might be able to induce IL-8 release.

We investigated also the involvement of MAPKs in the IL-8 release induced by thrombin from HEK-293 cells expressing PAR-3. The MAPKs have been shown to regulate the IL-8 expression and secretion induced by PAR activation in many different cells. Here, we demonstrate for the first time that activation of PAR-3 by thrombin mediates IL-8 synthesis via ERK1/2 phosphorylation, whereas the other members of the

MAPK family, JNK and p38 MAPK, were not significantly involved in thrombin-mediated PAR-3 activation. We have confirmed these observations by phosphorylation analysis and inhibitor studies. Silencing of PAR-1 in HEK-PAR3-GFP cells had no significant effect on the level of ERK1/2 phosphorylation, except for a slight reduction after 5 min of thrombin stimulation. These experiments confirm that PAR-3-mediated signaling does not require the presence of PAR-1. However, the existence of some proportion of PAR-1/PAR3 heterodimers cannot be excluded. Moreover, the relatively weak but significant JNK activation and its involvement in thrombin-mediated IL-8 secretion might be due to PAR-1/PAR-3 co-activation. Therefore, the concept of receptor dimerisation might be an important topic that has to be followed further in exploring PAR-3 signaling. It has been shown already that PAR-1 and PAR-4 are able to form stable heterodimers on human platelets and also when expressed in COS-7 fibroblasts. There PAR-1 acts as a cofactor and promotes the cleavage and activation of PAR-4 .

In conclusion, our investigations show that human PAR-3 might signal after activation by thrombin. The functional consequence of PAR-3 activation is elevation in ERK1/2 phosphorylation and increase in production of IL-8. Furthermore, PAR-3 responsiveness to thrombin is generally not dependent on the presence of PAR-1.

4.8 Conclusions

PARs on the airway epithelium can be activated both by exogenous proteases accessing the epithelium and by endogenous proteases secreted from resident or recruited cells. Under pathological conditions, PAR-activating proteases as well as pro-inflammatory mediators from pathogens are present at elevated level. We demonstrate that, among three trypsin isoforms, cationic and anionic isoforms interact with lung epithelial cells and activate PAR-2. Differently, mesotrypsin exhibits no activity on epithelial PARs (Fig. 4.5).

Simultaneous occurrence of PAR activation and bacterial pathogen invasion represents an additional relevant issue for the better understanding of the development of lung infection and chronic inflammatory diseases. Our studies present new evidence for separate and cooperative functions of PARs in the airway epithelial cells that are summarized in Figure 4.5. The numbered pathways illustrated in Figure 4.5 show the following findings:

- Pathway 1: The continuous activation of PAR-1 and PAR-2 by their agonists increases the expression level of these receptors.

- Pathway 2: The bacterial endotoxin LPS activates TLR-4 that causes the increase of the transcription level of PAR-2, but not of PAR-1.
- Pathway 3: The increased PAR-2 mRNA level persists upon simultaneous exposure to LPS, conditions that attenuate up-regulation of PAR-1 mRNA level.
- Pathway 4: Only activation of PAR-2 leads to increased production of chemokine IL-8. ERK1/2 and JNK are involved in this PAR-2 AP-mediated IL-8 release.
- Pathway 5: There is a cooperative action of PAR-2 and LPS in the production of the chemoattractant IL-8 and subsequent neutrophil recruitment.
- Pathway 6: PAR-1 and PAR-2 activation increase the production of the immunomodulatory cytokine TGF-β1. PAR-2 agonist exhibits higher effect than PAR-1 agonist on TGF-β1 synthesis.
- Pathway 7: The functional consequence of PAR-3 activation by thrombin is elevation in ERK1/2 phosphorylation and increase in production of IL-8.

PAR-3, as a receptor that mediates cytokine production, can be considered as an important modulator in the burst of inflammatory reactions. These findings presented here give new insights into the signaling and function of human PAR-3. With the help of HEK cells overexpressing PAR-3 we could confirm our hypothesis of PAR-3-mediated responses in airway epithelial cells.

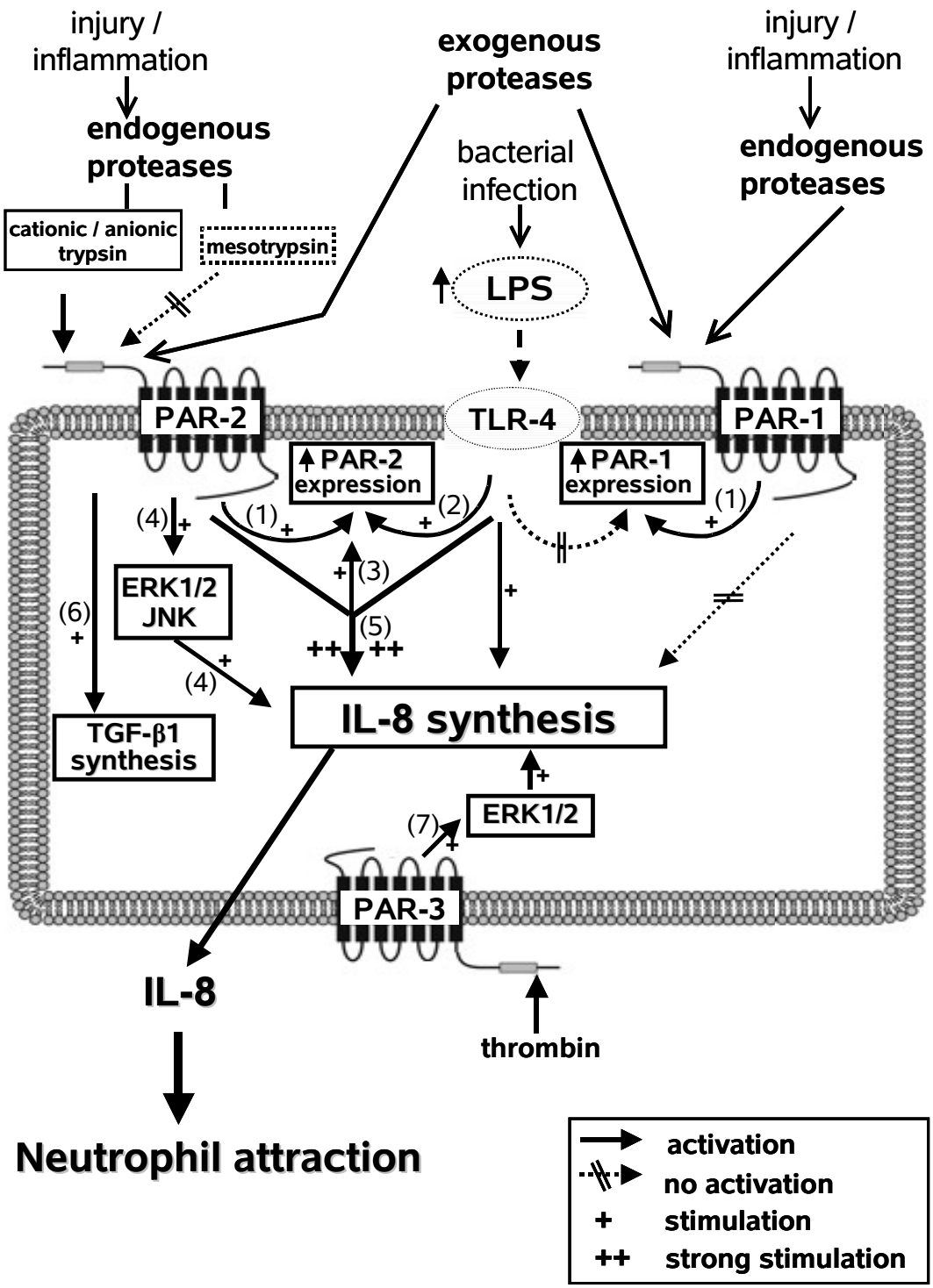

Figure 4.5: Scheme of separate and cooperative action of PARs and bacterial endotoxin (LPS) in regulation of the production of cytokines in airway epithelium. In lung epithelial cells PARs can be activated by airborne proteases and also by endogenous proteases e.g. cationic and anionic isoforms of trypsin that activate epithelial PAR-2. Pathway 1: The consequence of continuous activation of PAR-1 and PAR-2 is increased expression of both receptors. Pathway 2: Exposure of the cells to LPS up-regulates expression of PAR-2, but not of PAR-1 and PAR-3. Pathway 3: LPS in combination with PAR-2 activation induced increased transcription of PAR-2. Pathway 4: Activation of PAR-2 but not of PAR-1 triggered production of IL-8 through ERK1/2 and JNK. Pathway 5: Simultaneous LPS and PAR-2 activation causes potentiation in IL-8 synthesis. Pathway 6: Activation of PARs induces synthesis of TGF-β1. Pathway 7: Thrombin-induced PAR-3 activation leads to the ERK1/2 phosphorylation and finally to elevated IL-8 production.

5 Abstract

Asthma is a chronic inflammatory disease of the airways in which besides migratory cells of the immune system, many resident cells like smooth muscle cells, fibroblasts and epithelial cells play important roles. The airway epithelium acts not only as a physical barrier for inhaled infectious stimuli but also actively participates in acute and chronic inflammatory reactions by releasing pro- and anti-inflammatory mediators. Exposure of epithelial cells to deleterious factors, like allergens, bacteria, pollutants, and to endogenous proinflammatory factors, triggers defence mechanisms by modulation of expression and secretion of different bioactive molecules such as lipid mediators, cytokines, extracellular matrix proteins. It has been shown that the release of those agents is frequently mediated via activation of protease-activated receptors (PARs). PARs belong to the superfamily of G-protein coupled receptors with a 7-trans-membrane domain structure. They are activated by proteolytic cleavage of their N-terminus. For many potential PAR activators in airways elevated activity has been observed during chronic inflammation. Among those proteases are thrombin, tryptase, human airway trypsin-like protease (HAT) as well as proteases from airborne allergens. However, there is still limited information concerning the question which particular factors are responsible for the alteration of PAR expression and susceptibility in lung epithelial cells.

The findings of the present study are as follows:

1. Using RT-PCR, immunocytochemistry and Ca^{2+} mobilization measurements, we demonstrated that the airway epithelial cell line A549 expresses PAR-1, PAR-2, and PAR-3. Short-term stimulation of these cells with thrombin, trypsin, and activating peptides of PAR-1, PAR-2, but not PAR-3 and PAR-4, induced a transient rise of $[Ca^{2+}]_i$.
2. We showed that cationic and anionic trypsin induce Ca^{2+} mobilization in these cells. Mesotrypsin displays no effect on $[Ca^{2+}]_i$ rise. Furthermore, from desensitization study using PAR-2 AP we conclude that PAR-2 is substrate for cationic and anionic trypsin isoforms in human airway epithelial cells.
3. We evaluated the influence of inflammatory mediators LPS, TNF-α, IL-8 and PGE_2 on PAR expression level in A549 cells. We also investigated the influence of continuous PAR activation on PAR expression and release of the proinflammatory chemokine IL-8. We employed three different cells, two airway epithelial cell lines, A549 and HBE cells and primary airway epithelial cells (HSAEC). The bacterial endotoxin LPS after 4 h of stimulation up-regulated PAR-2 expression 2-fold, but the

effect disappeared after 24-h-term stimulation. TNF-α up-regulated PAR-1, -2 and -3 expression after 24 h of incubation. Exposure of the cells to IL-8 slightly decreased PARs mRNA level, mostly PAR-2. Similarly PGE_2 down-regulated PAR expression after 10 h of stimulation, whereas after 16 h PAR-2 mRNA level was up-regulated.

4. Continuous activation of PARs by exposure of epithelial cells to PAR-1 and PAR-2 agonists increased the PAR-1 expression level. The PAR-2 agonist exhibited higher potency than PAR-1 activators. However, in epithelial cells the combined incubation with LPS and PAR agonists abrogated the PAR-1 up-regulation induced by a single stimulus. Stimulation with PAR-1 or PAR-2 agonists also up-regulated the PAR-2 expression level (2.7-fold) that was higher than the effect of PAR agonists on PAR-1 level. In contrast to PAR-1, the PAR-2 level remained elevated under concomitant stimulation with LPS and PAR-2 agonist. PAR-3 mRNA level in A549 cells remained unaffected upon continuous PAR activation, whereas combined stimulation with PAR agonists and LPS resulted in slight down-regulation of PAR-3 level after 24 h.
5. Activation of PAR-2, but not of PAR-1 caused production of IL-8 from the epithelial cell lines. This effect was mediated in A549 cells by c-jun N-terminal kinase (JNK) and extracellular signal regulated kinase-1/2 (ERK1/2). We found synergistic modulation by PAR-2 agonist and LPS of the IL-8 synthesis and release both in the epithelial cell line and in primary epithelial cells.
6. PAR agonists induced also expression of the immunomodulatory cytokine TGF-β1. Simultaneous application of PAR agonists together with LPS attenuated or completely abolished the TGF-β1 up-regulation induced by PAR agonists alone.
7. With the help of HEK-293 cells expressing PAR-3, we demonstrated for the first time, that PAR-3 is involved in thrombin-mediated ERK1/2 activation and release of IL-8. Furthermore, generation of intracellular signals by PAR-3, such as enhancement of cytokine synthesis, does not require co-activation of PAR-1 or PAR-4.

In summary, these results underline the exclusive role of PAR-2 in human lung epithelial cells in regulation of receptor expression and mediating inflammatory responses. We show an intricate interplay between LPS and PAR agonists in affecting PAR regulation and production of IL-8 and TGF-β1 in lung epithelial cells. Our study reveals a new cooperative action of PAR-2 and endotoxin that contributes to the enhancement of inflammatory signaling in airways. In addition, we show that PAR-3, the elusive receptor among the PARs, can be activated by thrombin inducing functional

responses, such as IL-8 synthesis. Therefore PAR-3 participates actively in inflammatory reactions.

6 Zusammenfassung

Asthma ist eine chronische, entzündliche Erkrankung der Atemwege, in welcher neben den wandernden Zellen des Immunsystems auch die Zellen der glatten Muskulatur, sowie Fibroblasten und Zellen des Epithels eine wichtige Rolle spielen. Die Alveolarepithelzellen sind nicht nur ein physikalisches Hindernis für Infektionserreger, sondern spielen auch eine aktive Rolle in akuten und chronischen Entzündungsreaktionen, indem sie eine Reihe von entzündungsauslösenden und -hemmenden Mediatoren freisetzen. Die Exposition von Epithelzellen gegenüber schädlichen Faktoren, wie Allergenen, Bakterien, Schmutzstoffen und endogenen pro-inflammatorischen Stoffen lösen Abwehrmechanismen aus, wodurch Expression und Freisetzung von wichtigen bioaktiven Molekülen, wie z. B. Lipidbotenstoffen, Zytokinen, extrazellulären Matrixproteinen gesteuert werden. Es wurde gezeigt, dass die Freisetzung dieser Mediatoren oft durch Aktivierung von Protease-aktivierten Rezeptoren (PARs) vermittelt wird. PARs gehören zu der Superfamilie der G-Protein-gekoppelten Rezeptoren mit 7 Transmembran-Domänen. Aktivierung der PARs wird durch die proteolytische Spaltung durch extrazelluläre Proteasen eingeleitet. Die Spiegel vieler PAR Agonisten in den Atemwegen sind während chronischer Erkrankung erhöht. Dazu gehören die Proteasen wie Thrombin, Tryptase, HAT (human airway trypsin-like protease) und viele durch die Luft übertragene Allergene. Unsere Kenntnisse bezüglich der Faktoren, welche die PAR Expression und deren Erregbarkeit modifizieren, sind noch begrenzt.

In der vorliegenden Arbeit werden folgende Ergebnisse vorgestellt:

1. Wir haben mittels RT-PCR, Immunozytochemie und Ca^{2+}-Mobilisierungsstudien gezeigt, dass PAR-1, PAR-2 und PAR-3 in Epithelzellen der Lunge (Zelllinie A549) funktionell exprimiert werden. Kurzzeitstimulierung dieser Zellen mit Thrombin, Trypsin und Peptiden, die die „tethered-ligand“-Domäne von PAR-1, PAR-2, aber nicht von PAR-3 und PAR-4, darstellen, induzieren einen transienten Anstieg der intrazellulären Ca^{2+}-Konzentration ($[Ca^{2+}]_i$).
2. Unsere Untersuchungen von Isoformen des Trypsins ergaben, dass kationisches und anionisches Trypsin die Ca^{2+} Mobilisierung in Lungen-Epithelzellen induzieren. Mesotrypsin führte jedoch zu keiner $[Ca^{2+}]_i$-Antwort in diesen Zellen. Basierend auf Desensitisierungsversuchen durch Verwendung des PAR-2 Aktivierungspeptids (PAR-2-AP), konnten wir zeigen, dass PAR-2 in der Lunge ein Substrat für kationisches und anionisches Trypsin darstellt.

3. Weitere Untersuchungen befassten sich mit den Änderungen des PAR-mRNA-Spiegels nach Exposition der A549-Zellen gegenüber Entzündungsmediatoren wie LPS, TNF-α, IL-8 und PGE_2. Dazu wurden Real-Time PCR Experimente durchgeführt. Die Behandlung mit den oben genannten Mediatoren bewirkte unterschiedliche Effekte, wobei PAR-2 mRNA hauptsächlich beeinflusst wurde.
4. Für weitere Analysen haben wir noch andere Lungenepithelzellen eingesetzt, wie HBE Zellen und primäre Lungen Epithelzellen (HSAEC).

Eine kontinuierliche Aktivierung der PARs durch Stimulierung mit PAR Agonisten führte zu einer erhöhten Expression von PAR-1 mRNA, wobei das PAR-2 Aktivierungspeptid, verglichen mit PAR-1-AP, eine höhere Wirksamkeit aufwies. Allerdings führte die kombinierte Inkubation der Zellen mit PAR Agonisten und LPS zu einer verminderten Hochregulation von PAR-1 mRNA. PAR-2 mRNA wurde ebenfalls nach der Behandlung mit PAR-1 und PAR-2 Agonisten hochreguliert, und die Änderungen waren größer als die bei der PAR-1 Expression. Im Gegensatz zu PAR-1, war immer noch eine erhöhte PAR-2 Expression nach gleichzeitiger Behandlung mit LPS und PAR-2 Agonist zu beobachten. Die PAR-3-mRNA-Expression in A549 Zellen blieb jedoch unter kontinuierlicher PAR Aktivierung unverändert. Nur die kombinierte Inkubation der Zellen mit LPS und PAR Agonisten bewirkte eine Herunterregulation der PAR-3 Expression.

5. Weiterhin konnten wir zeigen, dass die Aktivierung von PAR-2, aber nicht die von PAR-1 die Freisetzung von IL-8, einem Entzündungsmarker, induziert. Darüber hinaus wurden die Signalübertragungswege, welche nach Stimulation mit Thrombin und dem PAR-2-AP in A549 Zellen aktiviert werden, untersucht. Die beiden Agonisten führten zu einer Aktivierung des MAPK-Weges, stimulierten die Phosphorylierung von ERK1/2 (extracellular signal regulated kinase-1/2) und JNK (c-jun N-terminal kinase). Außerdem haben wir in A549 Zellen und primären Lungenepithelzellen nachgewiesen, dass die durch PAR-2-AP und LPS-vermittelte IL-8 Freisetzung synergistisch stimuliert wurde.
6. Zudem erhöhten PAR Agonisten, hauptsächlich PAR-2-AP, die Expression von TGF-β1, einem immunmodulatorischen Zytokin. Simultane Behandlung der Zellen mit LPS und PAR Agonisten verminderte die durch PAR Aktivierung hervorgerufene TGF-β1 Hochregulation.
7. Mit Hilfe von HEK-293 Zellen, die PAR-3 überexprimieren, konnten wir als erste zeigen, dass PAR-3 an der Thrombin-vermittelten ERK1/2 Aktivierung und IL-8 Freisetzung beteiligt ist. Im Gegensatz zu ERK1/2 wurde JNK nur geringfügig

aktiviert, wobei die p38 MAPK bei der durch Thrombin induzierten Signalkaskade überhaupt nicht beteilig war. Die von PAR-3 vermittelten Effekte, wie die erhöhte IL-8 Synthese, erfordern keine Koaktivierung von PAR-1. Dieses haben wir mittels Herunterregulierung der Expression von PAR-1 durch siRNA bestätigen können.

Zusammenfassend ist diese Studie die erste, die folgende Befunde über Epithelzellen der Lunge zeigt: i) Die Entzündungsmediatoren modulieren die PAR Expression in A549 Zellen unterschiedlich. ii) Kontinuierliche PAR Aktivierung führt zur Änderung der PAR-Expression, wobei PAR-2 eine besonders herausragende Rolle spielt. iii) PAR-2 Aktivierung induziert IL-8 Freisetzung, wobei es mit LPS synergistisch wirkt. iv) PAR-induzierte IL-8 Freisetzung wird über den ERK1/2- und JNK-Signalweg vermittelt. iiv) PAR Aktivierung führt zur erhöhten TGF-β1-Expression.

Diese Studien zeigen dass PARs, insbesondere PAR-2, eine signifikante Funktion in entzündlichen Erkrankungen der Atemwege spielen. Das Wechselspiel zwischen PAR-2 und Endotoxinen wie LPS gibt wertvolle Einblicke in das Verständnis der Rolle von PARs bei Erkrankungen der Lunge, wie z. B. Asthma. Zusätzlich konnten wir zeigen, dass Aktivierung von PAR-3, des bisher am weinigsten erforschten Mitglieds der PAR-Familie, zu einer IL-8 Freisetzung führt, und dass dieser Rezeptor dadurch eine signifikante Rolle in Entzündungsprozessen spielen kann.

7 References

8 Abbreviations

AP	Activating peptide
A549	Human alveolar epithelial cell line
bp	Base pair
BSA	Bovine serum albumin
$[Ca^{2+}]_i$	Intracellular calcium concentration
COS-7	African green monkey kidney fibroblast-like cell line
cDNA	Complementary deoxyribonucleic acid
DMEM	Dulbecco's Modified Eagle's Medium
DNA	Deoxyribonucleic acid
dNTP	Deoxyribonucleoside triphosphate
DEPC	Diethyl pyrocarbonate
DMSO	Dimethyl sulfoxide
ds	Double stranded
DMSO	Dimethyl sulfoxide
ELISA	Enzyme Linked-Immuno-Sorbent Assay
ERK	Extracellular regulated kinase
Fura-2/AM	Fura-2/Acetoxymethyl Ester
FCS	Fetal calf serum
GAPDH	Glyceraldehyde phosphate dehydrogenase
GFP	Green fluorescent protein
GPCR	G-protein coupled receptor
GDP	Guanosine diphosphate
GTP	Guanosine triphosphate
HBE	Human bronchial epithial cell line
HBSS	Hank's balanced salt solution
HEK	Human embryonic kidney epithelial cell line
HSAEC	Human Small Airway Epitehlial Cells
$InsP_3$	Inositol 1,4,5-trisphosphate
JNK	c-jun related kinase
KCM	KCl- $CaCl_2$- $MgCl_2$
LB	Luria bertini
MMPs	Matrix Metalloproteinases

MAPK	Mitogen-activated protein kinase
mRNA	Messenger ribonucleic acid
MOPS	N-Morpholino-3-propansulphonic acid
p38 MAP	p38 mitogen activated protein
PBS	Phosphate buffered saline
PLC	Phospholipase C
PAR	Protease-activated receptor
PKC	Protein kinase C
PCR	Polymerase Chain Reaction
RT	Reverse Transcription
SDS-PAGE	Sodium dodecyl sulphate-polyacrylamide gel electrophoresis
SiRNA	Small interfering RNA
TCM	Tris/HCl- $CaCl_2$- $MgCl_2$
Tm	Melting temperature
TRag	Thrombin receptor agonist
TBE	Tris-boric acid-EDTA
TE	Tris-EDTA
WT	Wild-type